Chapter 6

Sensitivity Analysis of the Optimized LNA Specification

Following the results of optimization, the 2^{nd} order model with the stepwise regression is applied. We note that the models used should be the same with the optimization analysis. We will have three sensitivity analyses corresponding to the three optimal recipes obtained by optimization. In this chapter, we discuss variation of VB1 parameter, and take the case of satisfied all specifications with the largest D as the example. The procedure of other optimal recipes for sensitivity analysis is similar to that.

6.1 Sensitivity Analysis for LNA Circuit

By varying a set of critical circuit parameters, we will investigate the sensitivity of seven responses. Once a quadratic model for each response has been obtained, then it can save us a lot of time to run circuit simulator. To represent fluctuations of circuit performance, random values of parameters are selected from a normal distribution, and the corresponding circuit performance is calculated by their response surface models, respectively.

For example, the mean for VB1 input condition is equal to its optimized value, and the standard deviation is 1 % of its optimized value. In order to study the statistical nature of the LNA circuit performance, we have generated 100 normally and independently distributed pseudo-random numbers for VB1. The variation of seven circuit performance we obtained is calculated by the response surface models. Figures 6.1-6.7 are statistical distributions obtained by the sensitivity analysis on the models for the S11, S12, S21, S22, K , NF, and IIP3. Table 6.1 presents the results of sensitivity analysis by varying VB1 for the LNA circuit.

Among the seven figures, S12 obviously skewed to right, and is not a good result. But its standard deviation is very small so that we can ignore the phenomenon. However, the variation of each standard deviation is about 1 % of its optimal result, and the mean values of the seven responses calculated by the 2^{nd} order models are in good agreement with the simulated circuit performance.

Table 6.1: Sensitivity analysis for LNA circuit calculated from the response surface model which is obtained from circuit simulator by varying VB1. Calculated mean and standard deviation for seven circuit performances are shown.

Response	Predicted mean	Predicted Std. Dev.	Varied %	Actual mean	Actual Std. Dev	Varied %
S11 (dB)	-10.6494	0.1335	1.25	-10.3764	0.0629	0.059
S12 (dB)	-39.2682	0.00361	0.01	-39.2966	0.004969	0.01
S21 (dB)	14.3590	0.06470	0.45	14.3102	0.06005	0.42
S22 (dB)	-12.1912	0.01380	0.11	-12.2843	0.02931	0.24
K	7.8886	0.04506	0.57	7.9452	0.04918	0.62
NF (dB)	0.9459	0.00940	0.99	0.9793	0.008145	0.86
IIP3 (dB)	-5.8384	0.06295	1.08	-5.73435	0.080059	1.37

For the other examples, the mean for each input condition is set to be its optimized value, and the standard deviation is 1 % of the optimized value. In order to study the statistical nature of the LNA circuit performance, we generate 100 normally-and-independently distributed pseudo-random numbers for 10 factors. The variation of seven circuit performance we obtained is calculated by the response surface model. Table 6.1 presents the results of sensitivity analysis by varying 10 factors for the LNA circuit. Statistical distributions obtained by the sensitivity analysis on the models for the S11, S12, S21, S22, K , NF, and IIP3 are shown in Appendix E. Variation of all responses for the LNA circuit is less than ten percent of their nominal results, and the mean values of the seven responses calculated by the 2^{nd} order models are in good agreement with the simulated circuit performance.

Table 6.2: Sensitivity analysis for LNA circuit calculated from response surface models and obtained from circuit simulator by varied 10 factors, displaying calculated mean and standard deviation for seven circuit performances.

Response	Predicted mean	Predicted Std. Dev.	Varied %	Actual mean	Actual Std. Dev	Varied %
S11 (dB)	-10.573	0.558	5.38	-10.337	0.327	3.15
S12 (dB)	-39.271	0.089	0.23	-39.300	0.084	0.21
S21 (dB)	14.331	0.110	0.77	14.286	0.101	0.70
S22 (dB)	-12.146	0.217	1.76	-12.254	0.328	2.67
K	7.910	0.093	1.17	7.958	0.107	1.35
NF (dB)	0.951	0.0200	2.00	0.983	0.0175	1.73
IIP3 (dB)	-5.784	0.456	7.95	-5.780	0.551	9.61

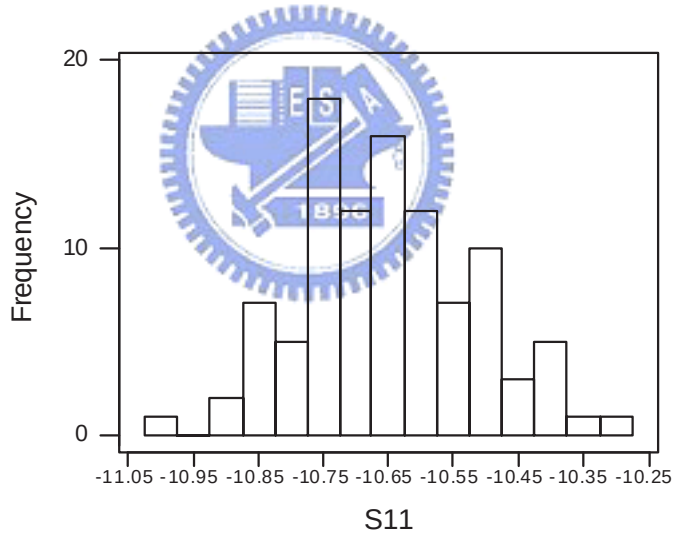

Figure 6.1: Statistical distribution of the model for S11, which is calculated by the sensitivity analysis and using the full 2^{nd} order response surface model by varying VB1.

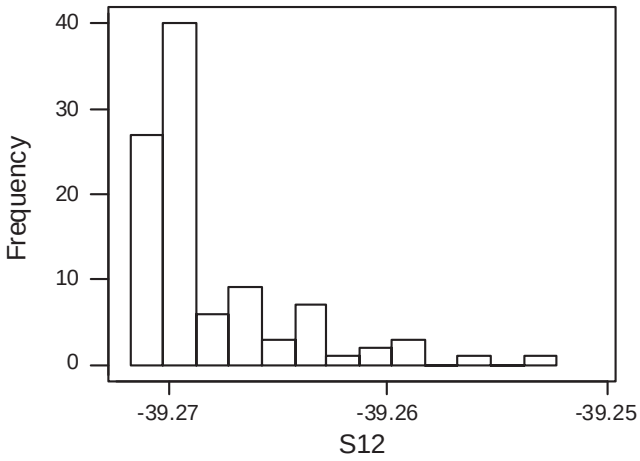

Figure 6.2: Statistical distribution of the model for S12, which is calculated by the sensitivity analysis and using the full 2^{nd} order response surface model by varying VB1.

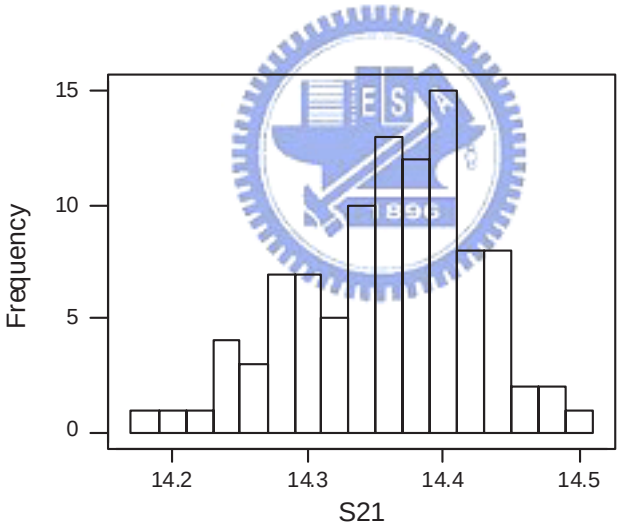

Figure 6.3: Statistical distribution of the model for S21, which is calculated by the sensitivity analysis and using the full 2^{nd} order response surface model by varying VB1.

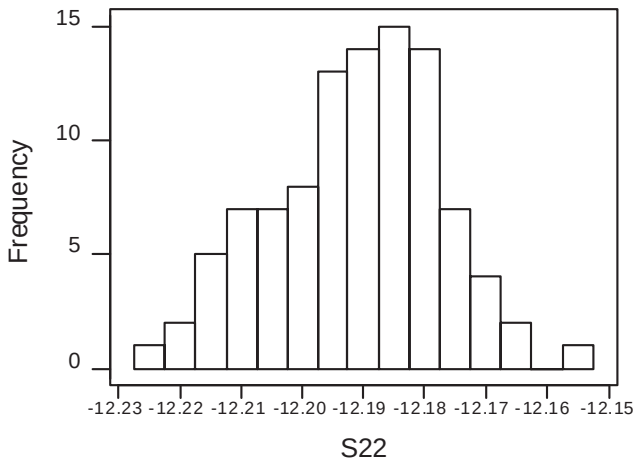

Figure 6.4: Statistical distribution of the model for S22, which is calculated by the sensitivity analysis and using the full 2^{nd} order response surface model by varying VB1.

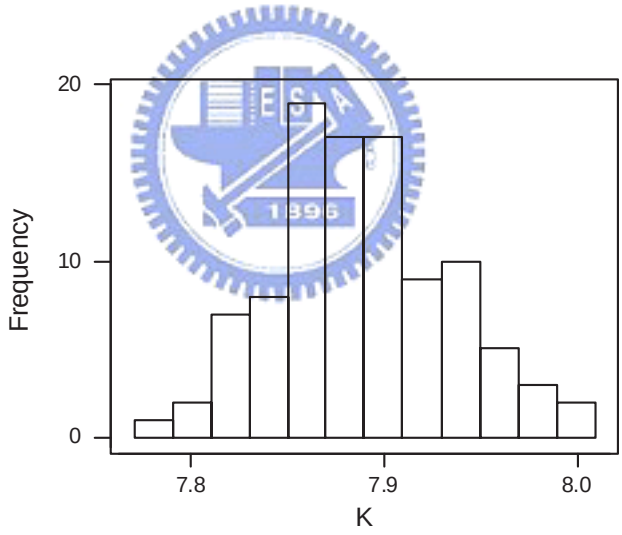

Figure 6.5: Statistical distribution of the model for K, which is calculated by the sensitivity analysis and using the full 2^{nd} order response surface model by varying VB1.

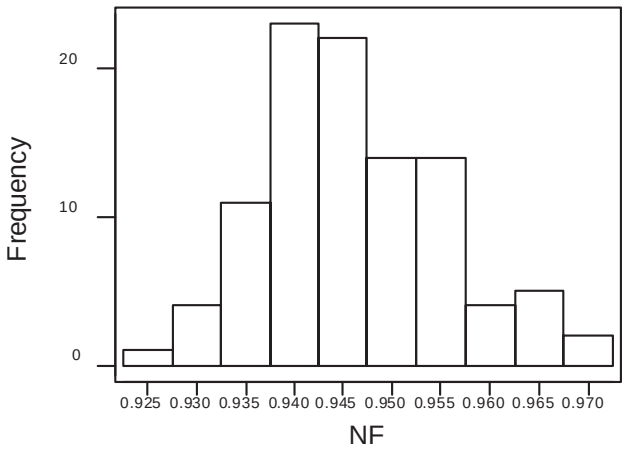

Figure 6.6: Statistical distribution of the model for NF, which is calculated by the sensitivity analysis and using the full 2^{nd} order response surface model by varying VB1.

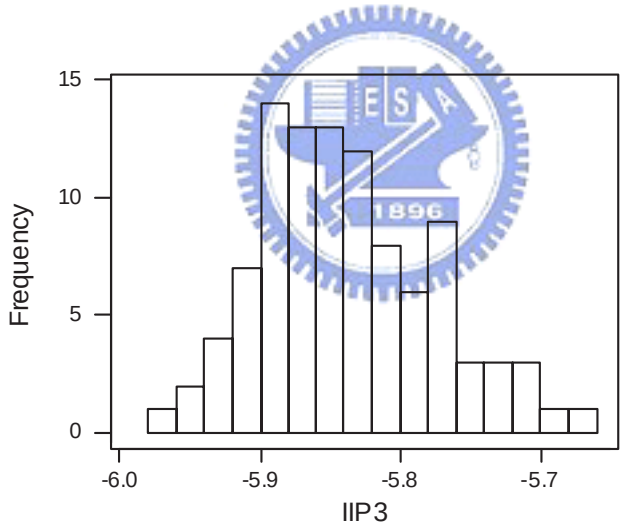

Figure 6.7: Statistical distribution of the model for IIP3, which is calculated by the sensitivity analysis and using the full 2^{nd} order response surface model by varying VB1.

6.2 Summary

In this chapter, the sensitivity analyses obtained from the case that satisfied all specifications with the largest D have been discussed. We calculate the fluctuations of the LNA circuit performance which is varied by 1 % VB1 and by 1 % 10 factors for the LNA circuit as an example. The recipe which we take is stable for studying the LNA circuit performance. In the next chapter, we will further discuss the sensitivity analysis of static noise margin of 6T and 4T SRAM cells.

Chapter 7

Application to Static Random Access Memory Cell

In this chapter, we firstly introduce 6T and 4T static random access memory (SRAM) cells with 65 nm MOSFETs in Sec. 7.1. The results of design of experiment will be discussed in Sec. 7.2. We will perform the sensitivity analysis of the static noise margin (SNM) of the sram cell by constructing the full 2^{nd} order response surface models in Sec. 7.3.

7.1 The 6T SRAM Cells

Figure 7.1 shows a typical static memory cell in CMOS technology. The MOSFETs used in our SRAM cells are with 65 nm devices. The SPICE model cards are from semiconductor

foundry directly. The circuit is a flip-flop comprising two cross-coupled inverters and two access transistors, M3 and M6. The flip-flop consists of two load elements (M4, M5) called pull-up (load) transistors and two storage elements (M1, M2) called pull-down (driver) transistors. Data are stored as voltage levels with the two sides of the flip-flop in opposite voltage configurations, that is, node Q is high and node QB is low in one state and node Q is low and node QB is high in the other resulting in two stable states. The access transistors are turned on when the world line is selected and its voltage raised to VDD, and they connect flip-flop to the column (bit or BL) line and column (bit or BLB) line. Note that both the BL and BLB lines are utilized.

Consider a first read operation, and assume that the cell is storage a ”1”. In this case, Q will be high at VDD, and QB will be low at 0 V. Before beginning of the read operation, the BL and BLB lines are precharged to a high voltage, usually VDD. (The circuit for precharging will be conjunct with the sensing amplifier.) When the word line is selected, and M3 and M6 are turned on, we see that current will flow from VDD through M4 and M6 and onto line BLB, charging the capacitance of line BLB. On the other side of the circuit, current will flow from the precharged BL line through M3 and M2 to ground [47].

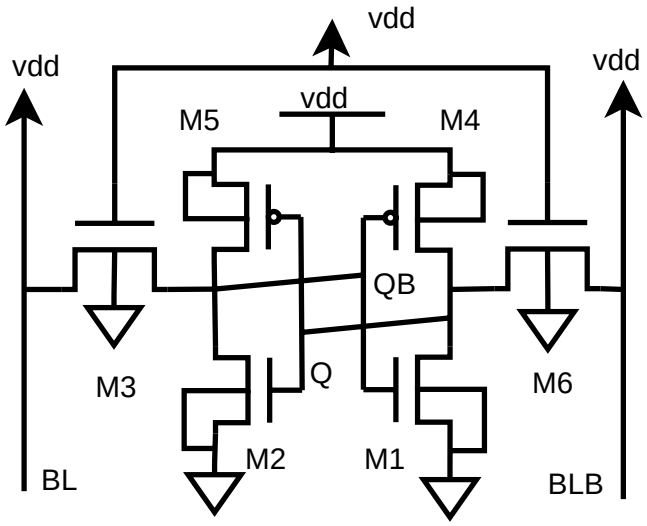

Figure 7.1: A circuit of 6T SRAM cell used in our circuit simulation.

7.2 The 4T SRAM Cells

Figure 7.2 shows a typical static memory cell in CMOS technology. Two storage elements (M1, M2) called pull-down (driver) transistors and two access transistors, M3 and M6 are included. Consider a first read operation, and assume that the cell is storage a ”1”. In this case, Q will be high at VDD, and QB will be low at 0 V. Before beginning of the read operation, the BL and BLB lines are precharged to an high voltage, usually VDD. When the word line is selected and M3 and M4 are turned on, we see that current will flow from the precharged BL line through M4 and M2 to ground.

We consider static noise margin (SNM) during hold and real modes in detail. The cell

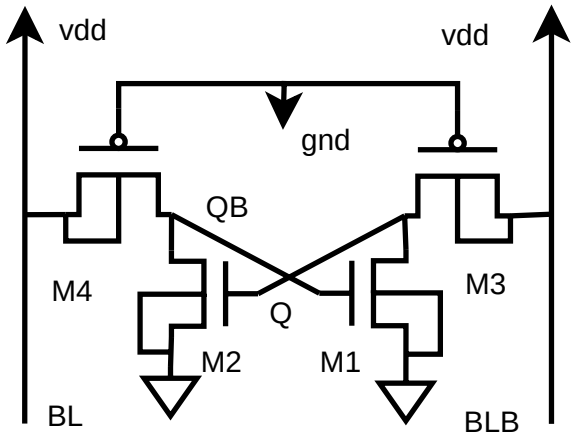

Figure 7.2: A circuit of 4T SRAM cell used in our circuit simulation.

stability is based on the ability of the cell to resist accidental overwrites during different operating conditions in the presence of electrical noise and process variations. The factors that influence the cell stability include the device sizing (channel widths and lengths), the supply voltage, and temperature [47].

7.3 The DOE of 6T and 4T SRAM Cells

Construction of the response surface model for the 6T and 4T SRAM cells use the 25-runs with face centered cube (CCF) design which consist of one center point, 8 axial points, and 2^4 cube points. The levels of CCF design for each factor are shown in Tab. 7.1.

Table 7.1: The levels of each factor for 6T and 4T SRAM cells .

Factor name	level -1	Level 0	level 1
L_1: channel length of the transistor M1 (nm)	60	65	70
L_2: channel length of the transistor M2 (nm)	60	65	70
L_3: channel length of the other transistors (nm)	60	65	70
VDD: supply voltage (V)	1.08	1.2	1.38

7.3.1 The Response Surface Model for 6T and 4T SRAM Cells

The full 2^{nd} order response surface models of 6T and 4T SRAM cells are shown in below with coded factors, where the unit of SNM is mV.

$$\begin{aligned} SNM(6T) = {} & 168.02 + 8.63L_1 - 4.55L_2 + 8.23L_3 + 5.28VDD \\ & - 1.49L_1^2 + 0.38L_2^2 - 0.82L_3^2 - 1.70VDD^2 \\ & - 0.011L_1L_2 + 0.052L_1L_3 + 1.075L_1VDD + 0.086L_2L_3 \\ & - 0.96L_2VDD + 0.70L_3VDD, \end{aligned} \tag{7.1}$$

$$\begin{aligned} SNM(4T) = {} & 170.03 + 6.23L_1 - 9.86L_2 + 10.54L_3 + 17.39VDD \\ & - 1.09L_1^2 + 0.69L_2^2 - 0.72L_3^2 - 1.24VDD^2 \\ & - 0.087L_1L_2 + 0.026L_1L_3 + 1.12L_1VDD + 0.31L_2L_3 \\ & - 1.25L_2VDD + 2.24L_3VDD, \end{aligned} \tag{7.2}$$

Table 7.2: The calculated results of SNM response surface model for the 6T and 4T SRAM cells using CCF design.

Response	R^2	Adj. R^2	Std. Dev.
SNM (6T)	0.9997	0.9993	0.097
SNM (4T)	0.9995	0.9998	0.22

where L_1 is the channel length of the M1 transistor, L_2 is the channel length of the M2 transistor, L_3 is the channel length of the M3, M4, M5, and M6 transistors for 6T SRAM cell and is the channel length of the M3 and M4 transistors for 4T SRAM cell, and VDD is the supply voltage. Table 7.2 is the information of the SNM response surface models for 6T and 4T SRAM cells using CCF design. We can observe that R-square of two models are high, and the model explanation is good. Figure 7.3 shows the trend of SNM for 6T and 4T SRAM cells which we vary L_1 and L_2. In our observation, the SNM of 4T SRAM cell is higher than 6T SRAM cell in some conditions but also lower than 6T SRAM cell in other conditions. Therefor, the range of variation of the 4T SRAM cell is larger than the 6T SRAM cell.

7.3.2 Model Adequacy Checking for 6T and 4T SRAM Cells

The residual normal probability plots and scatter plots of the SNM response for 6T and 4T SRAM cells are shown in Fig. 7.4. The results show that the model assumption is satisfied.

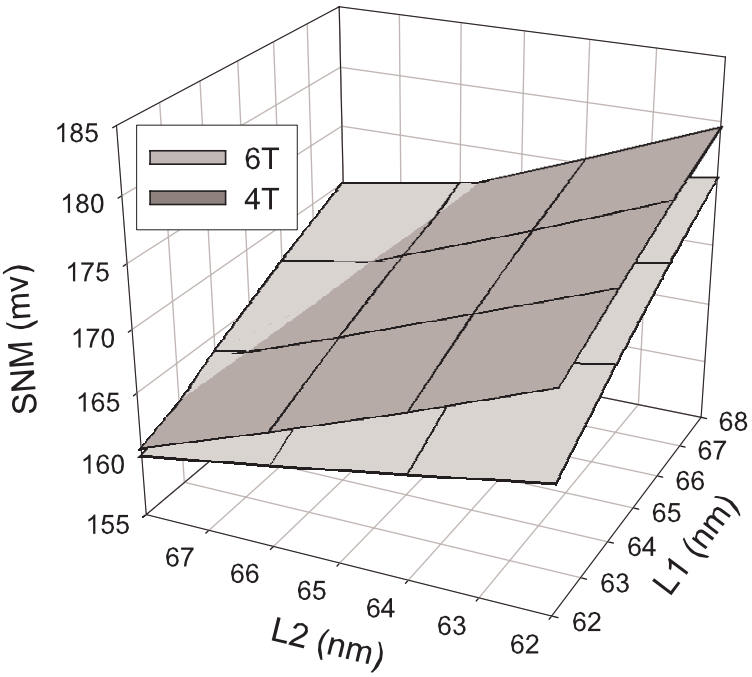

Figure 7.3: A 3D plot of SNM for 6T and 4T SRAM cells with respect to L_1 and L_2.

7.3.3 Accuracy Verification for 6T and 4T SRAM Cells

The results calculated from the response surface model and values obtained from circuit simulator are shown in Tab. 7.3. Scatter plots of values calculated from the response surface models versus the values obtained from circuit simulator for 6T and 4T SRAM cells are shown in Fig. 7.5, respectively. The results show that they are highly linear relationship.

Table 7.3: Accuracy verification of the response values calculated from the response surface model and obtained from circuit simulator for 6T and 4T SRAM cells.

Values calculated from the response surface models	6T SNM	4T SNM	Values calculated from circuit simulator	6T SNM	4T SNM
Mean (mV)	168.34	169.68	Mean (mV)	168.35	169.69
Std. Dev.	7.42	15.40	Std. Dev.	7.39	15.43

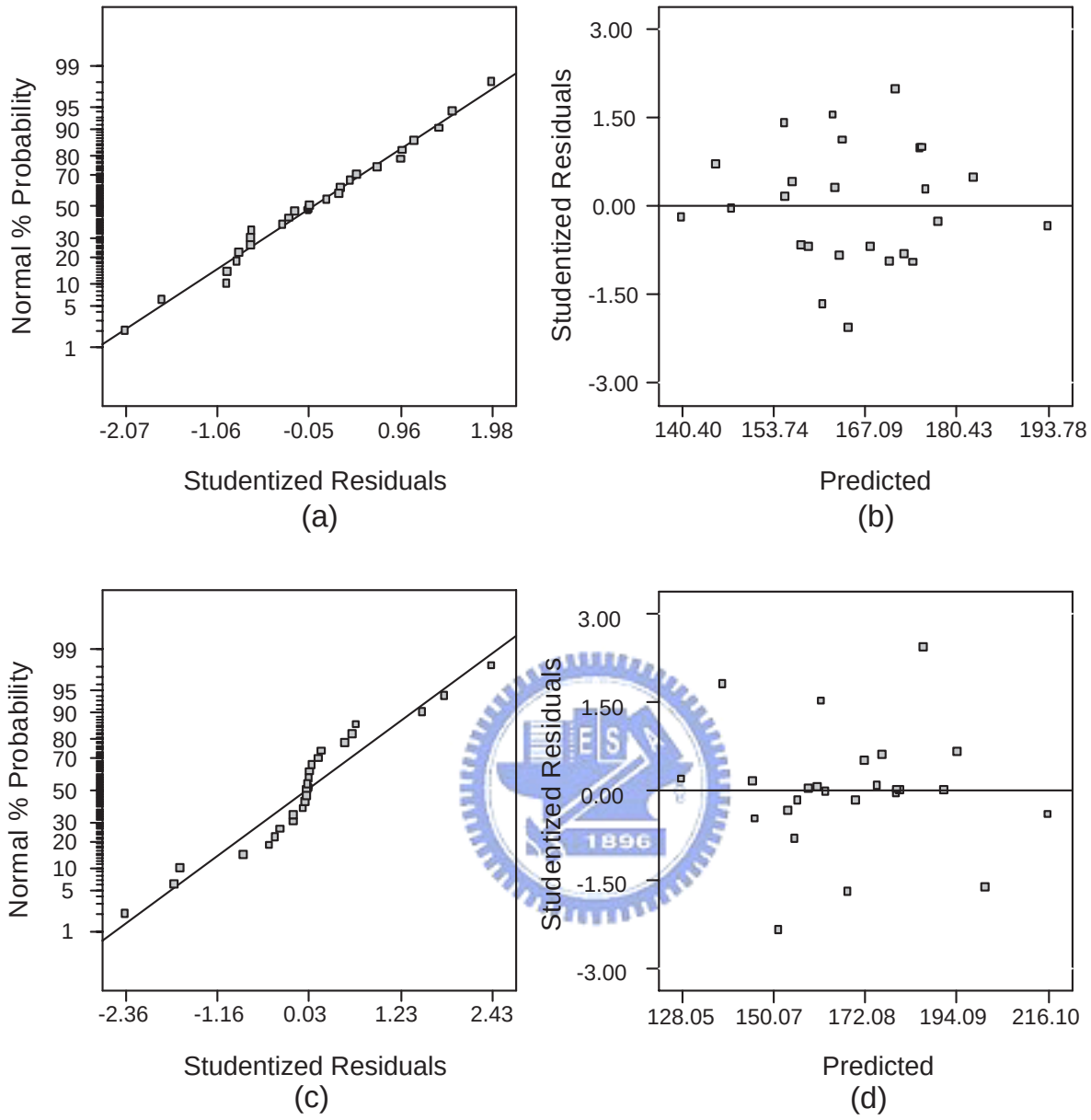

Figure 7.4: A model adequacy checking (a) the residual normal probability plot of SNM for 6T SRAM cell, (b) the residual scatter plot of SNM for 6T SRAM cell, (c) the residual normal probability plot of SNM for 4T SRAM cell, and (d) the residual scatter plot of SNM for 4T SRAM cell.

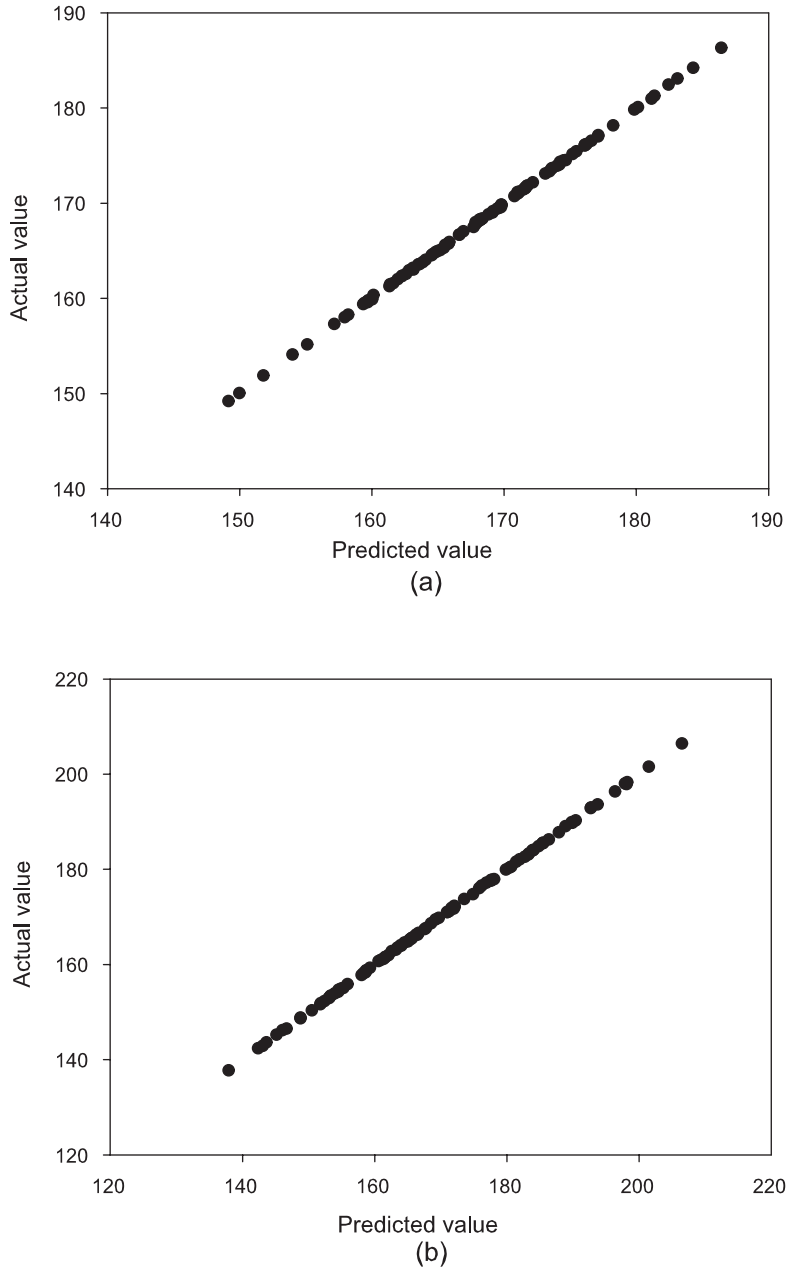

Figure 7.5: A scatter plot calculated from the response surface model versus values obtained from the circuit simulator. (a) 6T SRAM cell and (b) 4T SRAM cell. The results have highly linear relationship.

7.4 The Sensitivity Analysis for 6T and 4T SRAM Cells

We explore the sensitivity of SNM versus the channel length and the supply voltage for 6T and 4T SRAM cells. The sensitivity analysis is performed by assuming a normal distribution for each nominal value. The mean of $L_1, L_2, and L_3$ is set to be their nominal values 65 nm and VDD is equal to its nominal value 1.2 V. The standard deviation is 3.3 % of each nominal value. And we generate 500 normally and independently distributed pseudo-random numbers for four parameters. The variation of SNM we obtained is calculated by the response surface models for 6T and 4T SRAM cells. Figure 7.6 and Tab. 7.4 show the sensitivity analysis of SNM for 6T and 4T SRAM cells, and comparison between 4T SRAM cell and 6T SRAM cell. The results show the standard deviation of 6T SRAM cell is smaller than that of 4T SRAM cell. However in the test condition, we take 170 mV as nominal value and 3.3 % of 170 mV (5.61 mV) as 1-standard deviation. The result shows that 2 % variation of SNM is out of 3-standard deviation for the 6T SRAM cell. It is half of 4T SRAM cell (4.2 %). Thus, the comparison of sensitivity of 6T and 4T SRAM cells shows that 6T SRAM cell is more stable than 4T SRAM cell with 65 nm CMOS devices.

Table 7.4: Comparison of the sensitivity of the SNM for 6T SRAM cell between the sensitivity of the SNM for 4T SRAM cell. The mean of $L_1, L_2, and L_3$ is set to be its nominal values 65 nm, respectively; and VDD is set to be its nominal value 1.2 V. The standard deviation is 3.3 % for each nominal value. We generate 500 normally and independently distributed pseudo-random numbers for these four parameters.

	Mean	Std. Dev.
6T SNM	167.11	6.172
4T SNM	169.07	9.178

7.5 Summary

In this chapter, the full 2^{nd} order response surface models of 6T and 4T SRAM cells are shown in Eqs. 7.1 and 7.2. The residual normal probability plots and scatter plots of the SNM response are shown in Fig. 7.4. Then we generate 100 random numbers for each factor with *uniform(-1, 1)* distribution to verify the accuracy of the SNM response surface models for 6T and 4T SRAM cells within our high and low level settings. The results have highly linear relationship. And the results of CCF design are deemed adequate for the sensitivity analysis, and 4T SRAM cell is more sensitive than 6T SRAM cell. In the last chapter, we draw conclusions and suggest some issues for a future work.

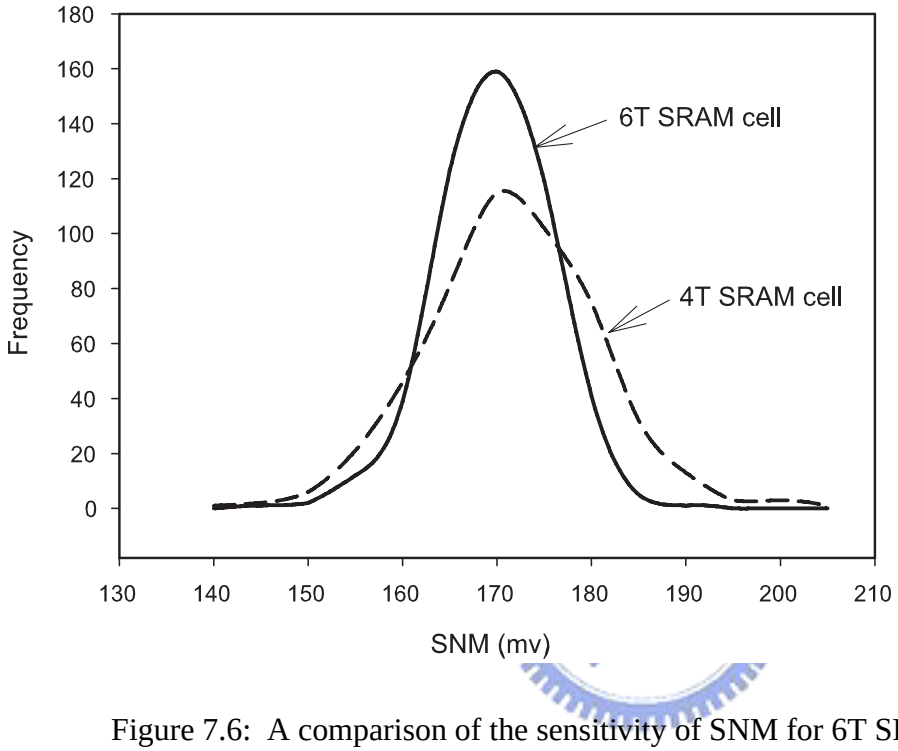

Figure 7.6: A comparison of the sensitivity of SNM for 6T SRAM cell and the sensitivity of SNM for 4T SRAM cell. The mean of $L_1, L_2, and L_3$ is set to be their nominal values 65 nm and VDD is equal to its nominal value 1.2 V. The standard deviation is 3.3 % of each nominal value. 4T SRAM cell shows more sensitive than 6T SRAM cell.

Chapter 8

Conclusions and Future Work

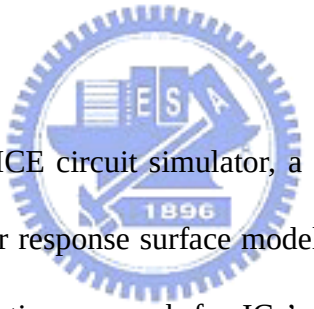

In this thesis, based upon SPICE circuit simulator, a screen design, a central composite design (CCD), and a 2^{nd} order response surface model (RSM). We have successfully developed a computational statistics approach for ICs' design optimization and sensitivity analysis. Two different circuits are explored. one is LNA circuit with 0.25um MOSFETs and the other is SRAM cells with 65 nm CMOS devices. The results of design of experiment which contain screening design, central composite design, construction of response surface model, model checking and accuracy verification were shown in Chap. 4. The three optimized cases which satisfy all specifications, minimize the noise figure, and maximize the voltage gain were provided in Chap. 5. Next the outcomes of the circuit sensitivity

analysis have been shown in Chap. 6. In the process of sensitivity analysis, the input factors have been assumed to be normally distributed about their mean. The standard deviation for each factor have been set as a percentage of its mean values. We note that the results were acceptable. The results presented in this work are promising in IC design. The 4T and 6T SRAM cells were also explored by using this methodology and the sensitivity analysis was successfully analyzed in Chap. 7.

8.1 Conclusions

Taking a low noise amplifier circuit with 0.25 μm MOSFETs as an example, we have stated the computational statistic algorithm. The circuit specification to be optimized includes (1) the input return loss $<$ -10 dB, (2) the output return loss $<$ -10 dB, (3) reverse isolation $<$ -25 dB, (4) voltage gain is as great as possible, (5) stability factor $>$ 1, (6) noise figure $<$ 2 dB, and (7) the third-order-intercept point $>$ -10 dB. To achieve the aforementioned seven circuit specifications, out-calling circuit simulator to obtain circuit performance was performed and then ten significant results among thirteen parameters were selected from the screening design. They were the Cmatch1, Cmatch2, Cmatch3, Ldeg, Lmatch1, L1, W1, VB1, VB2, and VDD. By simultaneously running circuit simulator, a ten-parameter face centered cube design was then performed in the step of central composite design. We used the 149 simulation which results in constructing the corresponding 2^{nd} order response

surface models for the seven circuit specification.With the 2^{nd} order RSM equations, design optimization and sensitivity analysis of performance have been explored. For the design optimization, we have obtained the improvement results in the LNA cirduit. For example, the input return loss in the original performance was -8.756 dB and it was too large. The output return loss of the original circuit performance -6.137dB was too large. Through our method, the input return loss of the circuit performance has been reduced and is smaller than -10 dB. The improved output return loss is smaller than -10 dB at the same time. Performance sensitivity with respect to certain optimized parameter and/or all parameters were also investigated by using RSM to an optimized recipe with 100 randomly generated normal samples. The optimized recipe was right the mean of the normal distribution; and one per centum of the optimized recipe was assumed to be the standard deviation. Our result has showed that the optimized recipe was stable to the circuit performance.

Similar methodology was further applied to explore the variation of static noise margin (SNM) for 6T and 4T SRAM cells with respect to channel length and supply voltage. For SRAM with 65 nm CMOS devices, our result has showed that 2 % variation of SNM was out of 3-sigma for the 6T SRAM cell with 3-sigma variation of parameters. It was half of 4T SRAM cell (4.2 %). Thus, it quantitatively confirmed that SRAM with 6T configuration was more stable than it with 4T configuration.

In conclusion, we have implemented systematically a computational statistics approach

to ICs' design optimization and sensitivity analysis. Successful application of the method to study analog and digital circuits has showed its computational efficiency and engineering accuracy, compared with large-scale SPICE circuit simulations. This approach was suitable for optimization problems and diagnosis of quantify trade-offs in IC industry.

8.2 Suggestions to Future Work

The result of Sec. 4.2 shows we run at least three experiments in order to achieve target. But it may not be an effective way to solve the problem when the target is far from the original performance with multiple responses. This is a demerit which restricts our optimization. In future work, one could develop a method which can solve the condition of target is far from the original performance. Thus, more problems will be solve efficiently. Furthermore, we can also apply the small composite designs to obtain the whole data if we want to design other complicated circuits to save more CPU time and computing cost. In addition, the recipes obtained by this work could be used to fabricate chips to compare with the results of simulation.

Application of the systematically statistical method can be extended to more RF, analog, and digital ICs, such as: (1) the operation amplifier; (2) the phase locked loop circuit; (3) the digital to analog converter; (4) the analog to digital converter and; and (5) other novel device architectures of SRAM cells.

Bibliography

[1] M. S. Phadke, *Quality Engineering Using Robust Design*, AT&T Bell Laboratories, 1989.

[2] C. K. Chen, *A Genetic Algorithm for Deep-Submicron MOSFET Parameters Extraction and Simulation*, National Chiao-Tung University, Master's thesis, Jun. 2002.

[3] Y. Li, Y. Y. Cho, C. S. Wang, and K. Y. Huang, *A Genetic Algorithm Approach to InGaP/GaAs HBT Parameters Extraction and RF Characterization*, Japanese Journal of Applied Physics, Vol. 42,pp. 2371-2374, Apr. 2003.

[4] Y. Y. Cho, *An Intelligent Hybrid Approach to Optimal Characterization of Nanoscale MOSFET Devices*, National Chiao Tung University, Master thesis, 2003. 6.

[5] Y. Li and S. M. Yu, *An Automatic Parameter Extraction Technique for Deep- Submicron and Nanoscale VLSI Devices Using Genetic Algorithm*, accepted for publication in Microelectronic Engineering.

[6] Y. Li, and S. M. Yu, *A Novel Approach to Compact Model Parameter Extraction for Excimer Laser Annealed Complementary Thin Film Transistors*, accepted for publication in Journal of Computational Electronics.

[7] H. M. Chou and Y. Li, *Three-Dimensional Simulation of Nanoscale Copper Interconnects*, , Accepted by 2005 IEEE Nanotechnology Conference (IEEE-NANO 2005), Nagoya Congress Center, Nagoya, Japan, pp. 11-15, Jul. 2005.

[8] Y. Li, H. M. Chou, J. W. Lee, and B. S. Lee, *A Three-Dimensional Simulation of Electrostatic Characteristics for Carbon Nanotube Array Field Effect Transistors*, accepted for publication in Microelectronic Engineering.

[9] B. R. S. Rodrigues and M. A. Styblinski, *Adaptive hierarchical multi-objective fuzzy optimization for circuit design*, Circuits and Systems, ISCAS, IEEE International Symposium: 1813 - 1816, May 1993.

[10] A. N. Lokanathan and J. B. Brockman, *A methodology for concurrent processcircuit optimization*, Computer-Aided Design of Integrated Circuits and Systems, IEEE Transactions on Volume 18, Issue 7, pp. 889 - 902, Jul. 1999.

[11] S. Liao, "*Microwave Circuit Analysis and Amplifier Design*," Prentice-Hall, pp. 123-160, 1988.

[12] G. Gonzalez, "*Microwave Transistor Amplifiers*," Prentice-Hall, pp. 139-193, 1984.

[13] N. Dye,H. Granberg, *"Radio Frequency Transistors Principles and Practical Applications,"* Butterworth- Heinemann, pp.204-231, 1993.

[14] N. Metropolis, A. Rosenbluth, and M. Rosenbluth, J. Chem. Phys., vol. 21, p. 1087, 1953.

[15] S. Kirkpatrick, C.D. Gelatt ,and M.P. Vecchi,,"*Optimization by Simulated Annealing,*"Science, vol.220,pp.671-680, 13 May 1983.

[16] Nobuo Yamashita, Masao Fukushima, *"On the rate of convergence of the Levenberg-Marquardt method"*, Comput. Suppl., 15, pp. 239-249, Springer, Vienna, 2001.

[17] Jian-zhong Zhang, L. H. Chen, *"Nonmonotone Levenberg-Marquardt algorithms and their convergence analysis"*, J. Optim. Theory Appl., 92(2), pp. 393-418, 1997.

[18] Qiao Ming Han, *"A Levenberg-Marquardt method for semidefinite programming*", J. Numer. Methods Comput. Appl., 19(2), pp. 99-106, 1998.

[19] Ralf Salomon, *"Evolutionary algorithms and gradient search: similarities and differences*", IEEE Transactions on Evolutionary Computation, 2(2), pp. 45-55, Jul, 1998.

[20] Helen G. Cobb, *"An investigation into the use of hypermutation as an adaptive operator in genetic algorithms having continuous, time-dependent nonstationary environments*", NRL Memorandum Report 6760, 1990.

[21] Kenneth A. De Jong, "*The analysis and behavior of a class of genetic adaptive systems*", University of Michigan, Ph.D. Thesis, 1975.

[22] Rainer Hackl and Ingo Morgenstern, "*Rapid Close-ro-Optimum Optimization by Genetic Algorithms*", International Journal of Modern Physics C, 8(5), pp. 1103-1117, 1997.

[23] Gary G. Yen and Nethrie Nithianandan, "*Automatic Facial Feature Extraction Using Edge Distribution and Genetic Search*", International Journal of Computational Intelligence and Applications, 3(1), pp. 89-100, 2003.

[24] Thomas Dandekar, Patrick Argos, "*Potential of genetic algorithms in protein folding and protein engineering simulations*", Protein Engineering, 5, pp. 637-645, 1992.

[25] Christine L Valenzuela, Pearl Y Wang, "*VLSI placement and area optimization using a genetic algorithm to breed normalized postfix expressions*", IEEE Transactions on Evolutionary Computation, 6(4), pp. 390-401. Aug, 2002.

[26] Benedetto Buttitta, Paolo Orlando, Filippo Sorbello, Giorgio Vassallo, "*Monreale: a new genetic algorithm for the solution of the channel routing problem*", 5th Annual European Computer Conference. Proceedings - Advanced Computer Technology, Reliable Systems and Applications, pp.462 -466, May, 1991.

[27] Roberto Menozzi, M. Borgarino, J. Tasselli, and A. Marty, "*HBT small-signal model extraction using a genetic algorithm*", Proc. 20th Annual IEEE GaAs IC Symposium, Atlanta, USA, November, pp.157-160, 1998.

[28] Chris Stergiou, "*What is a Neural Network?*".

[29] M. Sugawara, "*Numerical solution of the Schrödinger equation by neural network and genetic algorithm*", Computer Physics Communications, 140, pp. 366-380, 2001.

[30] Terrence J. Sejnowski and Charles R. Rosenberg, "*NETtalk: a parallel network that learns to read aloud*", The John Hopkins University Electrical Engineering and Computer Science Technical Repoert, JHU/EECS-86/01, 32 pp.

[31] Issac Elias Lagaris, Aristidis C. Likas, Dimitrios G. Papageorgiou, "Neural-Network Methods for Boundary Value Problems with Irregular Boundaries", IEEE transactions on Neural Networks, 11(5), 2000.

[32] Dimitris G. Triantafyllidis and Dimitris P. Labridis, "*A Finite-Element Mesh Generator Based on Growing Neural Networks*", IEEE transactions on Neural Networks, 13(6), 2002.

[33] Pekka Ojala, Jukka Saarinen, and Kimmo Kaski, "*Neurodevice-Neural Network Device Modelling Interface for VLSI Design*", Proceedings of the 1994 IEEE Workshop Neural Networks for Signal Processing IV, pp. 641-650, 1994.

[34] Eliasi, R., Elperin, T., and BarCohen, A., "*Monte Carlo thermal optimization of populated printed circuit board*", Thermal Phenomena in Electronic Systems, 1990. I-THERM II., InterSociety Conference on 23-25 pp. 74-84, 1990.

[35] Mateos, J., Gonzalez, T., Pardo, D., Hoel, V., and Cappy, A., "*Monte Carlo simulator for the design optimization of low-noise HEMTs*", Electron Devices, IEEE Transactions on Volume 47, Issue 10, pp. 1950 - 1956, 2000.

[36] *Engineering Statistics Handbook* [Online]. Available: http://www.itl.nist.gov/div898/handbook/

[37] C. F. J. Wu and M. Hamada, *Experiments: Planning, Analysis, and Parameter Design Optimization*, New York: John Wiley & Sons, Inc., 2000.

[38] R. H. Myers and D. C. Montgomery, *Response Surface Methodology: Process and Product Optimization Using Designed Experiments*, New York: John Wiley & Sons, Inc., 2002.

[39] Ying Shao Chou, *A Novel Statistical Methodology for Sub-100nm MOSFET Fabrication Optimization and Sensitivity Analysis*, A Thesis Submitted to the Department of Statistics National Chiao Tung University in partial Fulfillment of the Requirements for the Degree of Master in Statistics July 2005 Hsinchu, Taiwan.

[40] C. Daniel, Use of Half-normal Plots in Interpreting Factorial Two-level Experiments, *Technometrics*, Vol. 1, 1959, pp. 311-341.

[41] G. E. P. Box and Norman R. Draper, *Empirical Model-Building and Response Surfaces* , New York, Wiley, 1987.

[42] J. H. Dodgson, A Graphical Method for Assessing Mean Squares in Saturated Fractional Designs, *Journal of quality technology*, Apr. 2003, Vol. 35, No. 2, pp. 206-212.

[43] D. C. Montgomery, *Design and Analysis of Experiments*, New York: John Wiley & Sons, Inc., 1997.

[44] Carroll, J.and Kai Chang, *Statistical computer-aided design for microwave circuits*, Microwave Theory and Techniques, IEEE Transactions on Volume 44, Issue 1, Jan. 1996 Page(s):24 - 32 Digital Object Identifier 10.1109/22.481381

[45] J. S. Ramberg, S. M. Sanchez, P. J. Sanchez, and L. J. Hollick, *Designing simulation experiments: Taguchi methods and response surface metamodels*, in Proc. Winter Simulation Conference, 1991, pp.167-176.

[46] *Quality Engineering Seminar, Software, and Consulting* [Online]. Available: http://nutek-us.com/index.html

[47] E. Seevinck, F. J. List, and J. Lohstoh, Static-Noise Margin Analysis of MOS SRAM Cells, *IEEE J. Solid-state circuits*, vol. 22, no. 5, 1987, pp. 748-754.

Appendix A

Contour Plots of the Optimal Recipe for the CCF Design

In this appendix the completed contour plots of the optimal recipe for the case of satisfied all specifications have provided here.

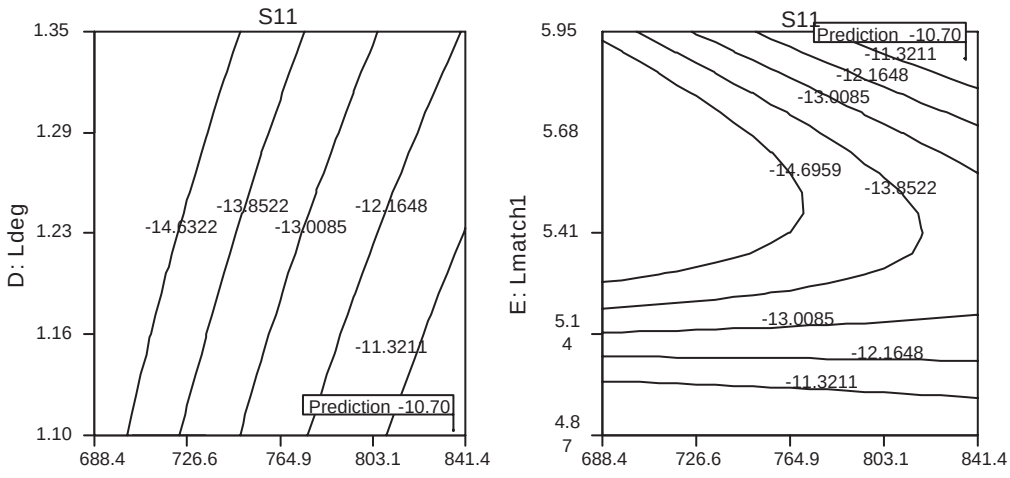
S11
D: Ldeg
A: Cmatch1
-14.6322
-13.8522
-13.0085
-12.1648
-11.3211
Prediction -10.70
1.35
1.29
1.23
1.16
1.10
688.4
726.6
764.9
803.1
841.4

S11
Prediction -10.70
E: Lmatch1
A: Cmatch1
-11.3211
-12.1648
-13.0085
-14.6959
-13.8522
-13.0085
-12.1648
-11.3211
5.95
5.68
5.41
5.14
4.87
688.4
726.6
764.9
803.1
841.4

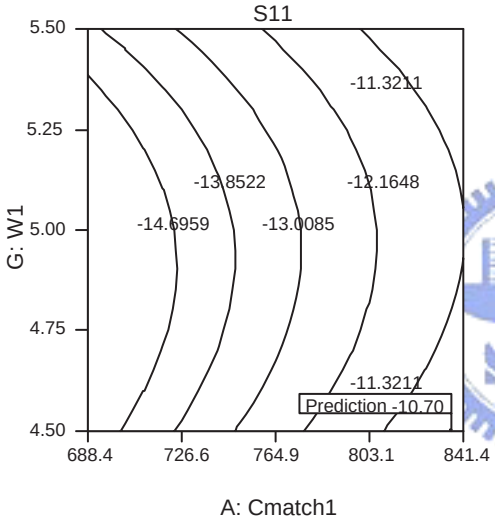
S11
G: W1
A: Cmatch1
-11.3211
-13.8522
-12.1648
-14.6959
-13.0085
-11.3211
Prediction -10.70
5.50
5.25
5.00
4.75
4.50
688.4
726.6
764.9
803.1
841.4

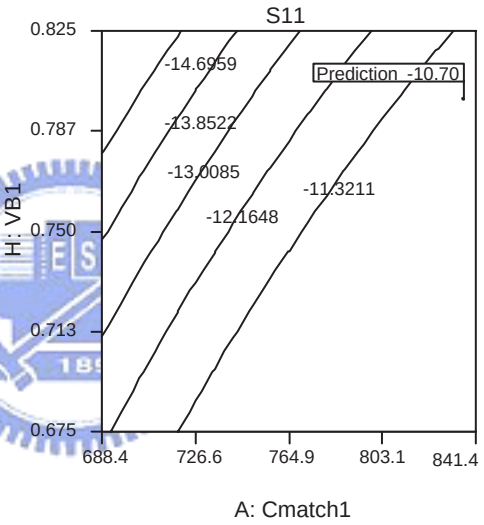
S11
H : VB1
A: Cmatch1
-14.6959
-13.8522
-13.0085
-12.1648
-11.3211
Prediction -10.70
0.825
0.787
0.750
0.713
0.675
688.4
726.6
764.9
803.1
841.4

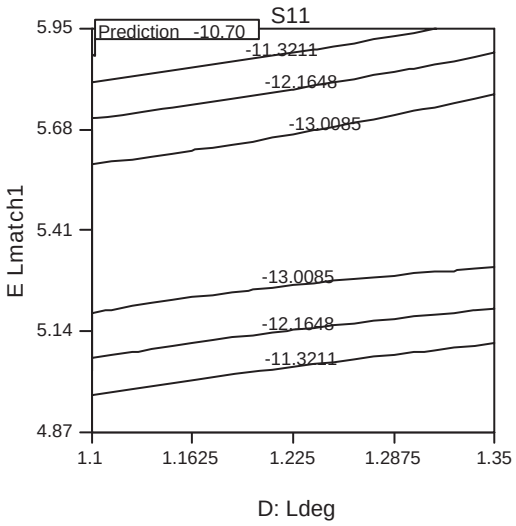
S11
Prediction -10.70
E Lmatch1
D: Ldeg
-11.3211
-12.1648
-13.0085
-13.0085
-12.1648
-11.3211
5.95
5.68
5.41
5.14
4.87
1.1
1.1625
1.225
1.2875
1.35

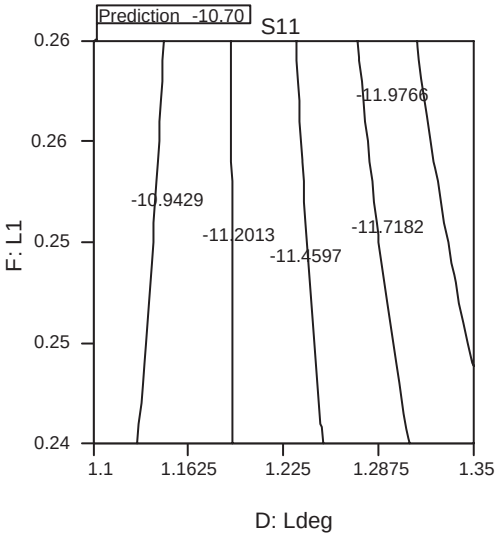
Prediction -10.70
S11
F: L1
D: Ldeg
-11.9766
-10.9429
-11.2013
-11.7182
-11.4597
0.26
0.26
0.25
0.25
0.24
1.1
1.1625
1.225
1.2875
1.35

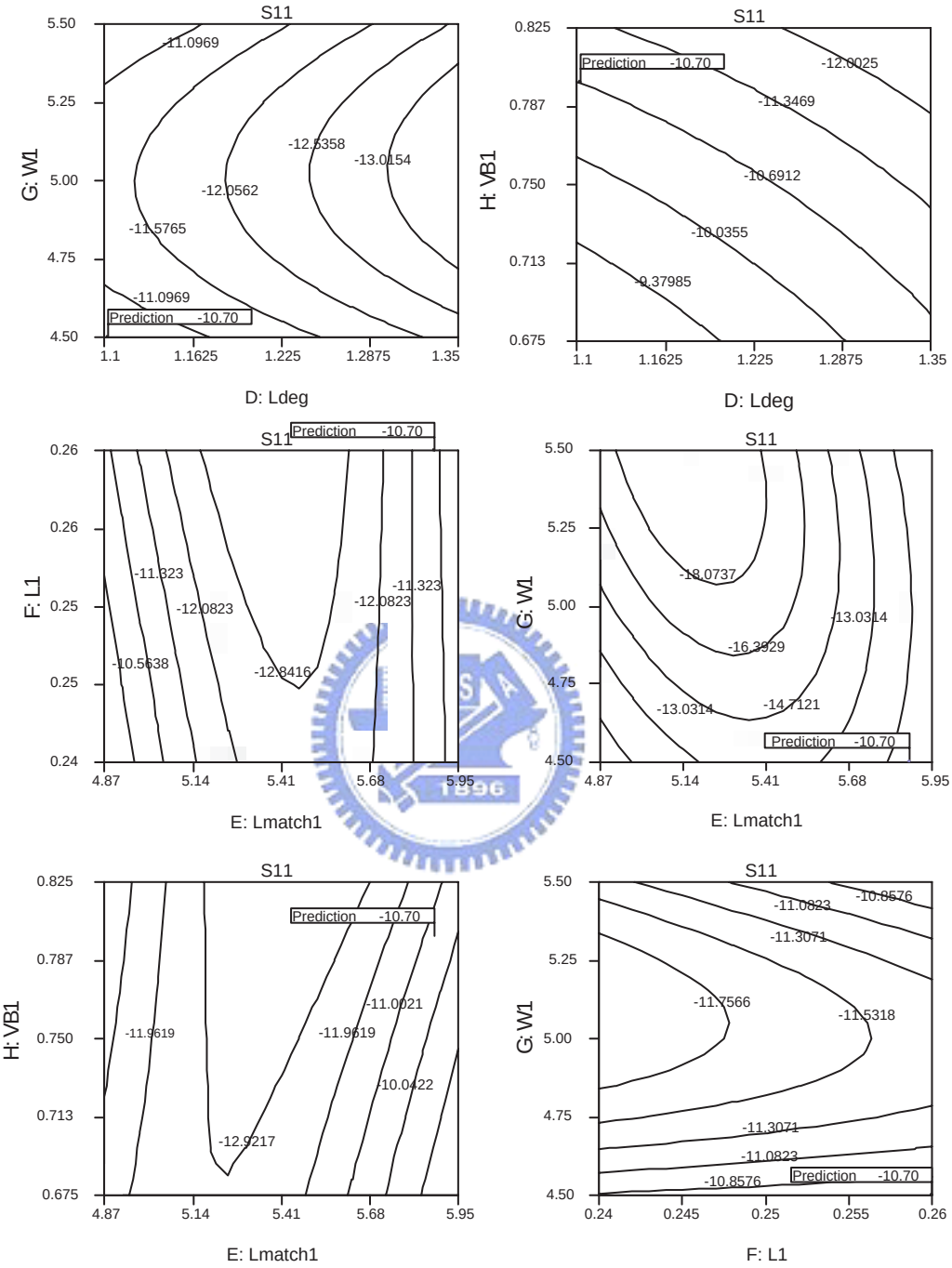
S11
G: W1
D: Ldeg
-11.0969
-12.5358
-13.0154
-12.0562
-11.5765
-11.0969
Prediction -10.70
S11
H: VB1
D: Ldeg
Prediction -10.70
-12.9025
-11.3469
-10.6912
-10.0355
-9.37985
S11
F: L1
E: Lmatch1
Prediction -10.70
-11.323
-12.0823
-11.323
-12.0823
-10.5638
-12.8416
S11
G: W1
E: Lmatch1
-18.0737
-13.0314
-16.3929
-13.0314
-14.7121
Prediction -10.70
S11
H: VB1
E: Lmatch1
Prediction -10.70
-11.9619
-11.0021
-11.9619
-10.0422
-12.9217
S11
G: W1
F: L1
-10.8576
-11.0823
-11.3071
-11.7566
-11.5318
-11.3071
-11.0823
-10.8576
Prediction -10.70

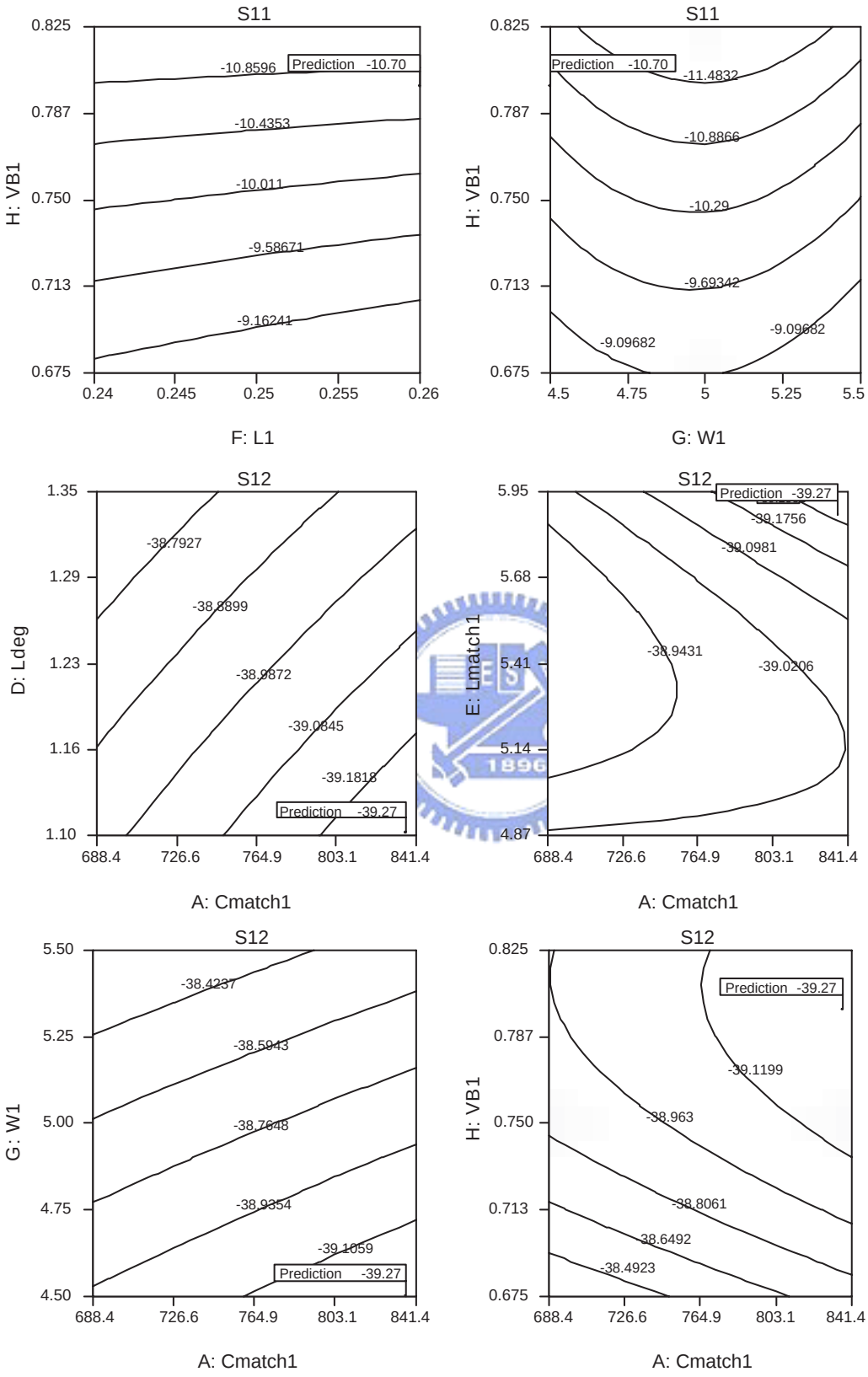
S11
Prediction -10.70
-10.8596
-10.4353
-10.011
-9.58671
-9.16241
H: VB1
F: L1
S11
Prediction -10.70
-11.4832
-10.8866
-10.29
-9.69342
-9.09682
-9.09682
H: VB1
G: W1
S12
-38.7927
-38.8899
-38.9872
-39.0845
-39.1818
Prediction -39.27
D: Ldeg
A: Cmatch1
S12
Prediction -39.27
-39.1756
-39.0981
-38.9431
-39.0206
E: Lmatch1
A: Cmatch1
S12
-38.4237
-38.5943
-38.7648
-38.9354
-39.1059
Prediction -39.27
G: W1
A: Cmatch1
S12
Prediction -39.27
-39.1199
-38.963
-38.8061
38.6492
-38.4923
H: VB1
A: Cmatch1

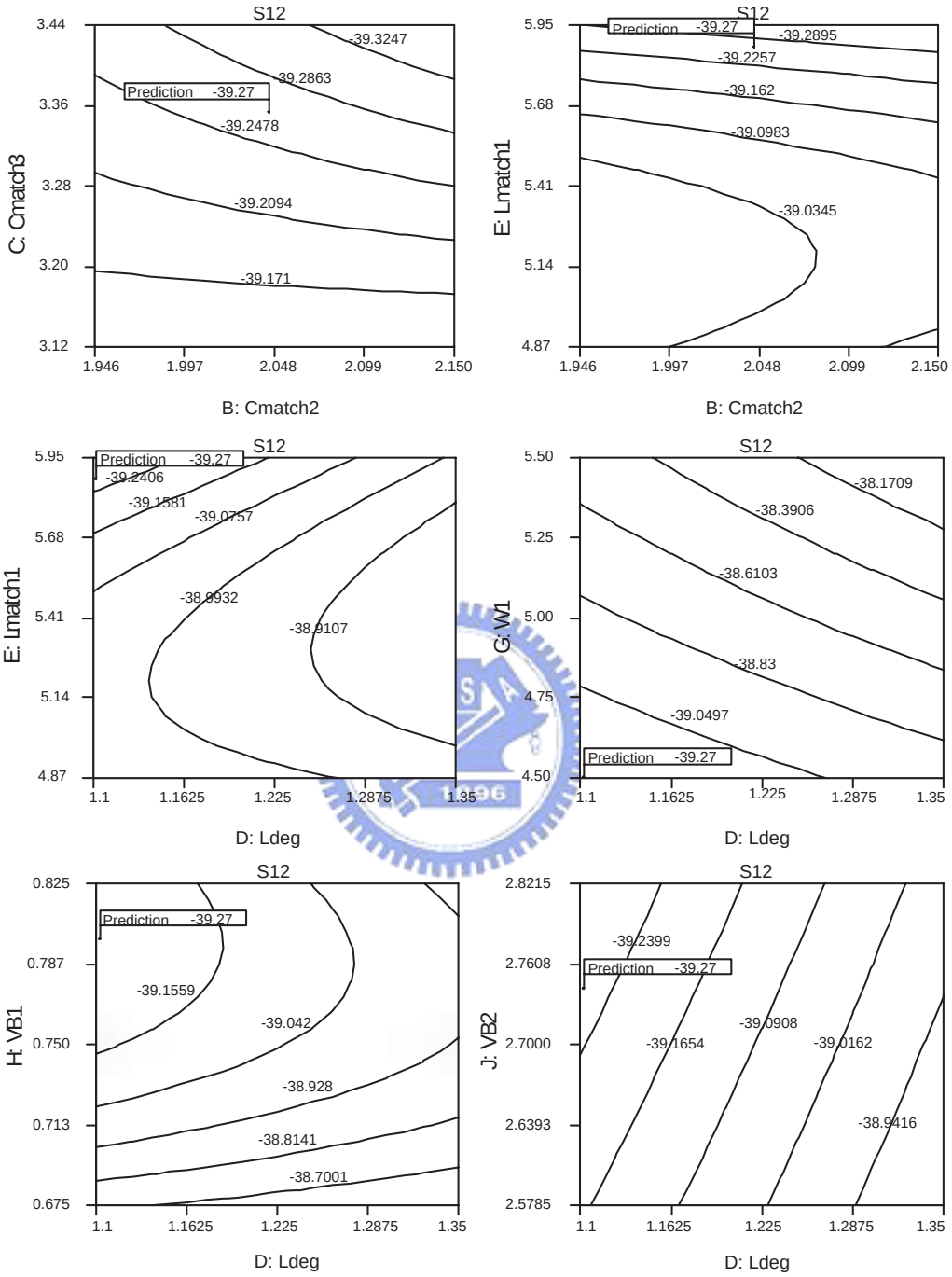
S12
C: Cmatch3
B: Cmatch2
Prediction -39.27
-39.3247
-39.2863
-39.2478
-39.2094
-39.171
S12
E: Lmatch1
B: Cmatch2
Prediction -39.27
-39.2895
-39.2257
-39.162
-39.0983
-39.0345
S12
E: Lmatch1
D: Ldeg
Prediction -39.27
-39.2406
-39.1581
-39.0757
-38.9932
-38.9107
S12
G: W1
D: Ldeg
-38.1709
-38.3906
-38.6103
-38.83
-39.0497
Prediction -39.27
S12
H: VB1
D: Ldeg
Prediction -39.27
-39.1559
-39.042
-38.928
-38.8141
-38.7001
S12
J: VB2
D: Ldeg
-39.2399
Prediction -39.27
-39.1654
-39.0908
-39.0162
-38.9416

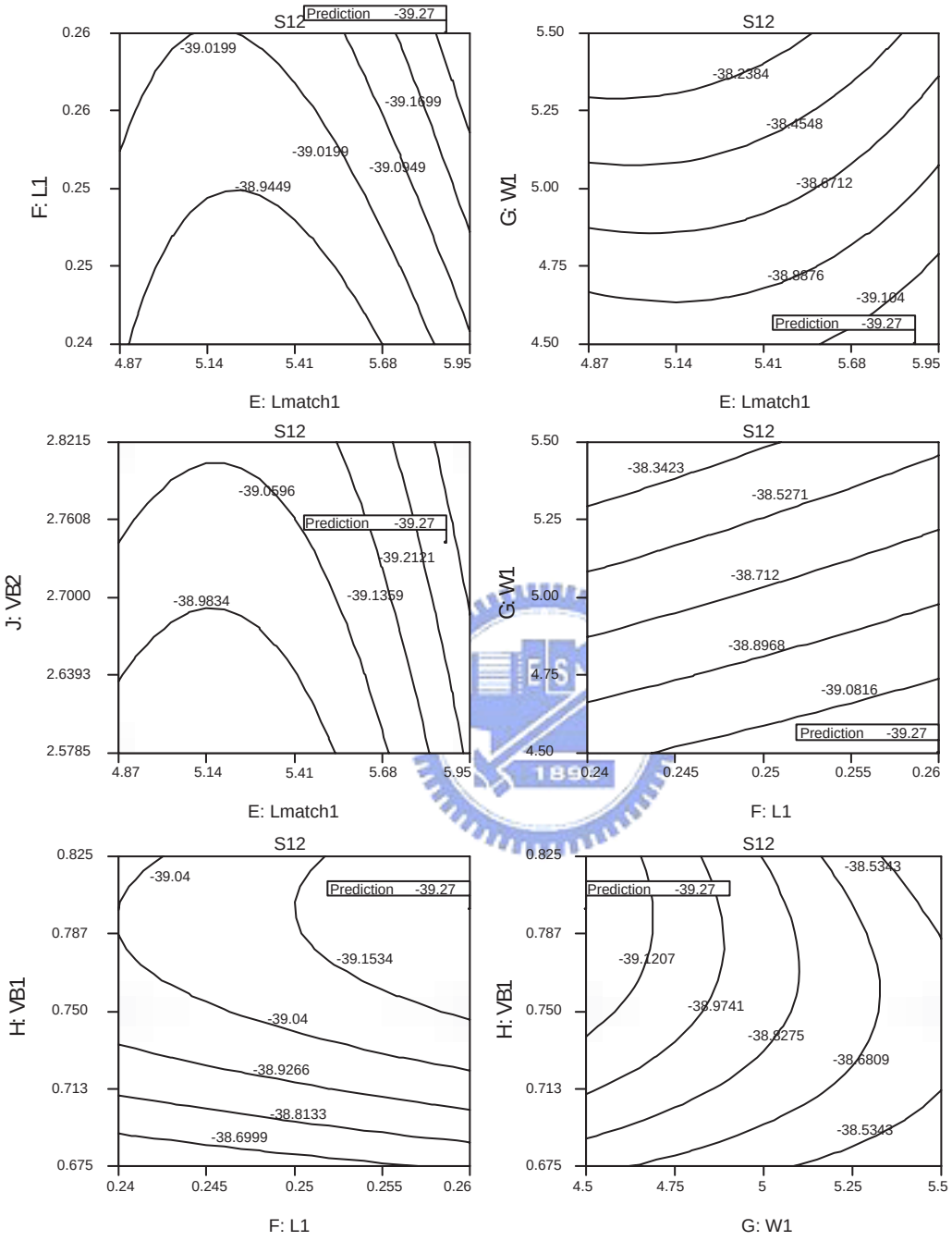
S12
Prediction -39.27
-39.0199
-39.1699
-39.0199
-39.0949
-38.9449
F: L1
E: Lmatch1
S12
-38.2384
-38.4548
-38.6712
-38.8876
-39.104
Prediction -39.27
G: W1
E: Lmatch1
S12
-39.0596
Prediction -39.27
-39.2121
-39.1359
-38.9834
J: VB2
E: Lmatch1
S12
-38.3423
-38.5271
-38.712
-38.8968
-39.0816
Prediction -39.27
G: W1
F: L1
S12
-39.04
Prediction -39.27
-39.1534
-39.04
-38.9266
-38.8133
-38.6999
H: VB1
F: L1
S12
Prediction -39.27
-38.5343
-39.1207
-38.9741
-38.8275
-38.6809
-38.5343
H: VB1
G: W1

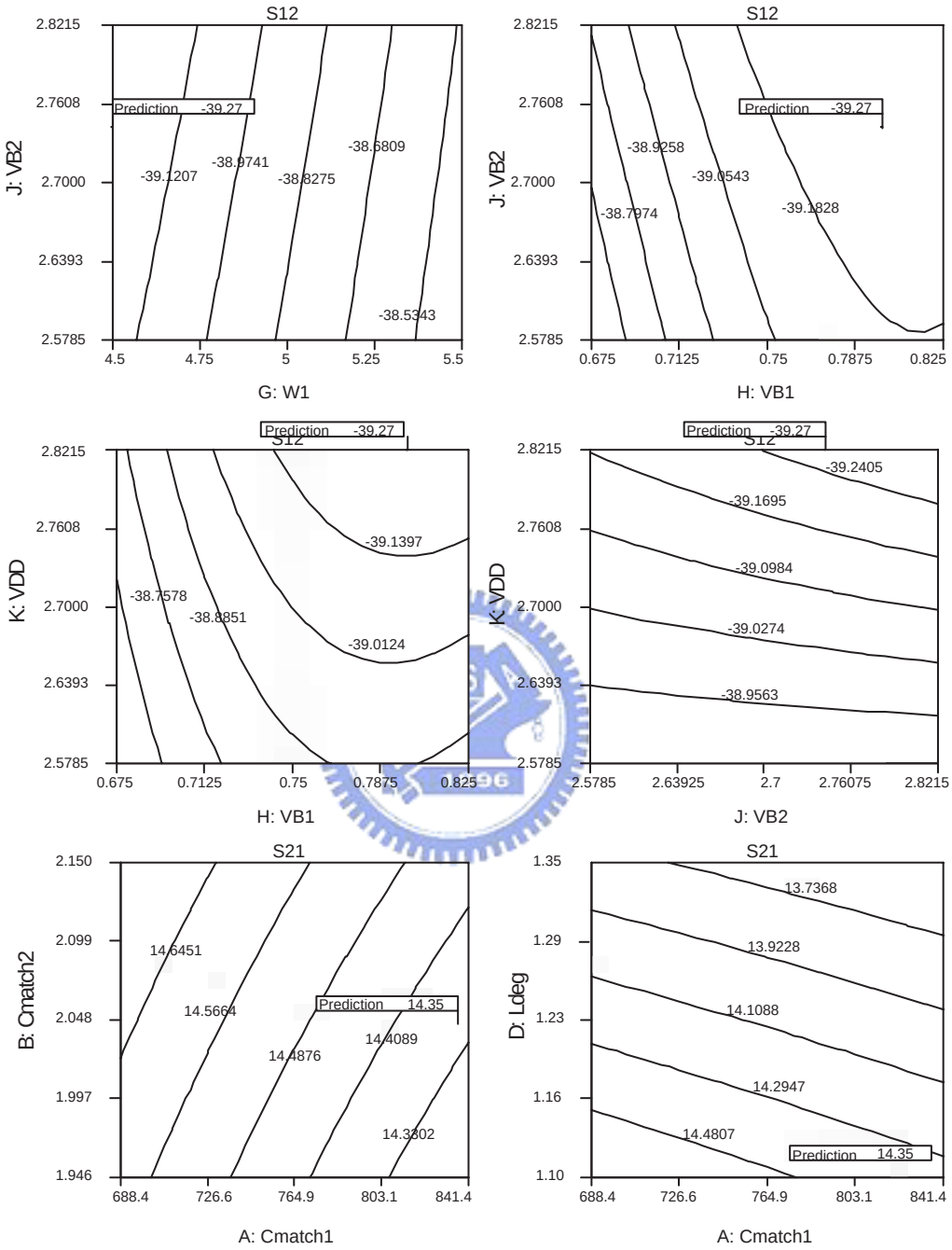
S12
Prediction -39.27
-39.1207
-38.9741
-38.8275
-38.6809
-38.5343
J: VB2
G: W1
S12
Prediction -39.27
-38.9258
-39.0543
-38.7974
-39.1828
J: VB2
H: VB1
Prediction -39.27
S12
-39.1397
-38.7578
-38.8851
-39.0124
K: VDD
H: VB1
Prediction -39.27
S12
-39.2405
-39.1695
-39.0984
-39.0274
-38.9563
K: VDD
J: VB2
S21
14.6451
14.5664
Prediction 14.35
14.4089
14.4876
14.3302
B: Cmatch2
A: Cmatch1
S21
13.7368
13.9228
14.1088
14.2947
14.4807
Prediction 14.35
D: Ldeg
A: Cmatch1

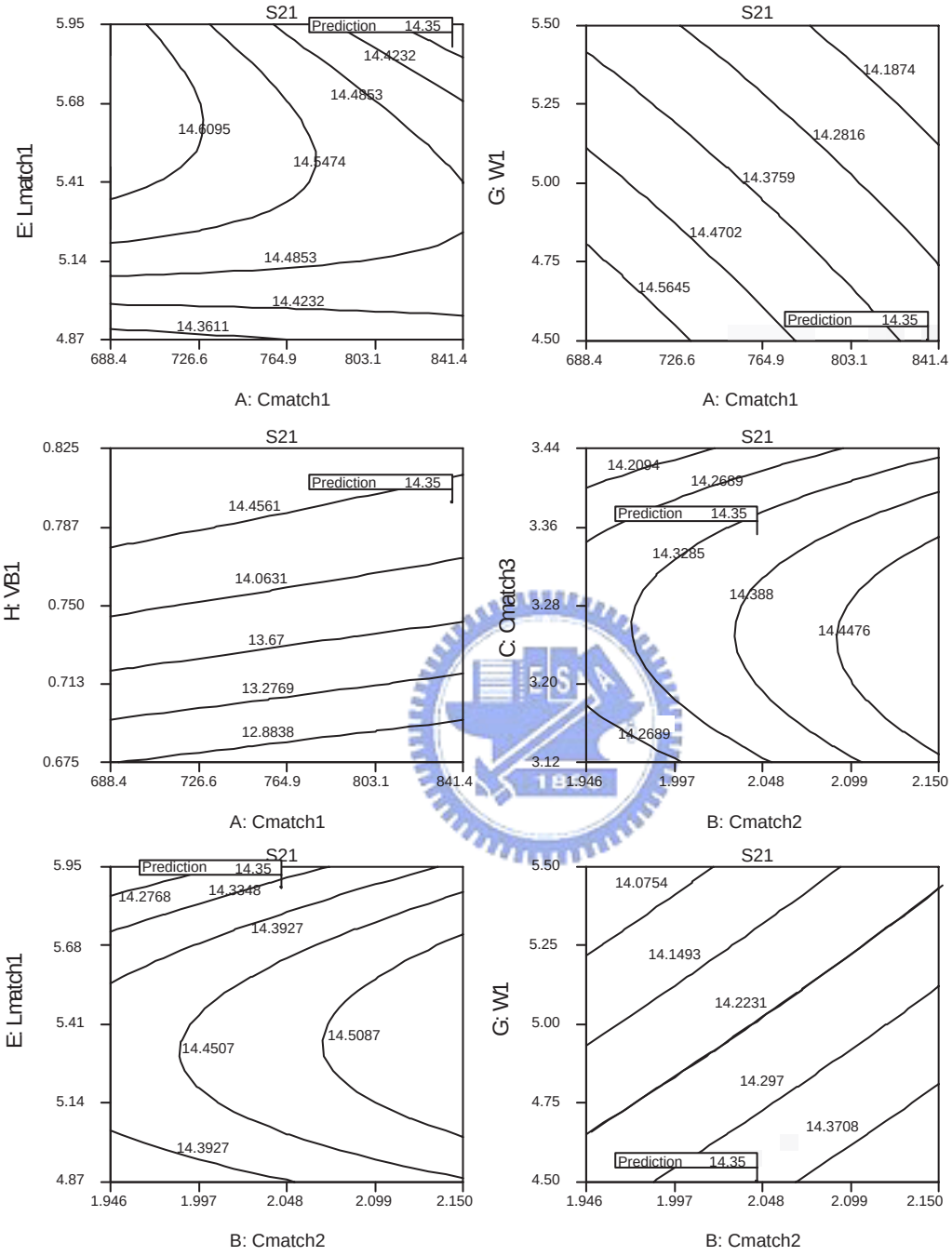
S21
Prediction 14.35
14.4232
14.4853
14.6095
14.5474
14.4853
14.4232
14.3611
E: Lmatch1
A: Cmatch1
S21
14.1874
14.2816
14.3759
14.4702
14.5645
Prediction 14.35
G: W1
A: Cmatch1
S21
Prediction 14.35
14.4561
14.0631
13.67
13.2769
12.8838
H: VB1
A: Cmatch1
S21
14.2094
14.2689
Prediction 14.35
14.3285
14.388
14.4476
14.2689
C: Cmatch3
B: Cmatch2
S21
Prediction 14.35
14.2768
14.3348
14.3927
14.4507
14.5087
14.3927
E: Lmatch1
B: Cmatch2
S21
14.0754
14.1493
14.2231
14.297
14.3708
Prediction 14.35
G: W1
B: Cmatch2

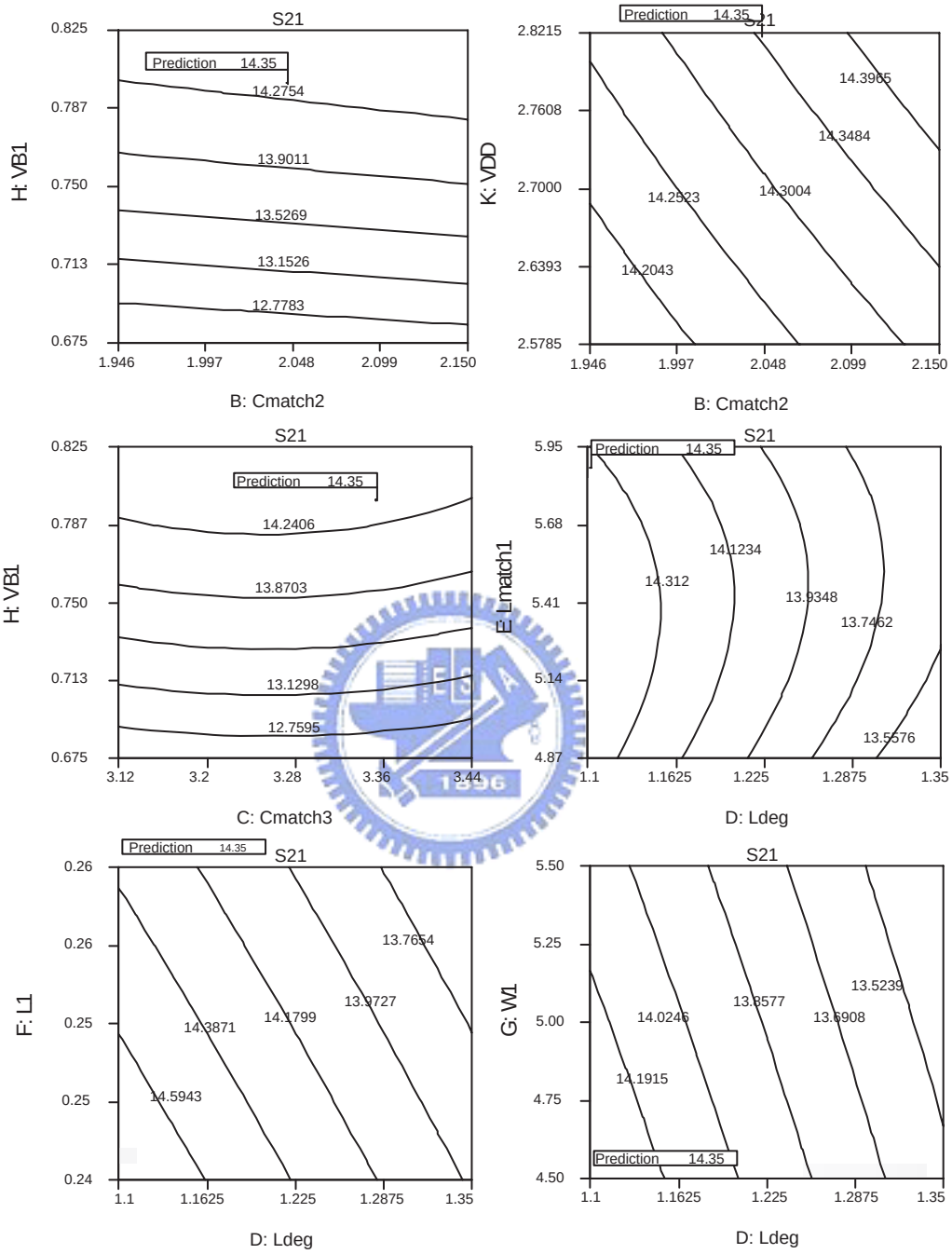
S21
Prediction 14.35
14.2754
13.9011
13.5269
13.1526
12.7783
H: VB1
0.825
0.787
0.750
0.713
0.675
1.946
1.997
2.048
2.099
2.150
B: Cmatch2
S21
Prediction 14.35
14.3965
14.3484
14.3004
14.2523
14.2043
K: VDD
2.8215
2.7608
2.7000
2.6393
2.5785
1.946
1.997
2.048
2.099
2.150
B: Cmatch2
S21
Prediction 14.35
14.2406
13.8703
13.1298
12.7595
H: VB1
0.825
0.787
0.750
0.713
0.675
3.12
3.2
3.28
3.36
3.44
C: Cmatch3
S21
Prediction 14.35
14.1234
14.312
13.9348
13.7462
13.5576
E: Lmatch1
5.95
5.68
5.41
5.14
4.87
1.1
1.1625
1.225
1.2875
1.35
D: Ldeg
S21
Prediction 14.35
13.7654
13.9727
14.1799
14.3871
14.5943
F: L1
0.26
0.26
0.25
0.25
0.24
1.1
1.1625
1.225
1.2875
1.35
D: Ldeg
S21
13.5239
13.8577
14.0246
13.6908
14.1915
Prediction 14.35
G: W1
5.50
5.25
5.00
4.75
4.50
1.1
1.1625
1.225
1.2875
1.35
D: Ldeg

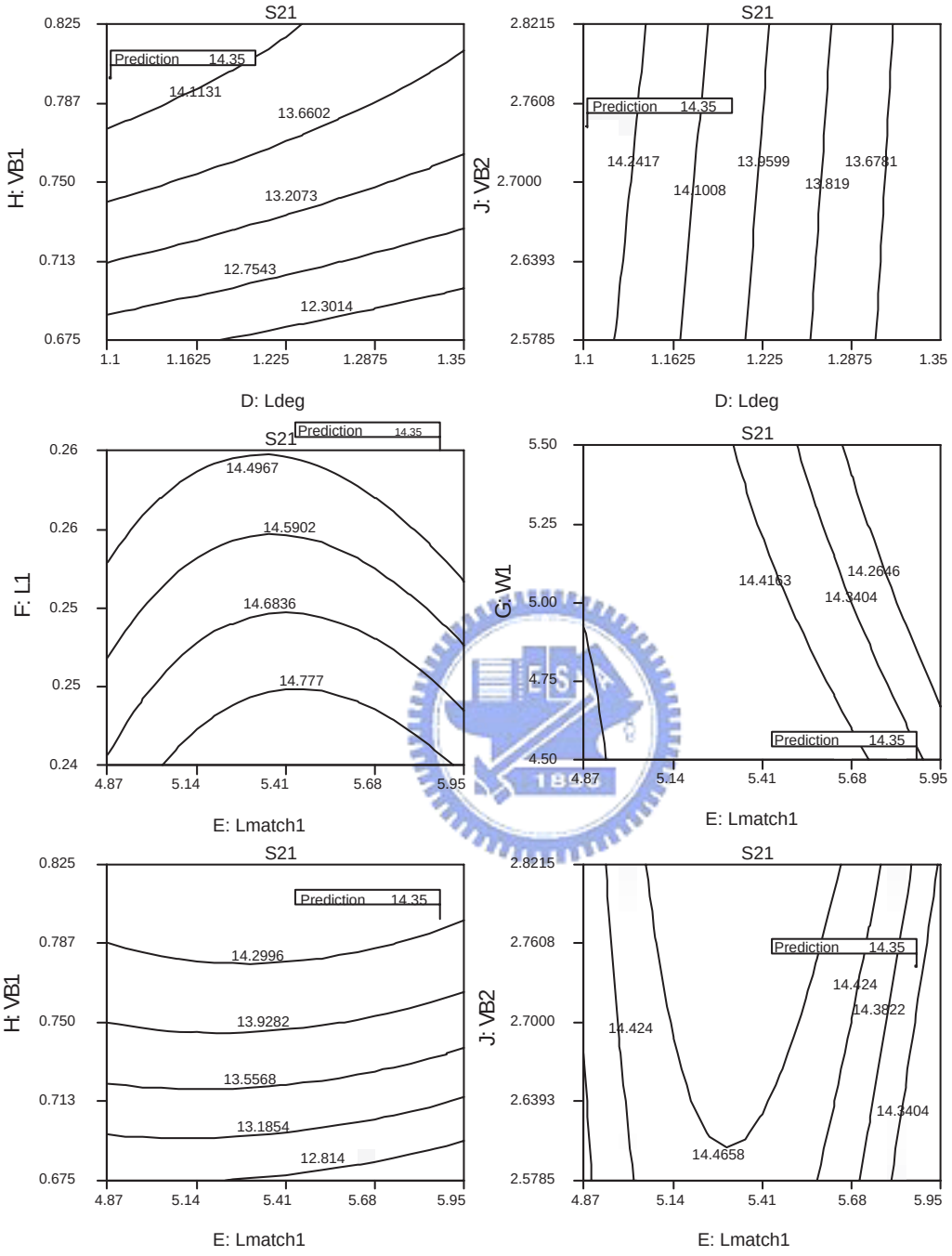
S21
Prediction 14.35
14.1131
13.6602
13.2073
12.7543
12.3014
H: VB1
D: Ldeg
S21
Prediction 14.35
14.2417
14.1008
13.9599
13.819
13.6781
J: VB2
D: Ldeg
S21
Prediction 14.35
14.4967
14.5902
14.6836
14.777
F: L1
E: Lmatch1
S21
14.4163
14.2646
14.3404
Prediction 14.35
G: W1
E: Lmatch1
S21
Prediction 14.35
14.2996
13.9282
13.5568
13.1854
12.814
H: VB1
E: Lmatch1
S21
Prediction 14.35
14.424
14.3822
14.424
14.3404
14.4658
J: VB2
E: Lmatch1

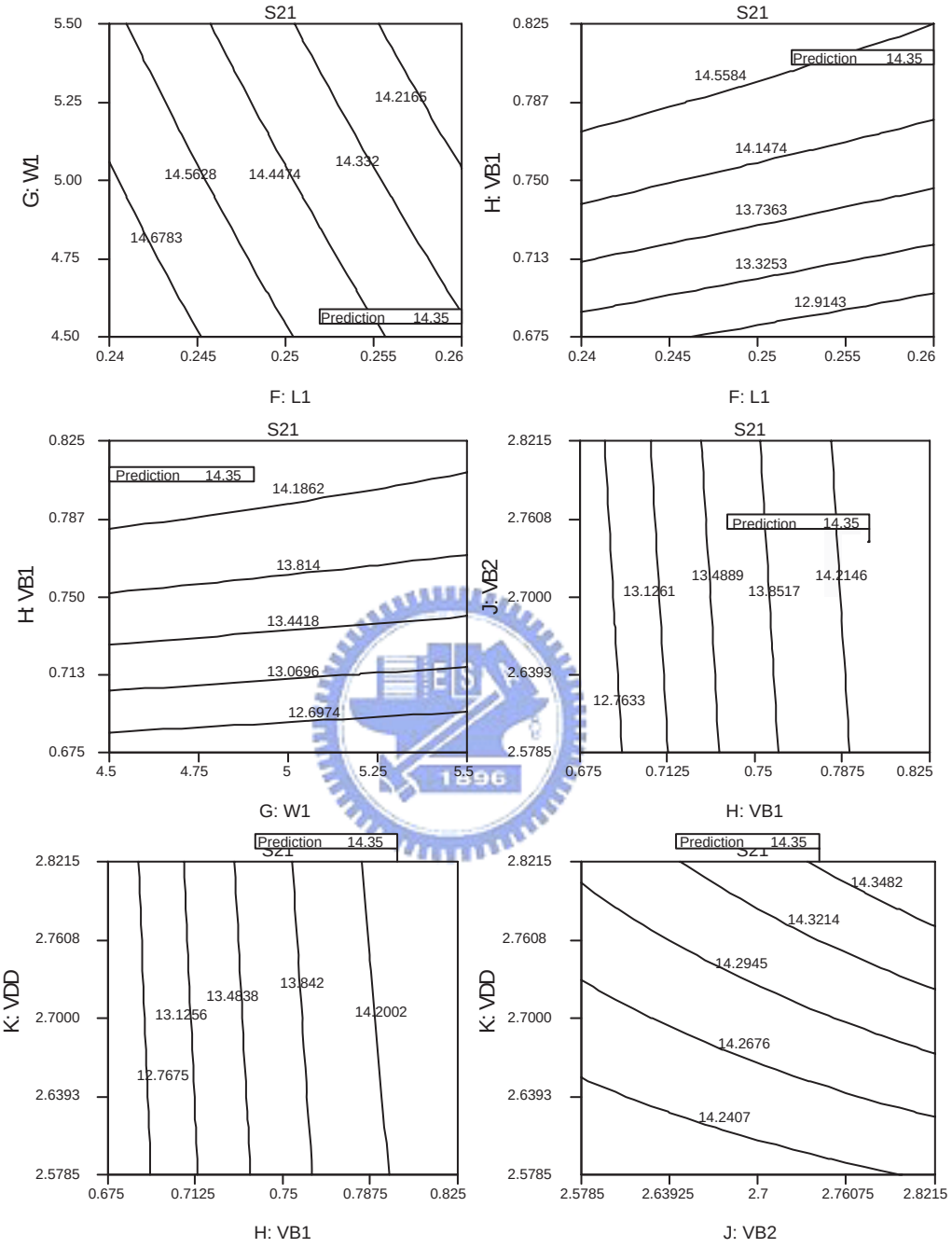
S21
G: W1
F: L1
14.2165
14.332
14.4474
14.5628
14.6783
Prediction 14.35
S21
H: VB1
F: L1
14.5584
14.1474
13.7363
13.3253
12.9143
Prediction 14.35
S21
H: VB1
G: W1
14.1862
13.814
13.4418
13.0696
12.6974
Prediction 14.35
S21
J: VB2
H: VB1
13.1261
13.4889
13.8517
14.2146
12.7633
Prediction 14.35
S21
K: VDD
H: VB1
13.1256
13.4838
13.842
14.2002
12.7675
Prediction 14.35
S21
K: VDD
J: VB2
14.3482
14.3214
14.2945
14.2676
14.2407
Prediction 14.35

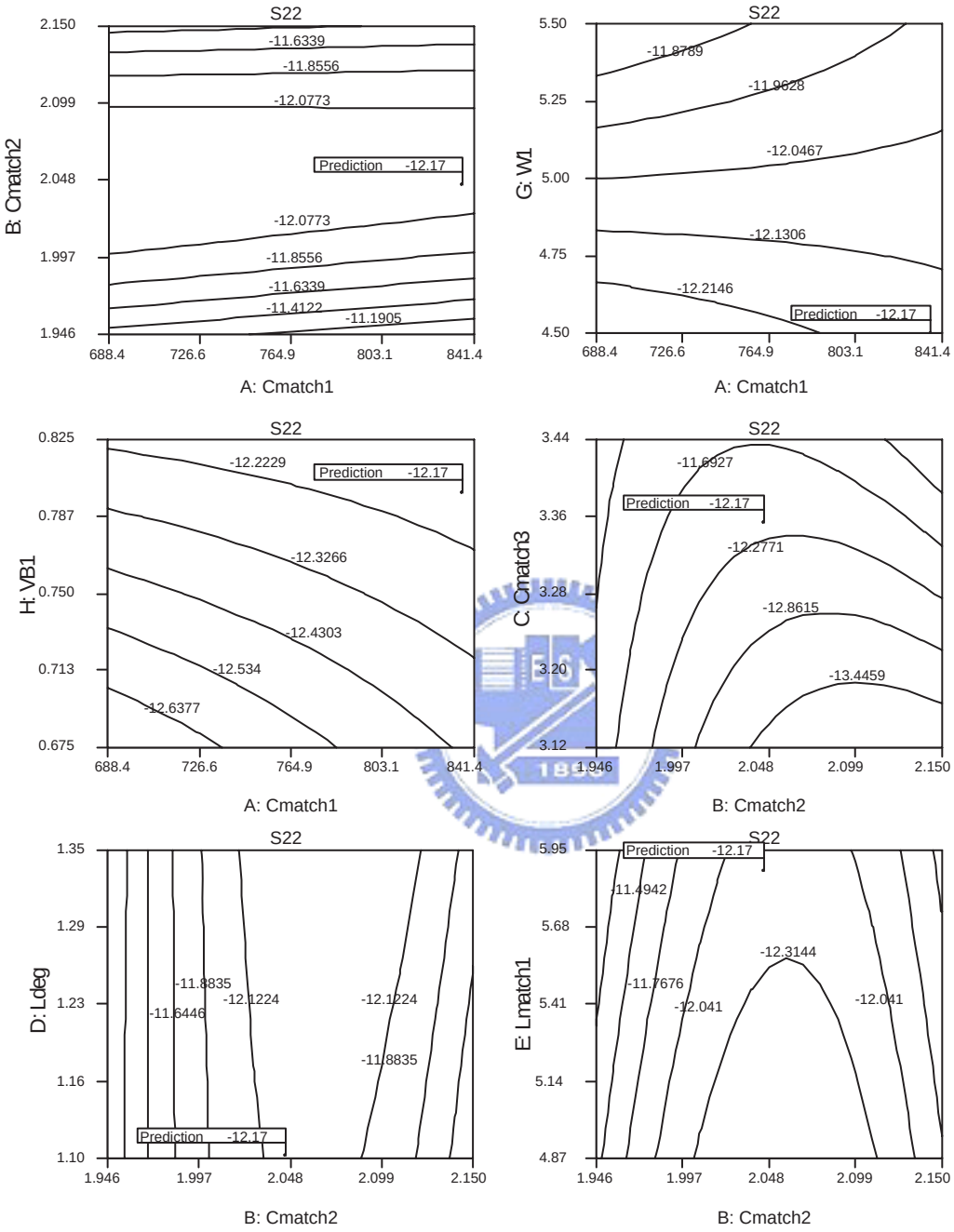
S22
B: Cmatch2
A: Cmatch1
-11.6339
-11.8556
-12.0773
Prediction -12.17
-12.0773
-11.8556
-11.6339
-11.4122
-11.1905
S22
G: W1
A: Cmatch1
-11.9789
-11.9628
-12.0467
-12.1306
-12.2146
Prediction -12.17
S22
H: VB1
A: Cmatch1
-12.2229
Prediction -12.17
-12.3266
-12.4303
-12.534
-12.6377
S22
C: Cmatch3
B: Cmatch2
-11.6927
Prediction -12.17
-12.2771
-12.8615
-13.4459
S22
D: Ldeg
B: Cmatch2
-11.8835
-12.1224
-11.6446
-12.1224
-11.8835
Prediction -12.17
S22
E: Lmatch1
B: Cmatch2
Prediction -12.17
-11.4942
-12.3144
-11.7676
-12.041
-12.041

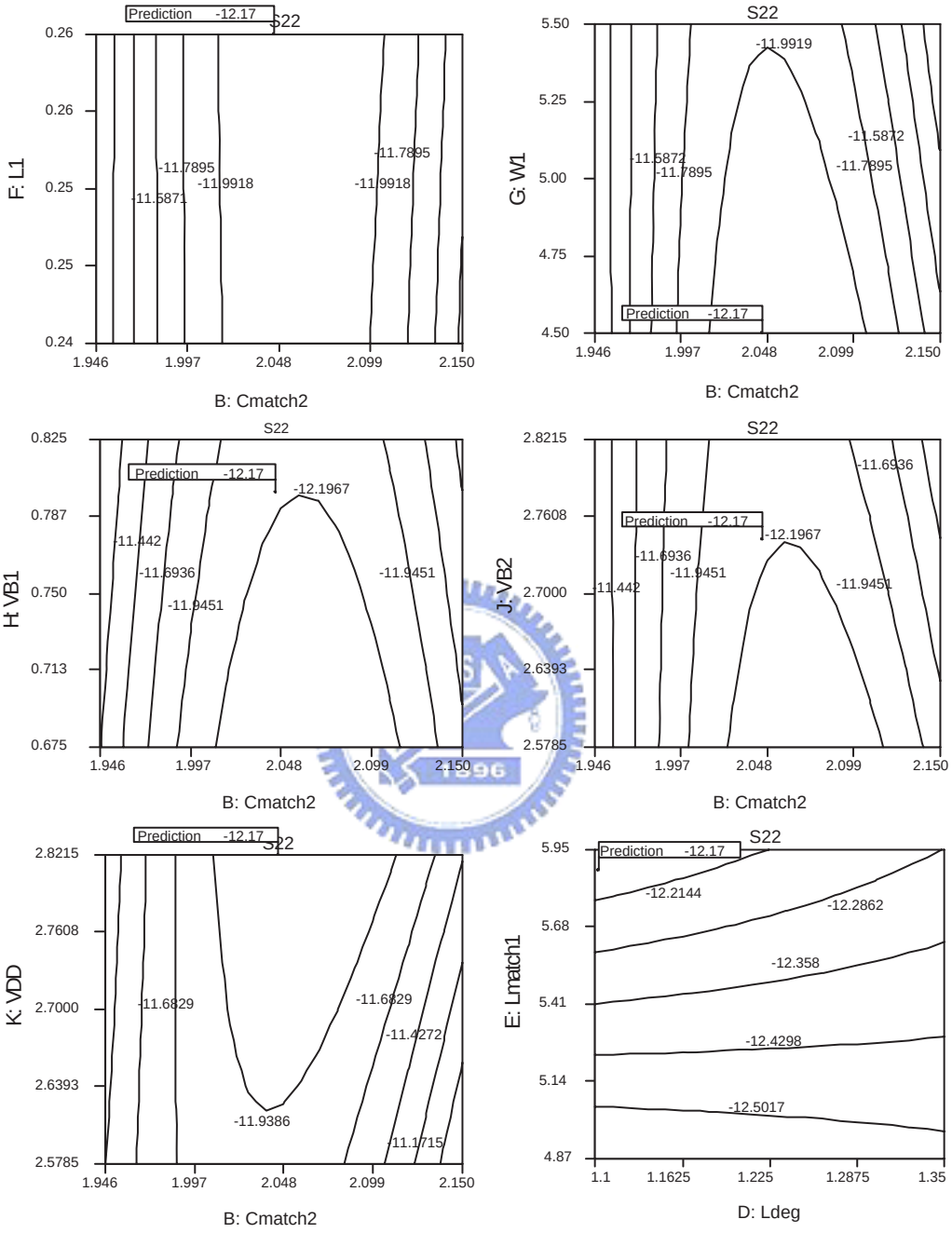
Prediction -12.17
S22
F: L1
0.26
0.26
0.25
0.25
0.24
-11.7895
-11.9918
-11.5871
-11.7895
-11.9918
1.946
1.997
2.048
2.099
2.150
B: Cmatch2
S22
G: W1
5.50
5.25
5.00
4.75
4.50
-11.9919
-11.5872
-11.5872
-11.7895
-11.7895
Prediction -12.17
1.946
1.997
2.048
2.099
2.150
B: Cmatch2
S22
H: VB1
0.825
0.787
0.750
0.713
0.675
Prediction -12.17
-12.1967
-11.442
-11.6936
-11.9451
-11.9451
1.946
1.997
2.048
2.099
2.150
B: Cmatch2
S22
J: VB2
2.8215
2.7608
2.7000
2.6393
2.5785
-11.6936
Prediction -12.17
-12.1967
-11.6936
-11.9451
-11.442
-11.9451
1.946
1.997
2.048
2.099
2.150
B: Cmatch2
Prediction -12.17
S22
K: VDD
2.8215
2.7608
2.7000
2.6393
2.5785
-11.6829
-11.6829
-11.4272
-11.9386
-11.1715
1.946
1.997
2.048
2.099
2.150
B: Cmatch2
S22
Prediction -12.17
E: Lmatch1
5.95
5.68
5.41
5.14
4.87
-12.2144
-12.2862
-12.358
-12.4298
-12.5017
1.1
1.1625
1.225
1.2875
1.35
D: Ldeg

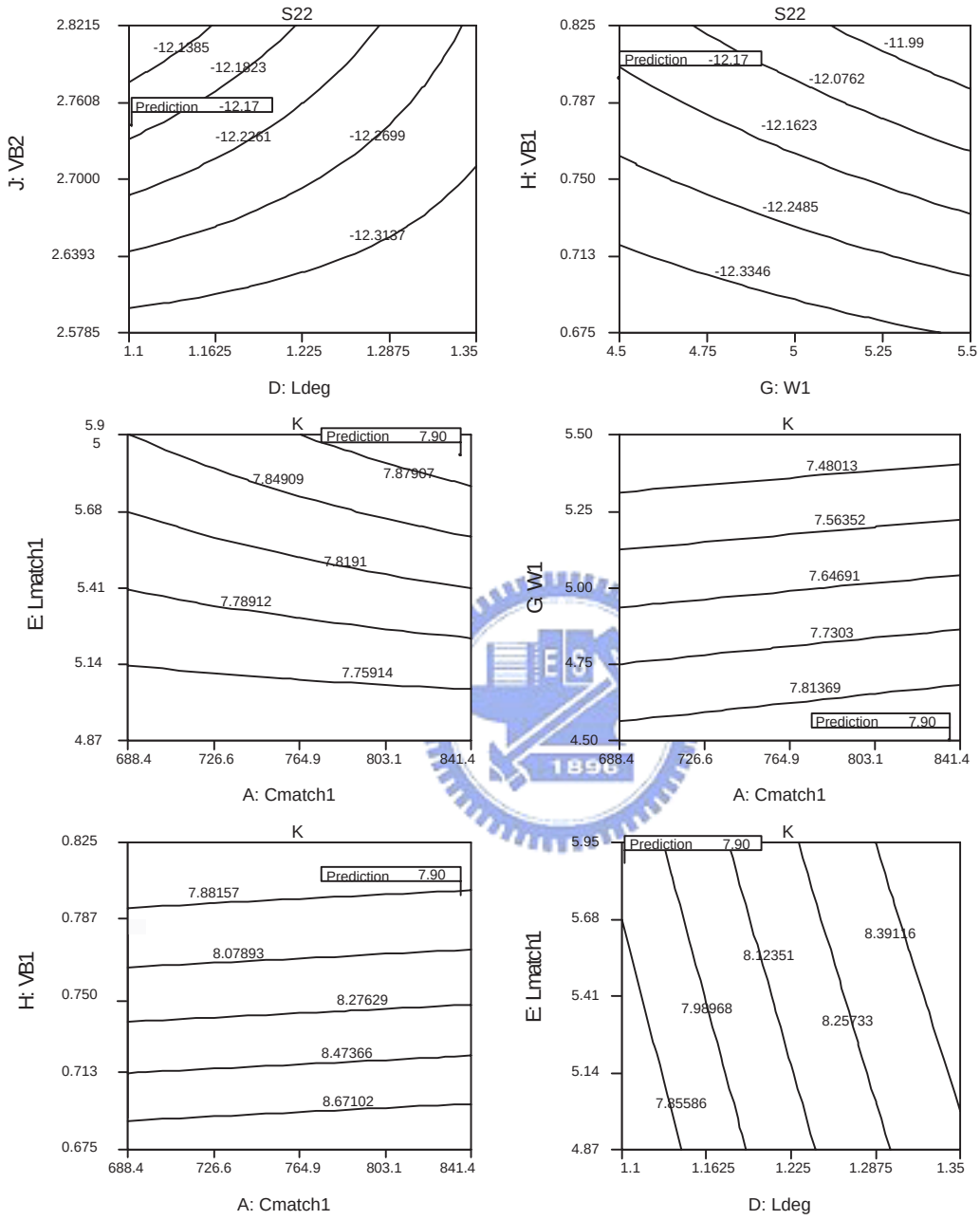
S22
J: VB2
D: Ldeg
Prediction -12.17
-12.1385
-12.1823
-12.2261
-12.2699
-12.3137
S22
H: VB1
G: W1
Prediction -12.17
-11.99
-12.0762
-12.1623
-12.2485
-12.3346
K
E: Lmatch1
A: Cmatch1
Prediction 7.90
7.84909
7.87907
7.8191
7.78912
7.75914
K
G: W1
A: Cmatch1
7.48013
7.56352
7.64691
7.7303
7.81369
Prediction 7.90
K
H: VB1
A: Cmatch1
Prediction 7.90
7.88157
8.07893
8.27629
8.47366
8.67102
K
E: Lmatch1
D: Ldeg
Prediction 7.90
8.39116
8.12351
7.98968
8.25733
7.85586

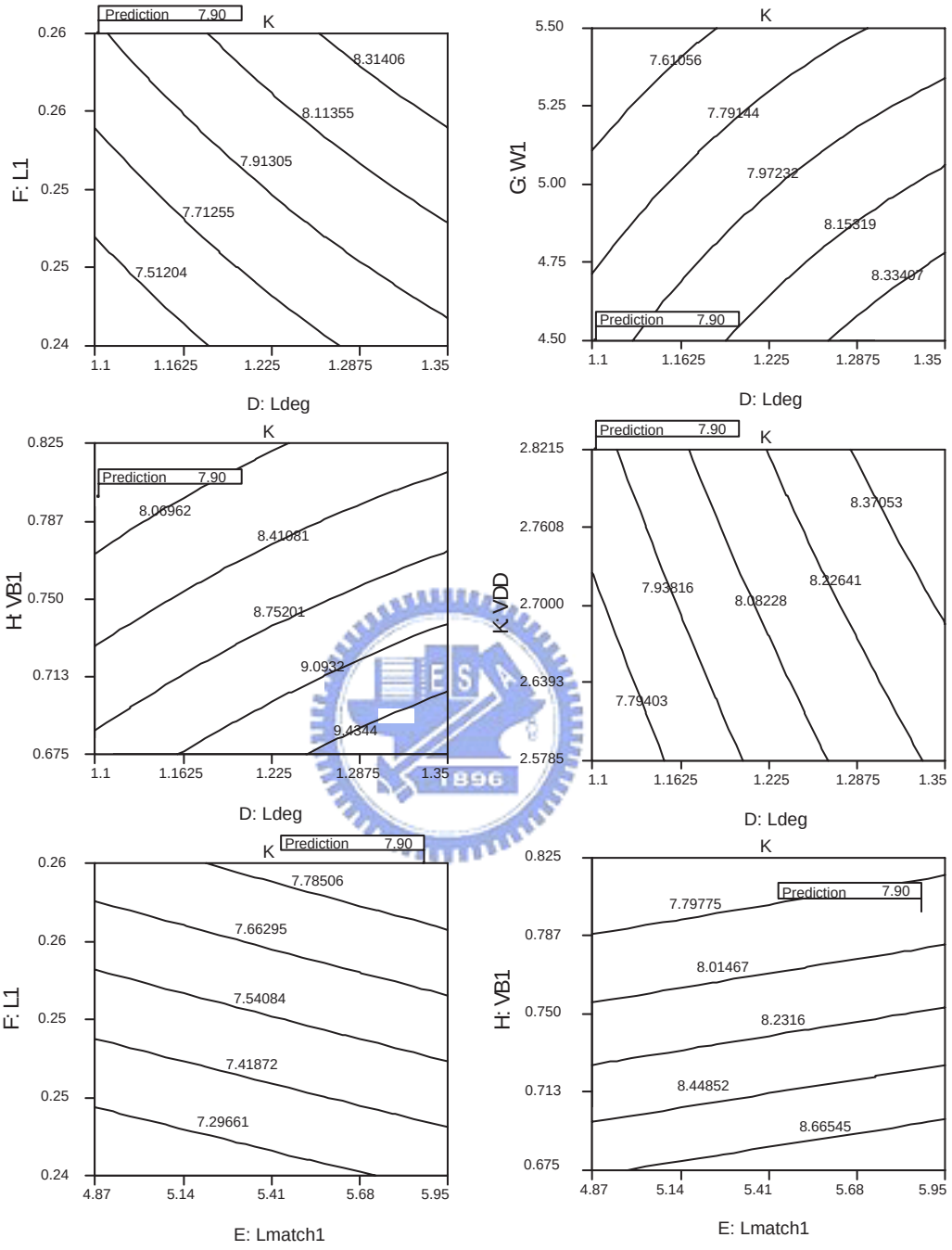
Prediction 7.90
K
8.31406
8.11355
7.91305
7.71255
7.51204
F: L1
D: Ldeg
G: W1
7.61056
7.79144
7.97232
8.15319
8.33407
H: VB1
8.06962
8.41081
8.75201
9.0932
9.4344
K: VDD
8.37053
8.22641
8.08228
7.93816
7.79403
E: Lmatch1
7.78506
7.66295
7.54084
7.41872
7.29661
7.79775
8.01467
8.2316
8.44852
8.66545

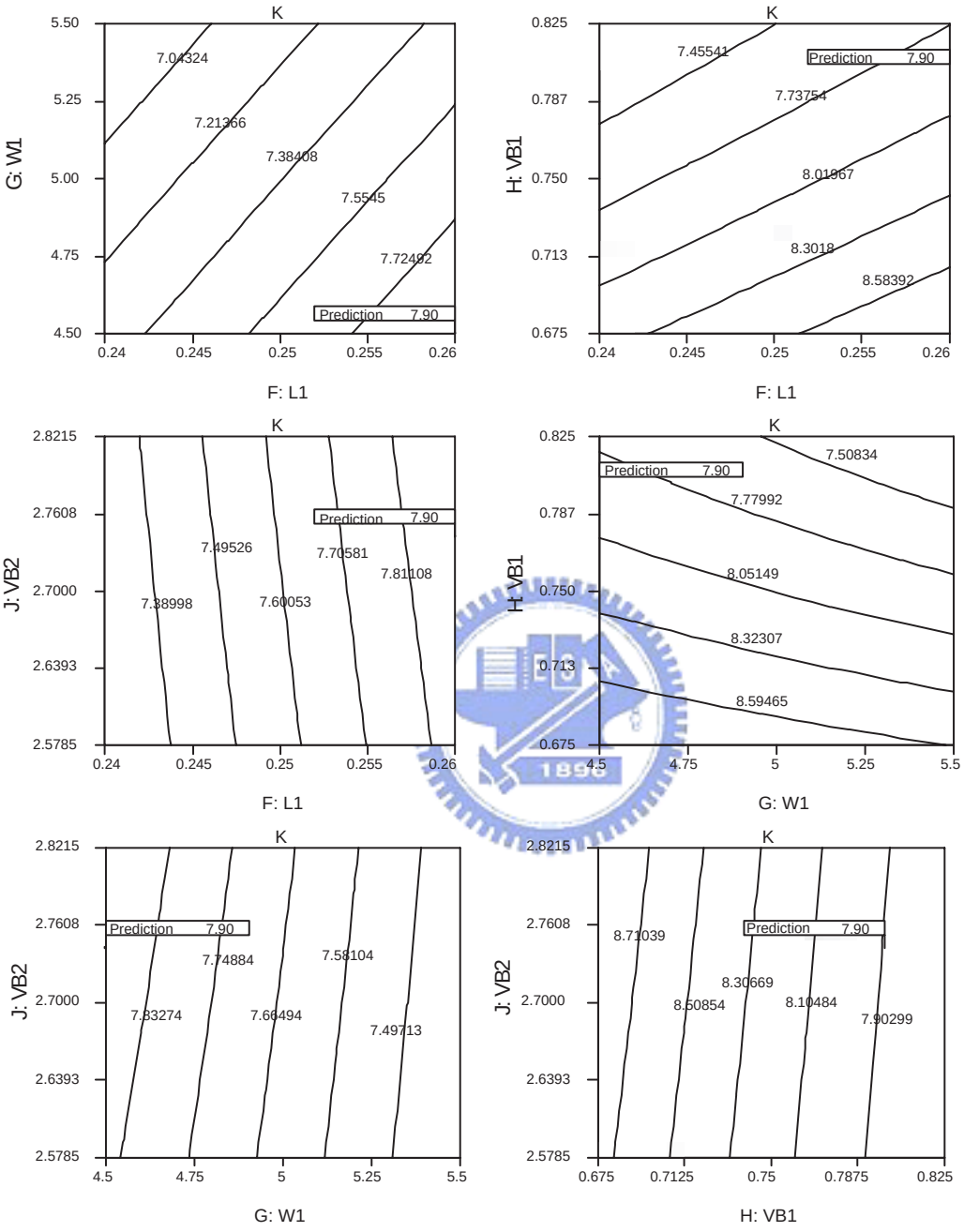
K
G: W1
F: L1
7.04324
7.21366
7.38408
7.5545
7.72492
Prediction 7.90
H: VB1
7.45541
7.73754
8.01967
8.3018
8.58392
J: VB2
7.38998
7.49526
7.60053
7.70581
7.81108
7.50834
7.77992
8.05149
8.32307
8.59465
7.83274
7.74884
7.66494
7.58104
7.49713
8.71039
8.50854
8.30669
8.10484
7.90299

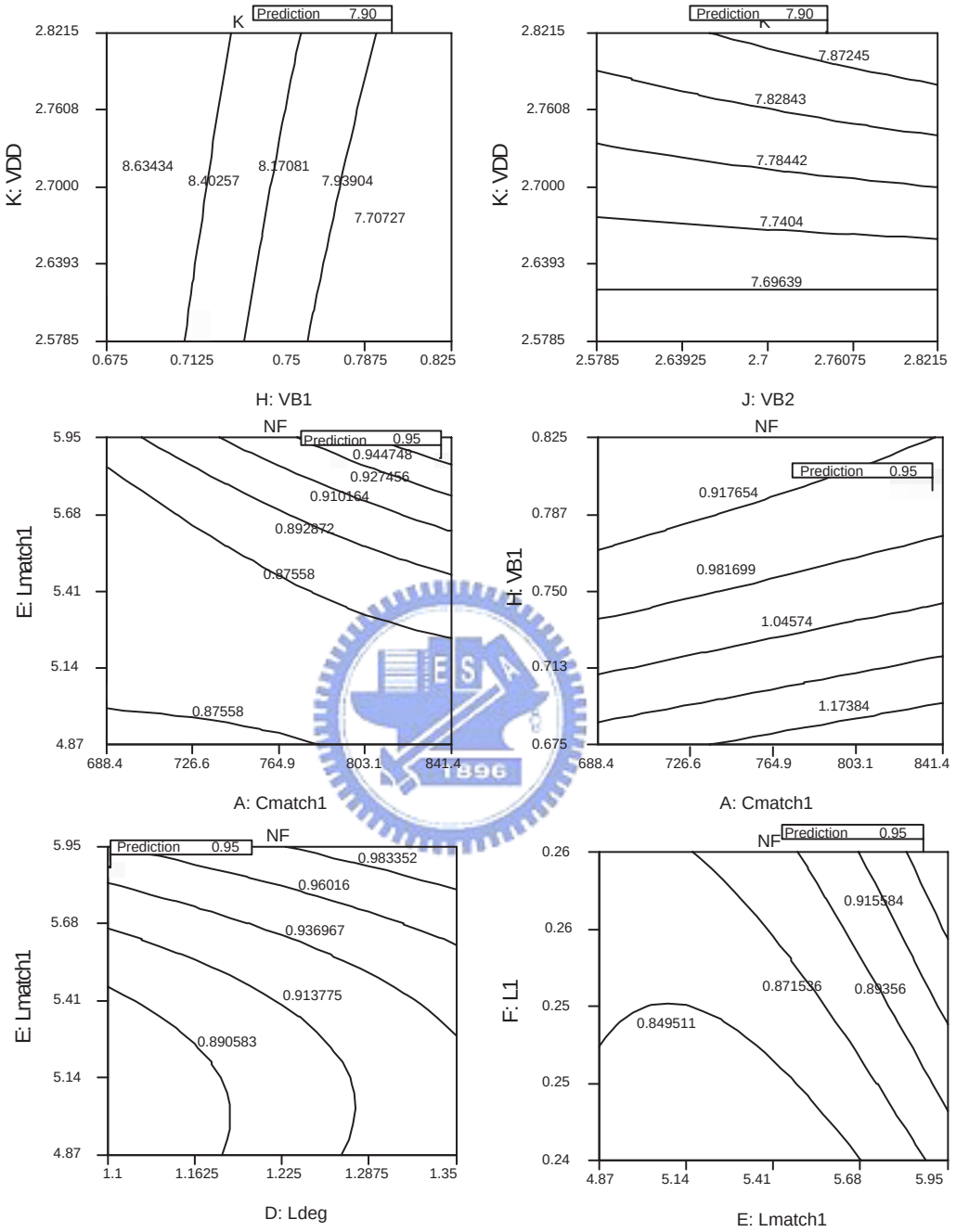
Prediction 7.90
K
2.8215
2.7608
2.7000
2.6393
2.5785
K: VDD
8.63434
8.40257
8.17081
7.93904
7.70727
0.675
0.7125
0.75
0.7875
0.825
H: VB1
Prediction 7.90
K
7.87245
7.82843
7.78442
7.7404
7.69639
2.5785
2.63925
2.7
2.76075
2.8215
J: VB2
NF
Prediction 0.95
5.95
5.68
5.41
5.14
4.87
E: Lmatch1
0.944748
0.927456
0.910164
0.892872
0.87558
0.87558
688.4
726.6
764.9
803.1
841.4
A: Cmatch1
NF
Prediction 0.95
0.825
0.787
0.750
0.713
0.675
H: VB1
0.917654
0.981699
1.04574
1.17384
688.4
726.6
764.9
803.1
841.4
A: Cmatch1
NF
Prediction 0.95
5.95
5.68
5.41
5.14
4.87
E: Lmatch1
0.983352
0.96016
0.936967
0.913775
0.890583
1.1
1.1625
1.225
1.2875
1.35
D: Ldeg
NF
Prediction 0.95
0.26
0.26
0.25
0.25
0.24
F: L1
0.915584
0.871536
0.89356
0.849511
4.87
5.14
5.41
5.68
5.95
E: Lmatch1

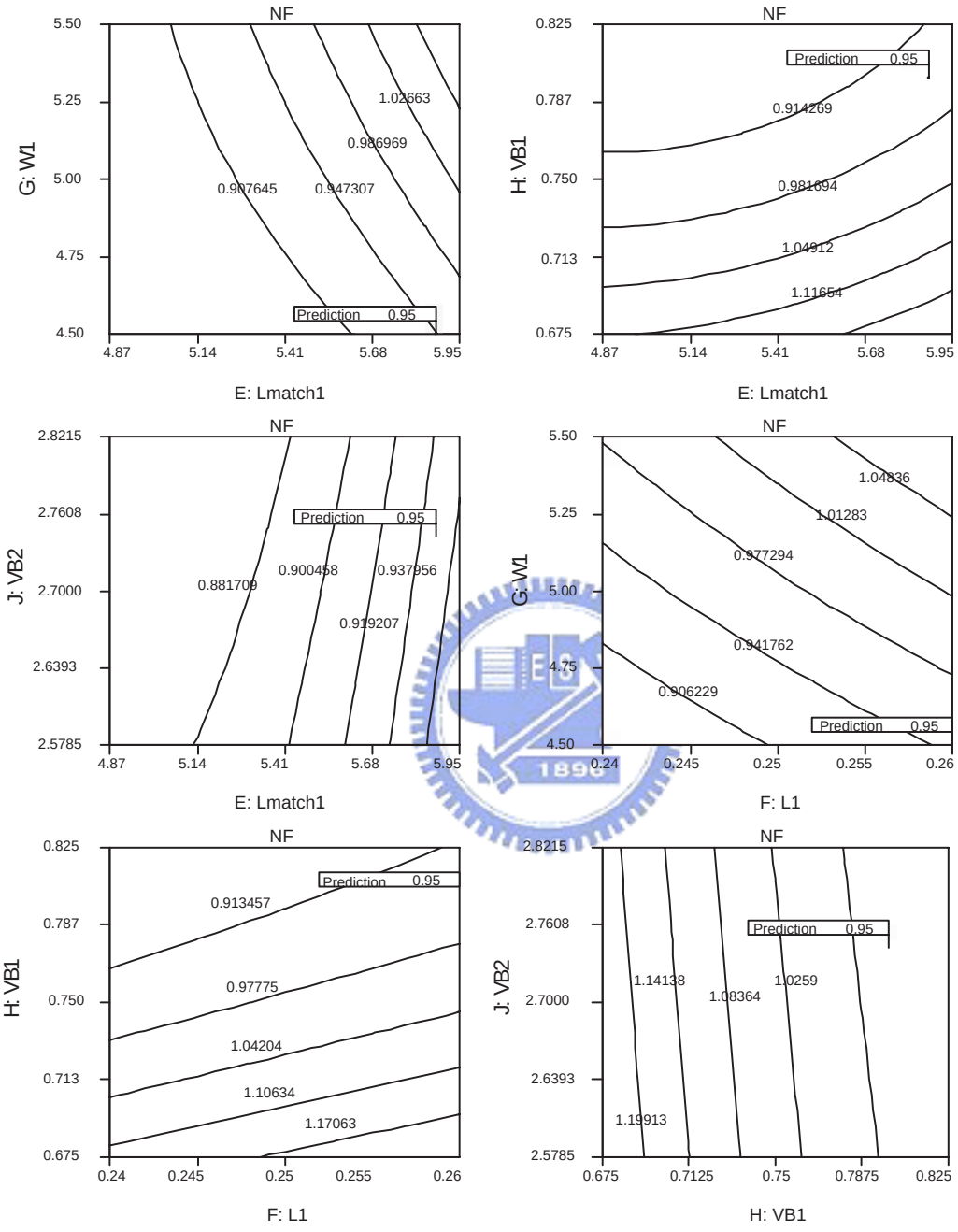
NF
G: W1
E: Lmatch1
1.02663
0.986969
0.947307
0.907645
Prediction 0.95
NF
H: VB1
E: Lmatch1
Prediction 0.95
0.914269
0.981694
1.04912
1.11654
NF
J: VB2
E: Lmatch1
Prediction 0.95
0.881709
0.900458
0.937956
0.919207
NF
G: W1
F: L1
1.04836
1.01283
0.977294
0.941762
0.906229
Prediction 0.95
NF
H: VB1
F: L1
Prediction 0.95
0.913457
0.97775
1.04204
1.10634
1.17063
NF
J: VB2
H: VB1
Prediction 0.95
1.14138
1.08364
1.0259
1.19913

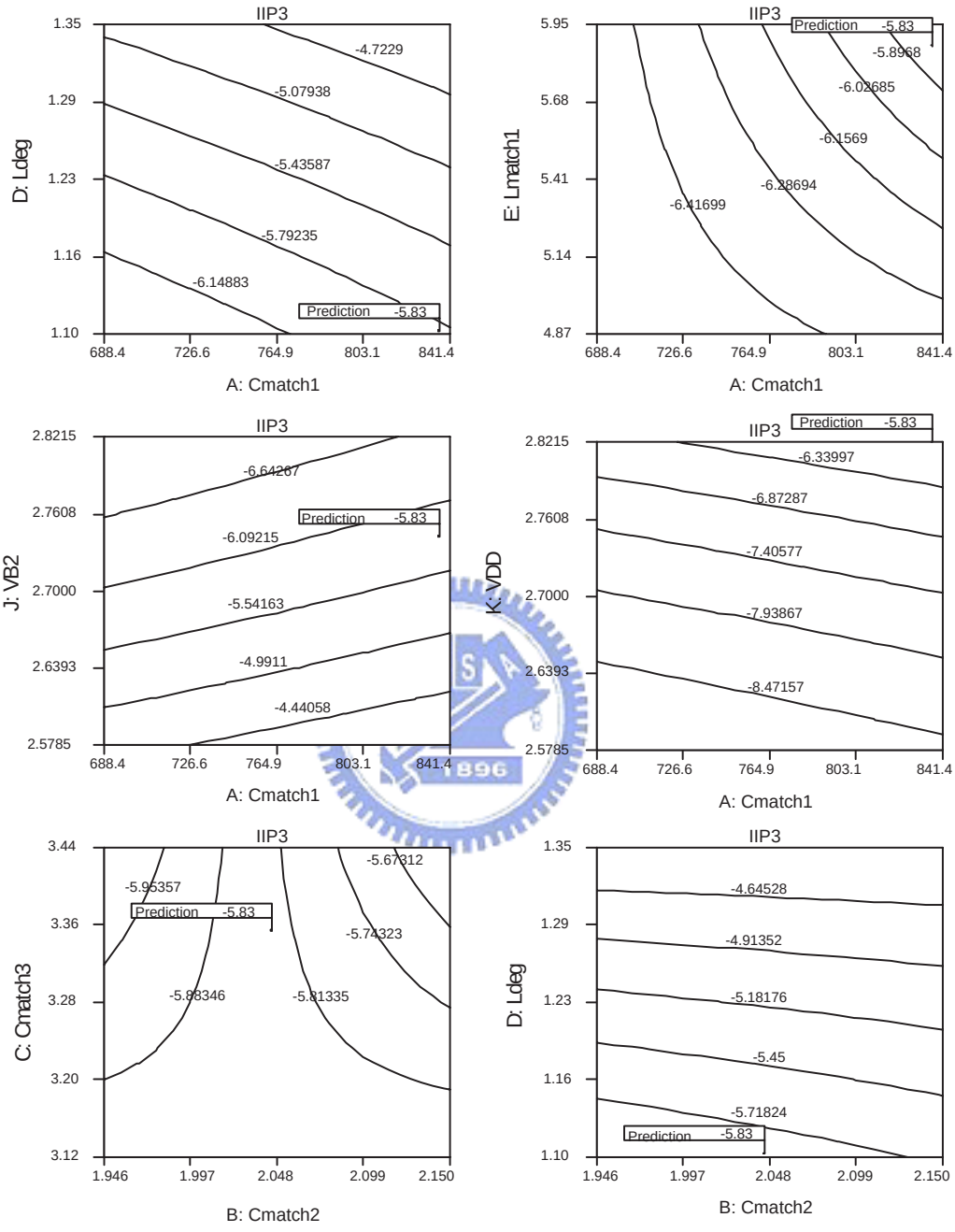
IIP3
D: Ldeg
A: Cmatch1
-4.7229
-5.07938
-5.43587
-5.79235
-6.14883
Prediction -5.83
IIP3
E: Lmatch1
A: Cmatch1
Prediction -5.83
-5.8968
-6.02685
-6.1569
-6.28694
-6.41699
IIP3
J: VB2
A: Cmatch1
-6.64267
Prediction -5.83
-6.09215
-5.54163
-4.9911
-4.44058
IIP3
K: VDD
A: Cmatch1
Prediction -5.83
-6.33997
-6.87287
-7.40577
-7.93867
-8.47157
IIP3
C: Cmatch3
B: Cmatch2
-5.67312
-5.95357
Prediction -5.83
-5.74323
-5.88346
-5.81335
IIP3
D: Ldeg
B: Cmatch2
-4.64528
-4.91352
-5.18176
-5.45
-5.71824
Prediction -5.83

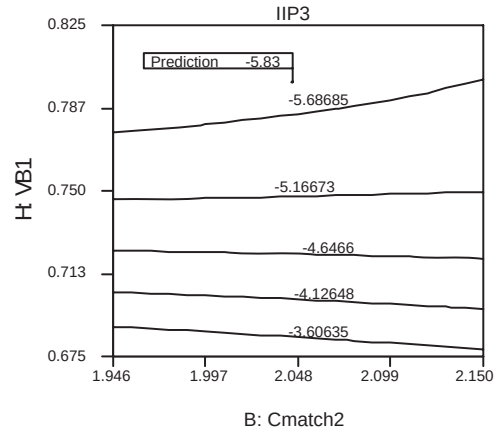
IIP3
Prediction -5.83
-5.68685
-5.16673
-4.6466
-4.12648
-3.60635
H: VB1
0.825
0.787
0.750
0.713
0.675
1.946
1.997
2.048
2.099
2.150
B: Cmatch2

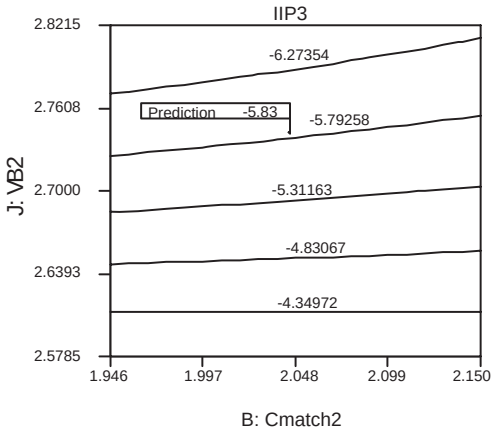
IIP3
-6.27354
Prediction -5.83
-5.79258
-5.31163
-4.83067
-4.34972
J: VB2
2.8215
2.7608
2.7000
2.6393
2.5785
1.946
1.997
2.048
2.099
2.150
B: Cmatch2

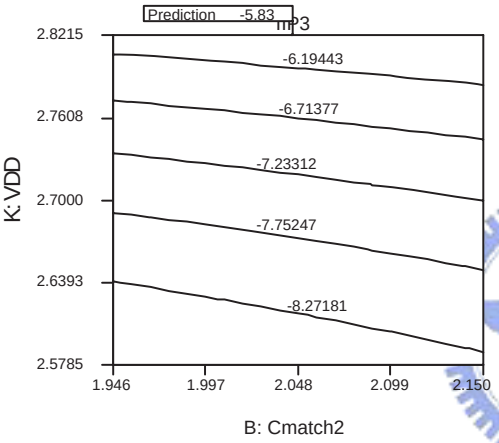
Prediction -5.83
IIP3
-6.19443
-6.71377
-7.23312
-7.75247
-8.27181
K: VDD
2.8215
2.7608
2.7000
2.6393
2.5785
1.946
1.997
2.048
2.099
2.150
B: Cmatch2

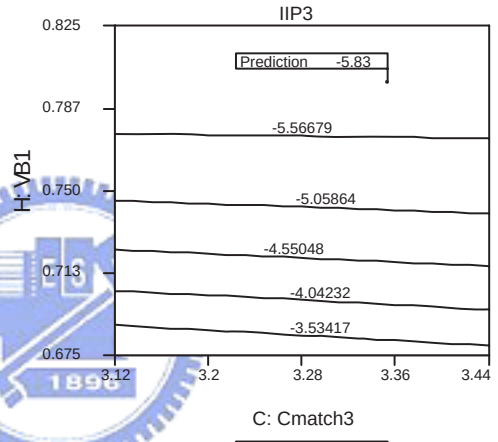
IIP3
Prediction -5.83
-5.56679
-5.05864
-4.55048
-4.04232
-3.53417
H: VB1
0.825
0.787
0.750
0.713
0.675
3.12
3.2
3.28
3.36
3.44
C: Cmatch3

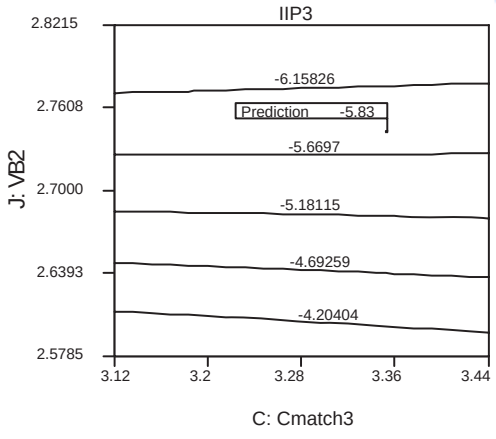
IIP3
-6.15826
Prediction -5.83
-5.6697
-5.18115
-4.69259
-4.20404
J: VB2
2.8215
2.7608
2.7000
2.6393
2.5785
3.12
3.2
3.28
3.36
3.44
C: Cmatch3

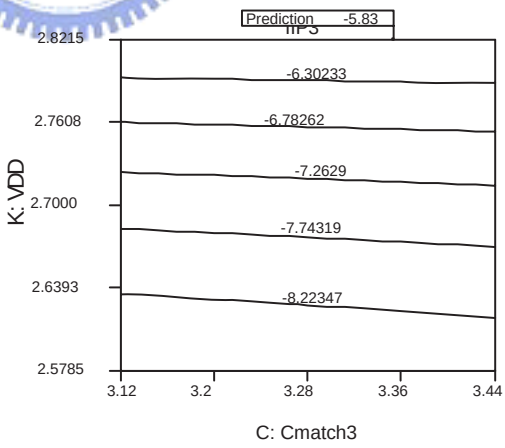
Prediction -5.83
IIP3
-6.30233
-6.78262
-7.2629
-7.74319
-8.22347
K: VDD
2.8215
2.7608
2.7000
2.6393
2.5785
3.12
3.2
3.28
3.36
3.44
C: Cmatch3

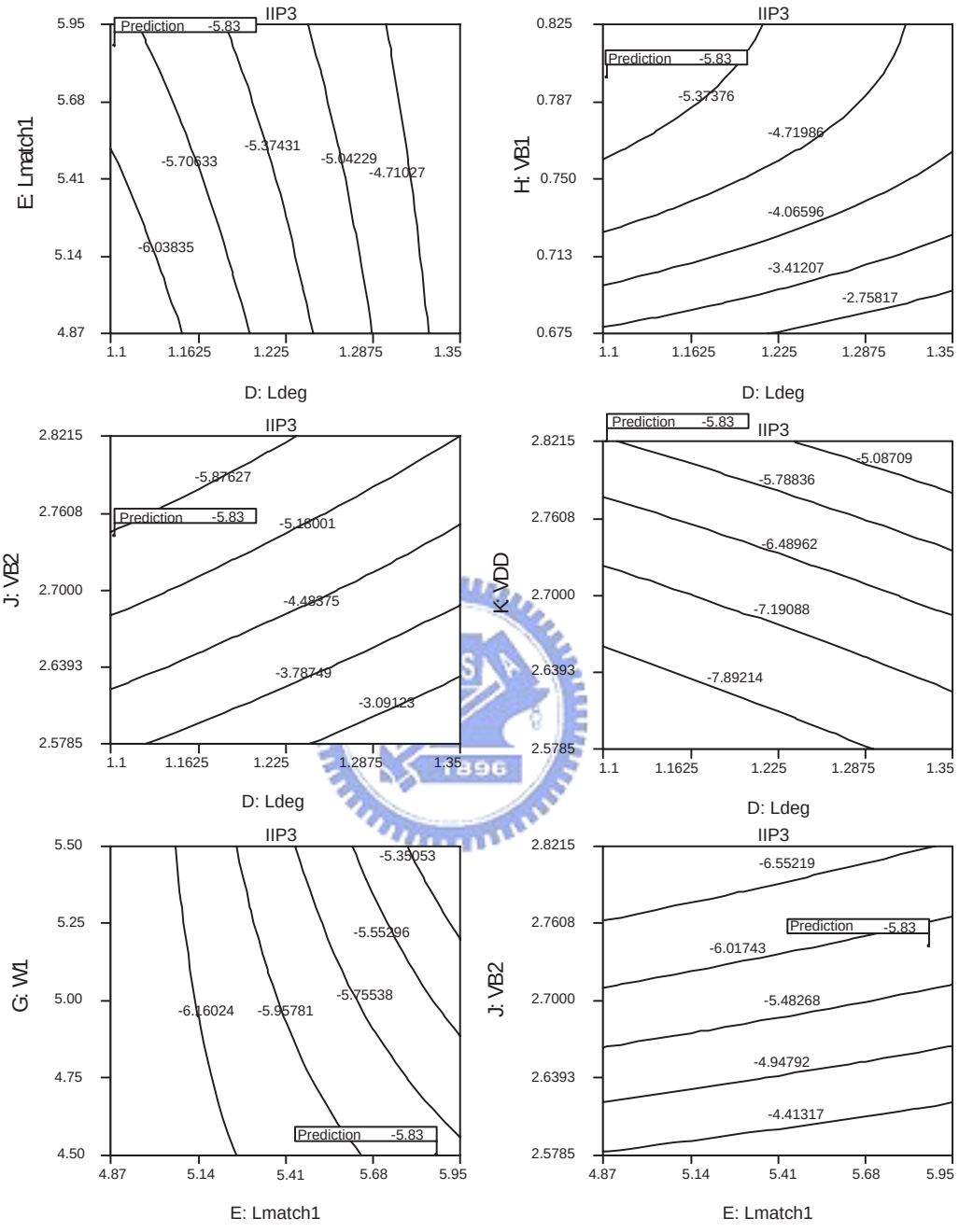
IIP3
Prediction -5.83
E: Lmatch1
D: Ldeg
-5.70633
-5.37431
-5.04229
-4.71027
-6.03835
IIP3
Prediction -5.83
H: VB1
D: Ldeg
-5.37376
-4.71986
-4.06596
-3.41207
-2.75817
IIP3
Prediction -5.83
J: VB2
D: Ldeg
-5.87627
-5.18001
-4.48375
-3.78749
-3.09123
IIP3
Prediction -5.83
K: VDD
D: Ldeg
-5.08709
-5.78836
-6.48962
-7.19088
-7.89214
IIP3
Prediction -5.83
G: W1
E: Lmatch1
-5.35053
-5.55296
-5.75538
-6.16024
-5.95781
IIP3
Prediction -5.83
J: VB2
E: Lmatch1
-6.55219
-6.01743
-5.48268
-4.94792
-4.41317

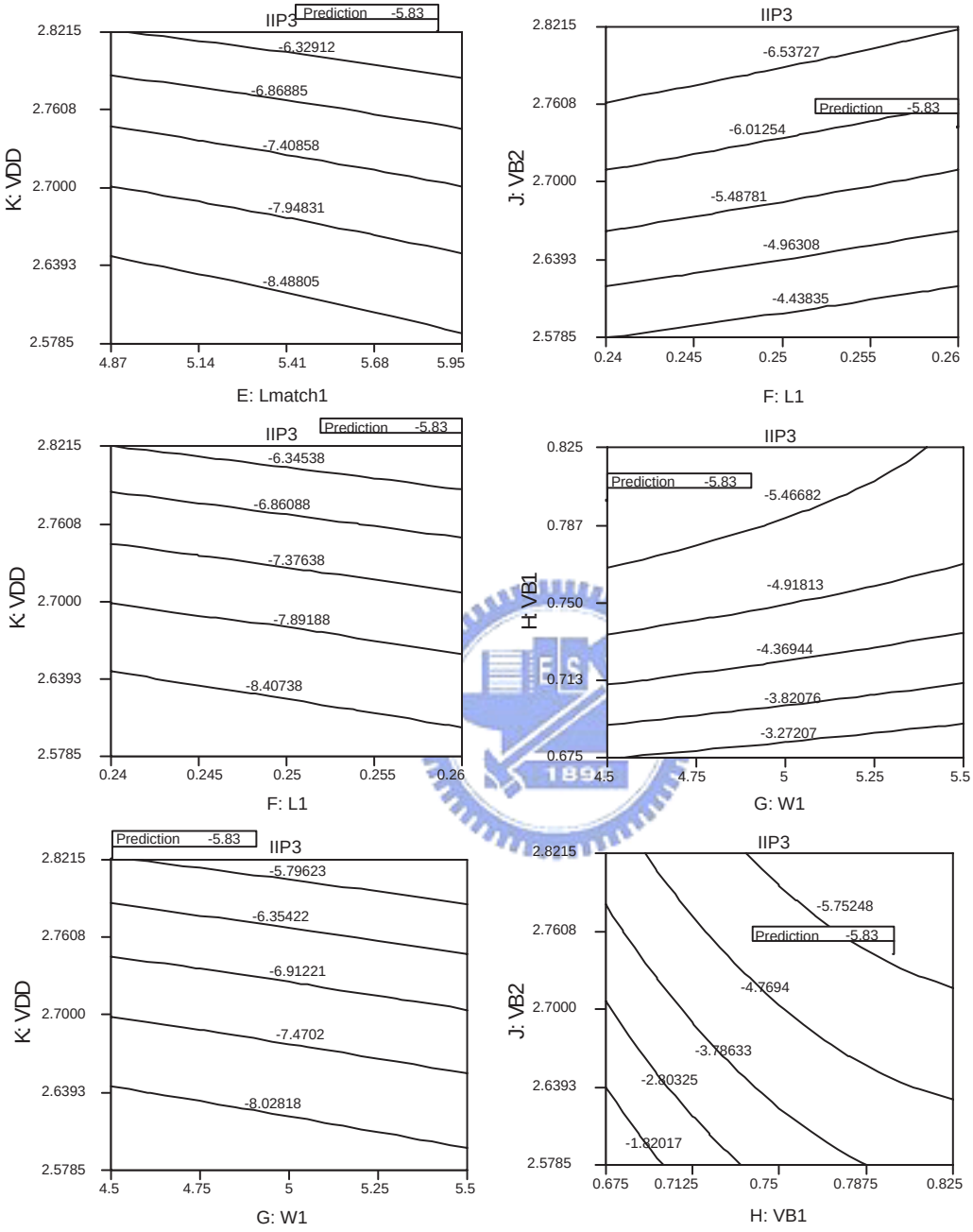
IIP3
Prediction -5.83
-6.32912
-6.86885
-7.40858
-7.94831
-8.48805
K: VDD
E: Lmatch1
IIP3
-6.53727
Prediction -5.83
-6.01254
-5.48781
-4.96308
-4.43835
J: VB2
F: L1
IIP3
Prediction -5.83
-6.34538
-6.86088
-7.37638
-7.89188
-8.40738
K: VDD
F: L1
IIP3
Prediction -5.83
-5.46682
-4.91813
-4.36944
-3.82076
-3.27207
H: VB1
G: W1
IIP3
Prediction -5.83
-5.79623
-6.35422
-6.91221
-7.4702
-8.02818
K: VDD
G: W1
IIP3
-5.75248
Prediction -5.83
-4.7694
-3.78633
-2.80325
-1.82017
J: VB2
H: VB1

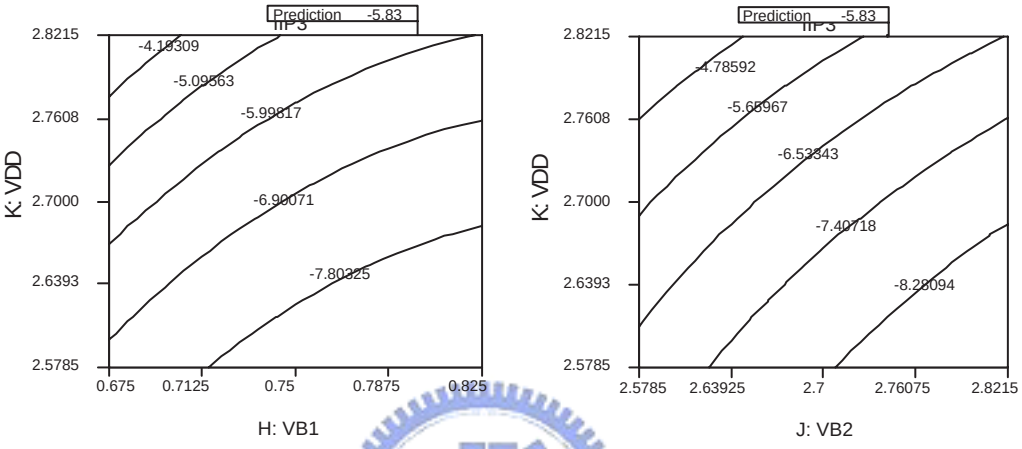

Figure A.1: Contour plots of the optimal recipe for the CCF Design. Plots 1-14, from the left column to the right one, are for S11; plots 15-34 are for S12; plots 35-60 are for S21; plots 61-74 are for S22; plots 75-92 are for K; plots 93-102 are for NF; and plots 103-126 are for IIP3. The X-axis and Y-axis are constraint of factors, and contour plots show the spread of seven circuit performance.

Appendix B

Netlist of LNA Circuit

In this appendix the netlists of the LNA circuit are shown below.

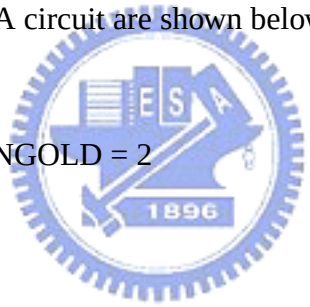

.options brief nomod accurate probe INGOLD = 2

.lib 'RFMODEL.l' TT_RFMOS

.lib 'RFMODEL.l' RF_MACRO

.global .param rfpower=-30 rfamp='sqrt(0.4*pwr(10,(rfpower/10)))' temperature=300

.inc "lnaparameters"

XLNA OUT VDD_L GND_L VB1 VB2 IN LNA

VRF IN2 GND sin(0 'rfamp' 2.15g 0 0 0) ac 1

VB1 VB1 GND 0.75

VB2 VB2 GND 2.7

```
VDD_L VDD_L GND 2.7

Vnull GND_L GND 0

Rout1 OUT GND 10MEG

Rsource IN IN2 50

Rstab IN GND 2K

.op

.net v(out) VRF rin=50 rout=50

.noise v(out) VRF 1

.probe noise inoise onoise

.probe nf=par('10*log10(inoise(m)*inoise(m)/(1.66e-20*50))')

.ac DEC 500 500meg 5g

.print noise(m)inoise onoise nf=par('10*log10(inoise(m)*inoise(m)/(1.66e-20*50))')

.end
```

To make a general working environment, a replacing mask scheme is proposed for simulation based circuit optimization. A example mask file is shown below:

```
.SUBCKT LNA OUT VDD_L GND_L VB1 VB2 IN

CCIN N_10 N_9 20p

CCMATCH1 N_10 IN $CCMATCH1$f
```

CCMATCH2 N_5 OUT $**CCMATCH2**$p

CCMATCH3 GND_L OUT $**CCMATCH3**$p

LLBOND N_9 N_6 $**LLBOND**$n

LLCHOKE VB1 N_6 1u

LLDEG N_8 GND_L $**LLDEG**$n

XLLOAD VDD_L N_5 spiral_turn

LLMATCH1 N_10 GND_L $**LLMATCH1**$n

XM1 N_7 N_6 N_8 GND_L NMOS_RFW5 LR=$**XM1L**$u WR=$**XM1W**$u NR=$**XM1N**$

XM2 N_5 VB2 N_7 GND_L NMOS_RFW5 LR=$**XM2L**$u WR=$**XM2W**$u NR=$**XM2N**$

XRRLOAD VDD_L N_5 spiral_turn

.ENDS LNA

As shown above the keyword covered with $ is the position where parameters should paste on. The RF compact spice netlist we apply is show below.

mcore n1 n2 n3 n4 nch_rf33w5 w=5u l=lr m=nr ad=0.0 as=0.0 pd=0.0 ps=0.0

rd D n1 1e-5

rg G n2 ’(0.175+173.8/nr-9.532/(nr*lr*1e6))*nmos_rgfac’

rs S n3 ’1.3574/(log10(nr/2+1.0))+1.26722’

rsub1 n6 n4 ’(99.5294/nr-0.11765)*nmos_rsubfac’

rsub2 n5 n4 ’(99.5294/nr-0.11765)*nmos_rsubfac’

rsub3 n4 B ’(-42.43+5469.1/nr)*nmos_rsubfac’

rds n7 n3’373.76-34.76/(nr*sqrt(lr*1e6))’

ddb n6 n1 ndio_rf33w5 area=’nr/2.0*0.82u*5u’ pj=’nr*(0.82u+5u)’

dsb n5 n3 ndio_rf33w5 area=’(nr/2.0+1.0)*0.82u*5u’ pj=’(nr/2+1.0)*(0.82u+5u)*2’

cds n1 n7 ’(-7.87+0.873*nr/sqrt(lr*1.0e6))*1.0e-15’

Appendix C

Netlist of SRAM Cells

In this appendix the netlists of SRAM Cells are shown below.

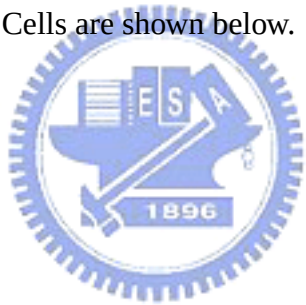

(1) The netlist of 6-T SRAM

.protect

.lib ’cln651p_1k_postsim_V1d0.l’ tt

.unprotect

.options post = 2 acct = 2 dccap = 1 nomod

.global vdd! gnd!

.param gnd! = 0 sup = $**sup**$ vdd vdd! 0 DC sup

vw1 4 0 DC sup

vb1 5 0 DC sup

vb1b 6 0 DC sup

M1 3 2 gnd! gnd! nch w = 1u l = $**L1**$

M2 2 3 gnd! gnd! nch w = 1u l = $**L2**$

M3 5 4 2 gnd! nch w = 1u l = $**L3**$

M6 3 4 6 gnd! nch w = 1u l = $**L3**$

M4 3 2 vdd! vdd! pch w = 1u l = $**L3**$

M5 2 3 vdd! vdd! pch w = 1u l = $**L3**$

vq 2 0

.DC vq 0 sup 0.0012 *sweep ln1 60n 70n 1n

.END

(2) The netlist of 4-T SRAM

.protect

.lib ’cln651p_1k_postsim_V1d0.l’ tt

.unprotect

.options post = 2 acct = 2 nomod

.global vdd! gnd!

.param gnd! = 0 sup = $**sup**$

vw1 4 0 DC gnd!

vb1 5 0 DC sup

vb1b 6 0 DC sup

M1 3 2 gnd! gnd! nch w = 1u l = $**L1**$

M2 2 3 gnd! gnd! nch w = 1u l = $**L2**$

M3 4 6 6 pch w = 1u l = $**L3**$

M4 2 4 5 5 pch w = 1u l = $**L3**$

vq 2 0

.DC vq 0 sup 0.0011 *sweep ln1 60n 70n 1n

.END

As shown above the keyword covered with $ is the position where parameters should paste on.

Appendix D

A Example of Design Expert 6.0.6

1. Execute Design-Expert 6.0.6 Trial

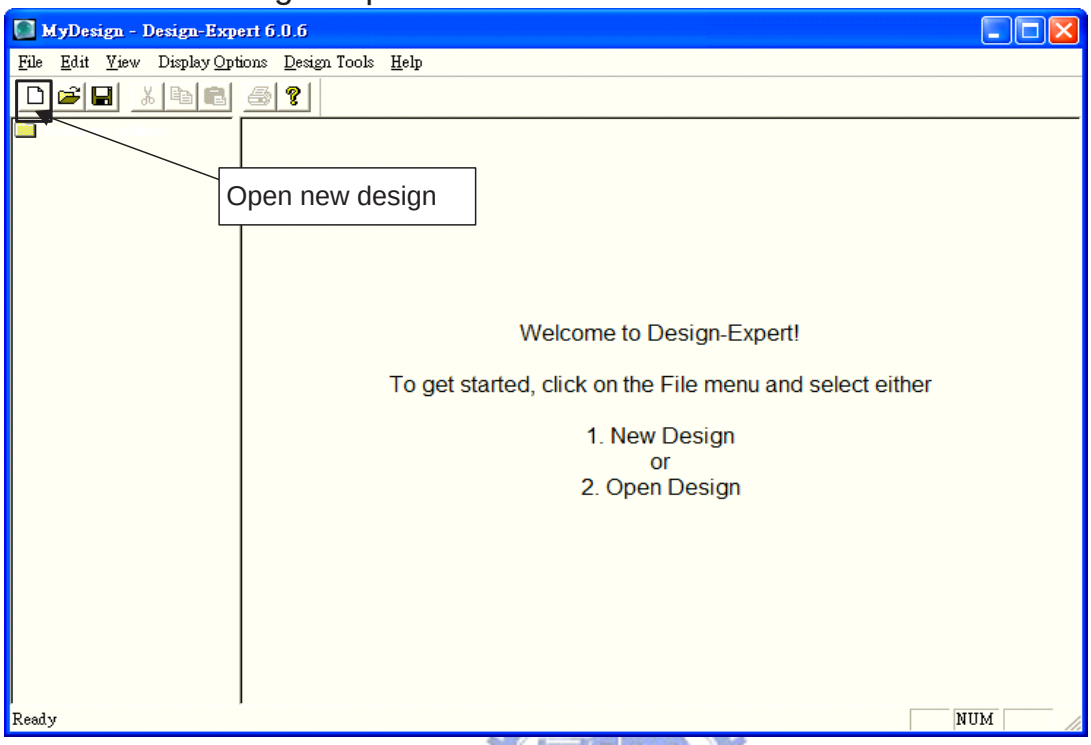

2. Choose one design

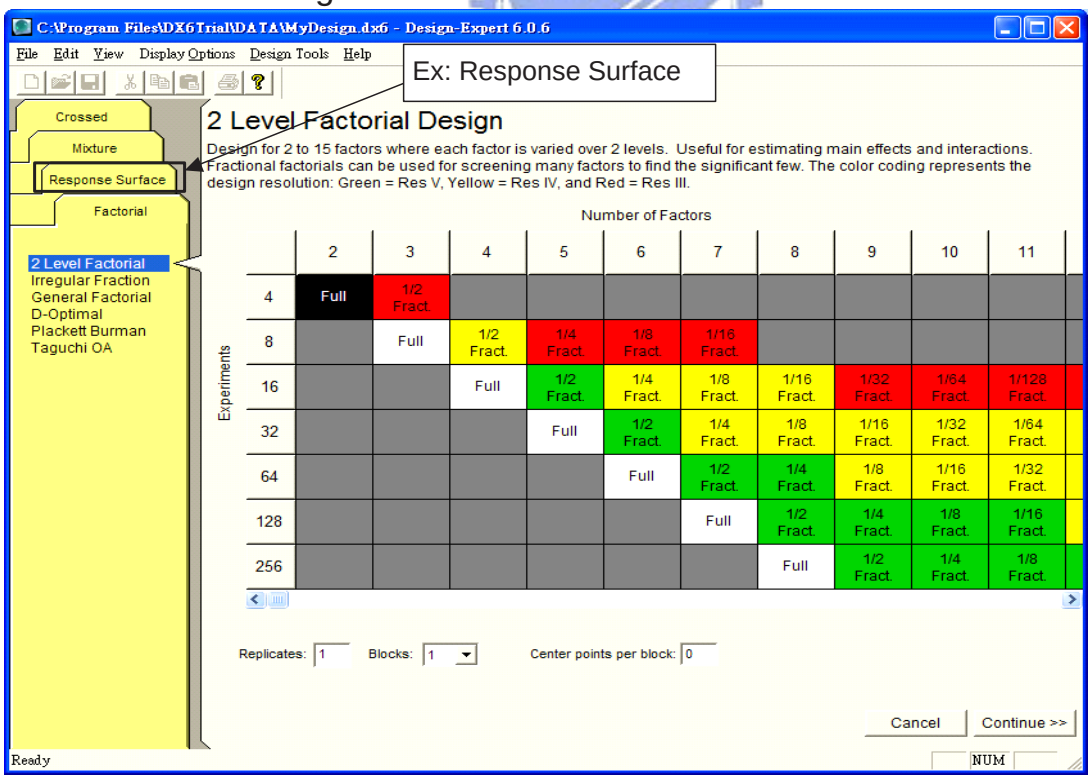

3. Determine the number of factors

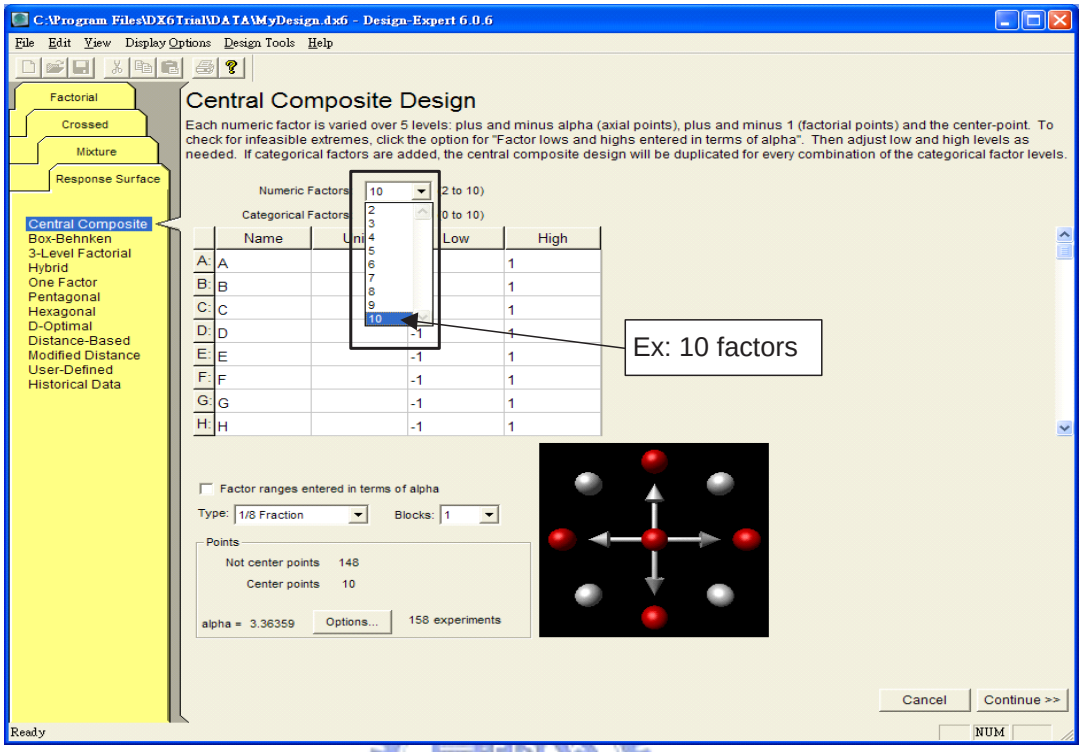

4. Key in the factor names

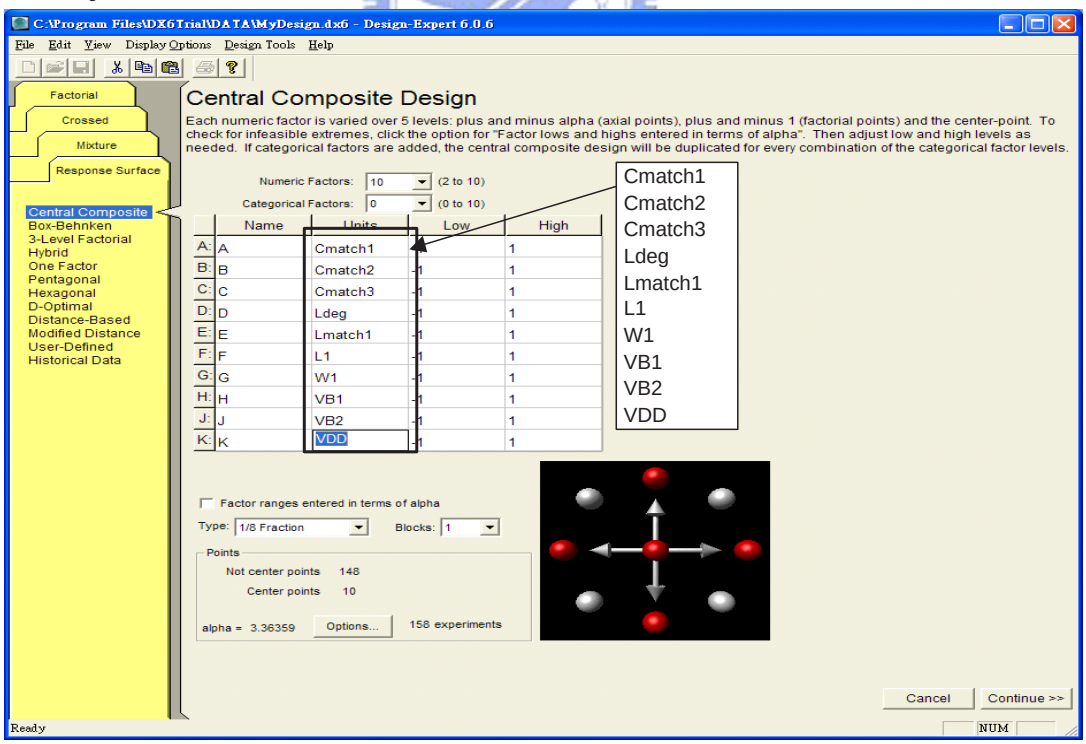

5. Key in natural values

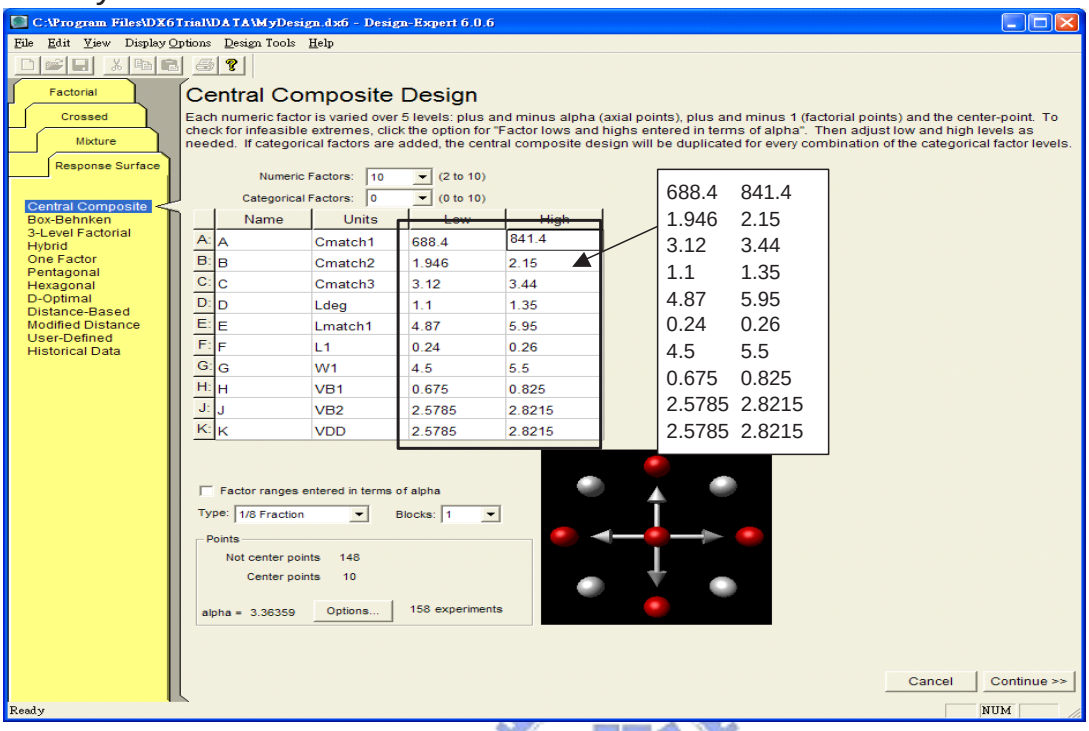

6. Choose one type of design

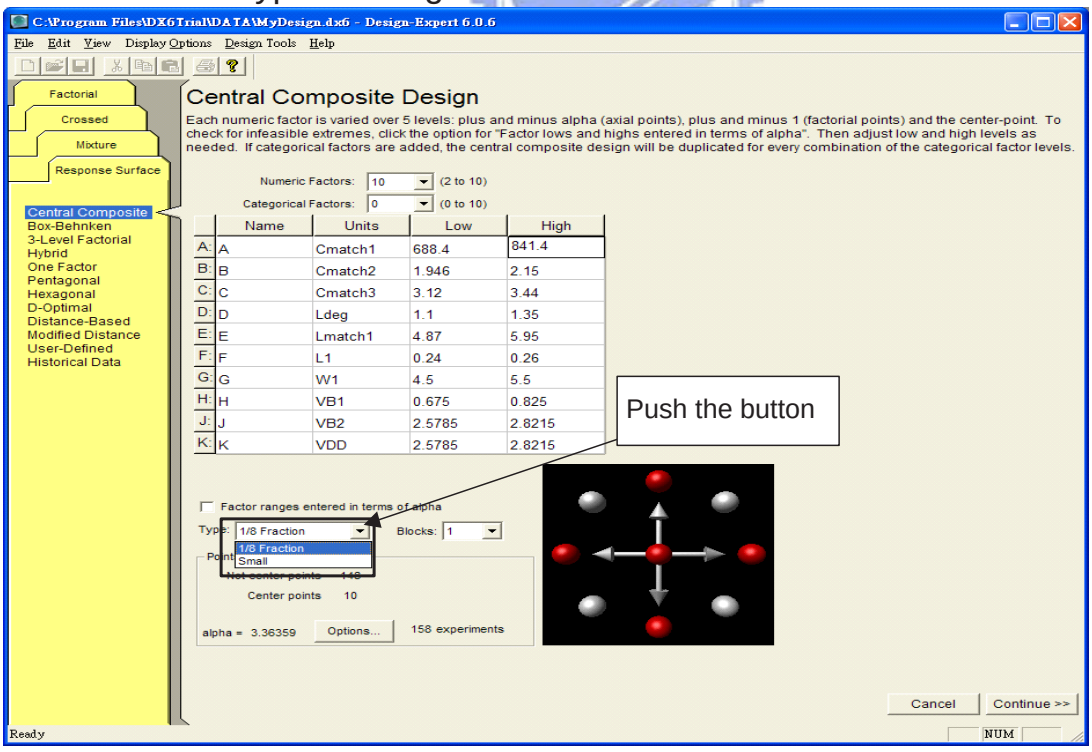

7. Determine the replication of the center points

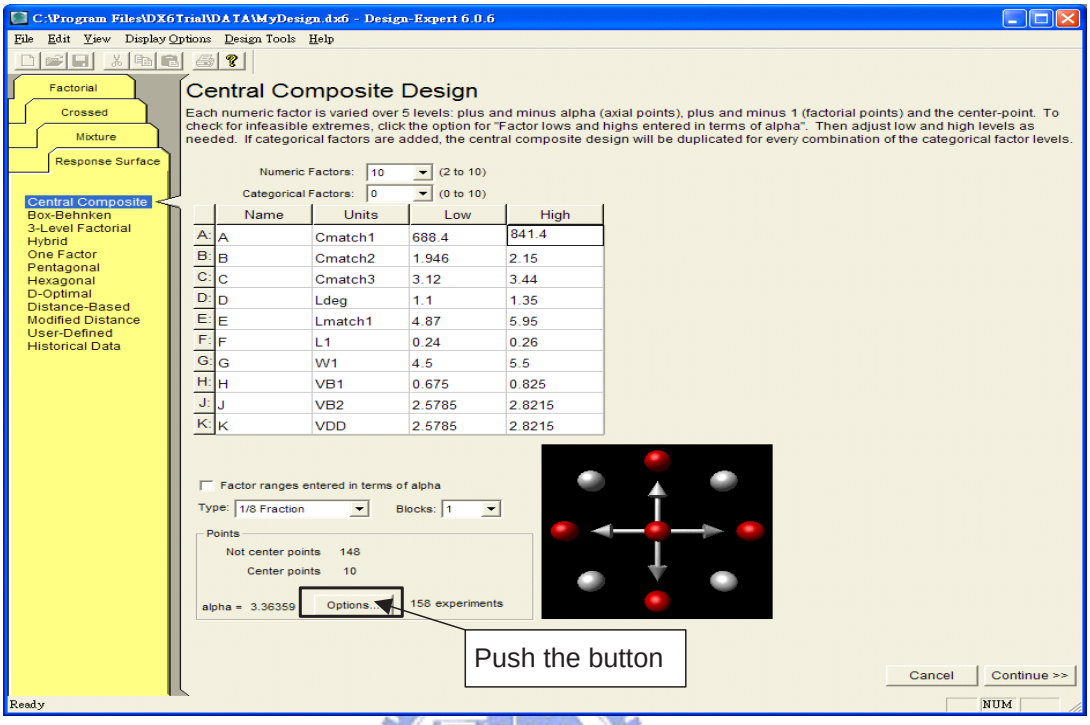

8. Change the replication of the center points

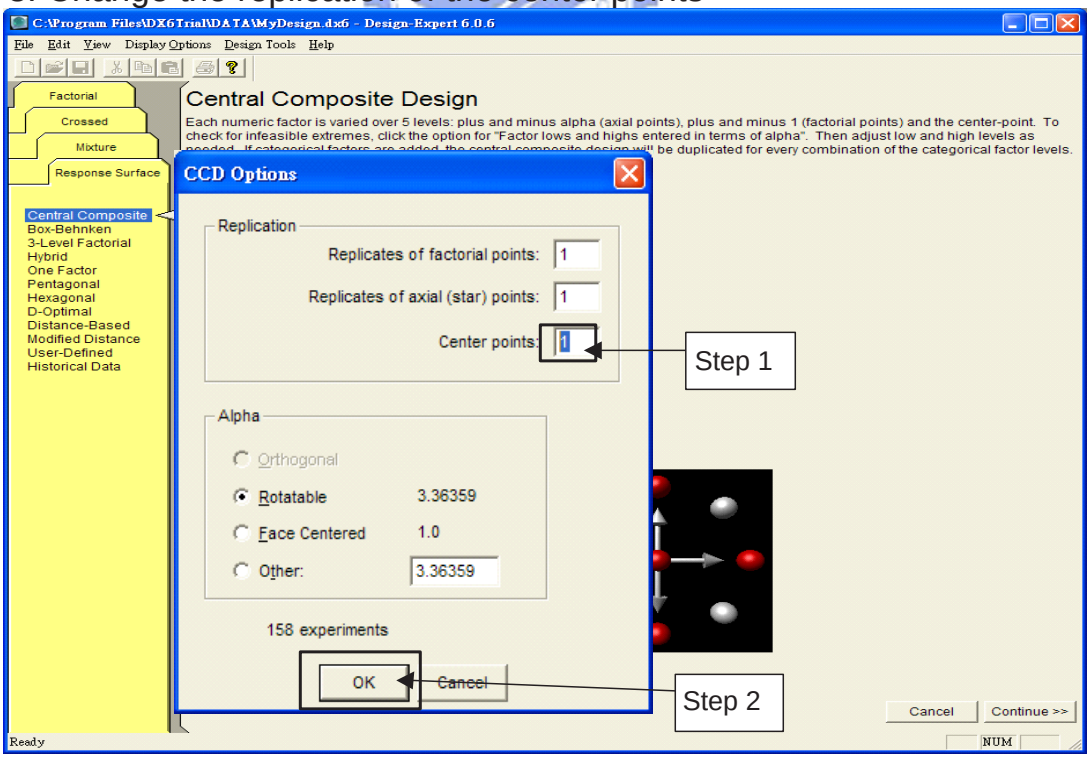

9. Finish design matrix construction, next step

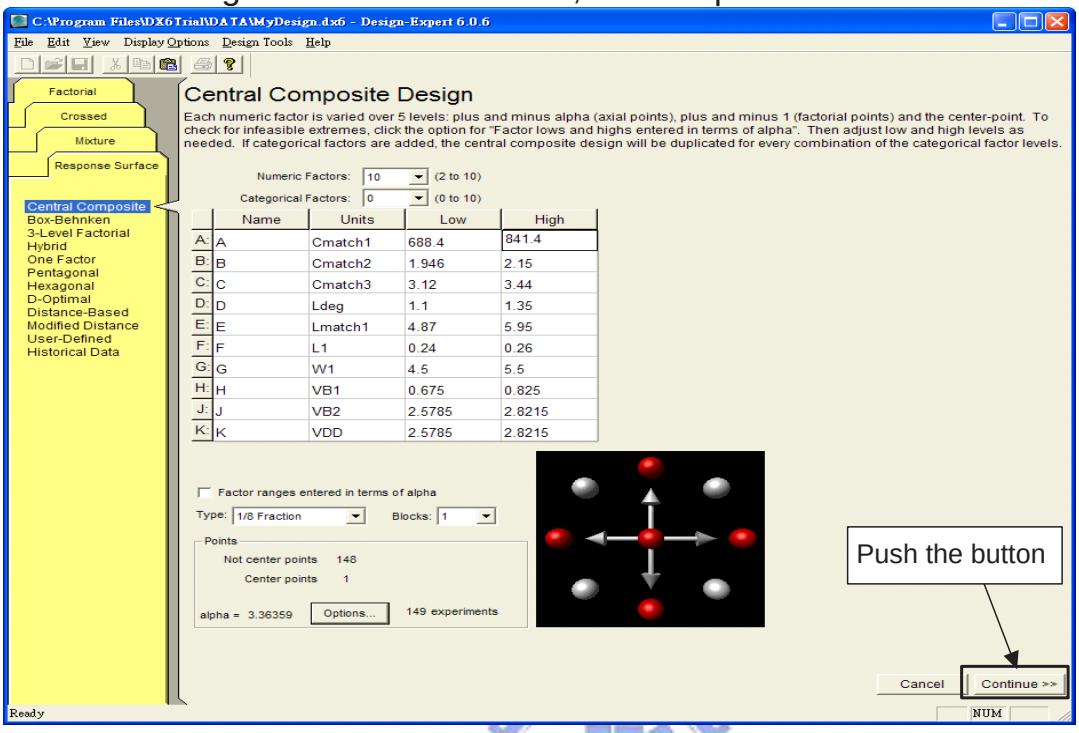

10. Determine the number of responses

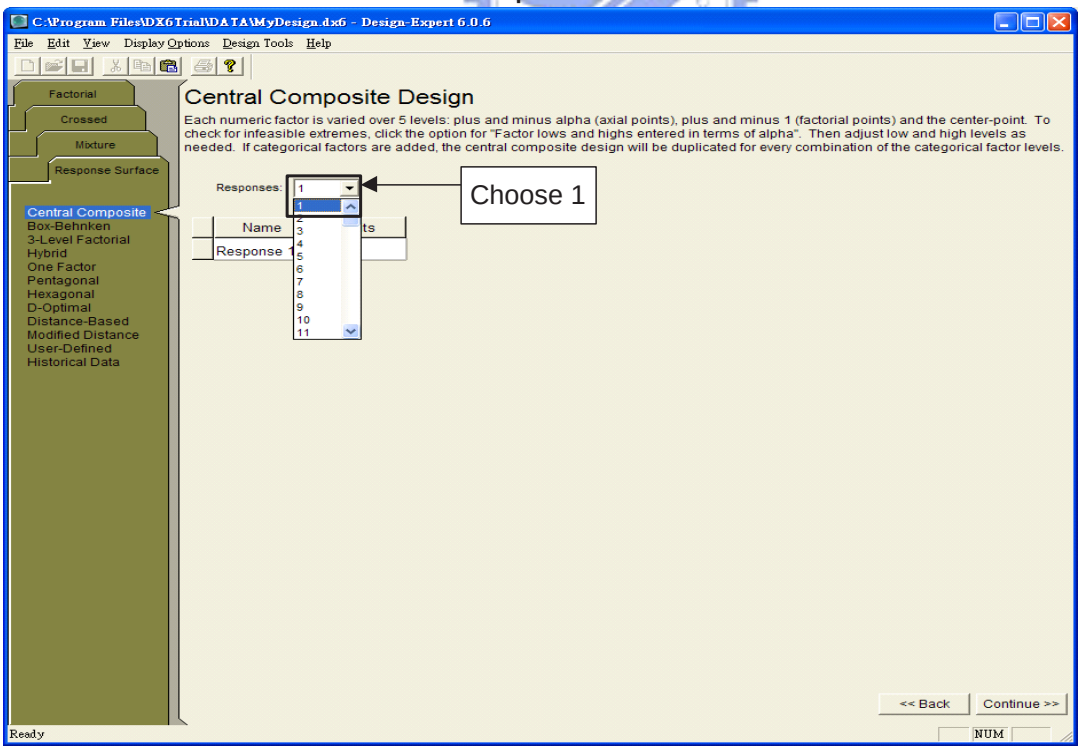

11. Input the response name

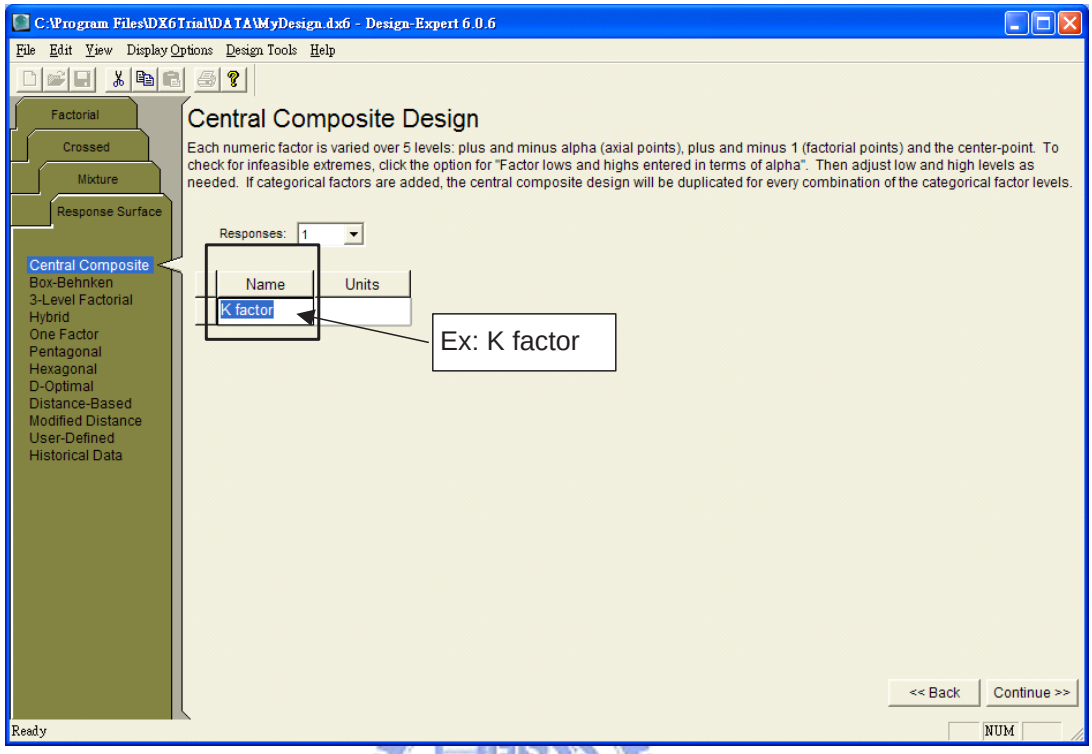

12. Finish response construction, next step

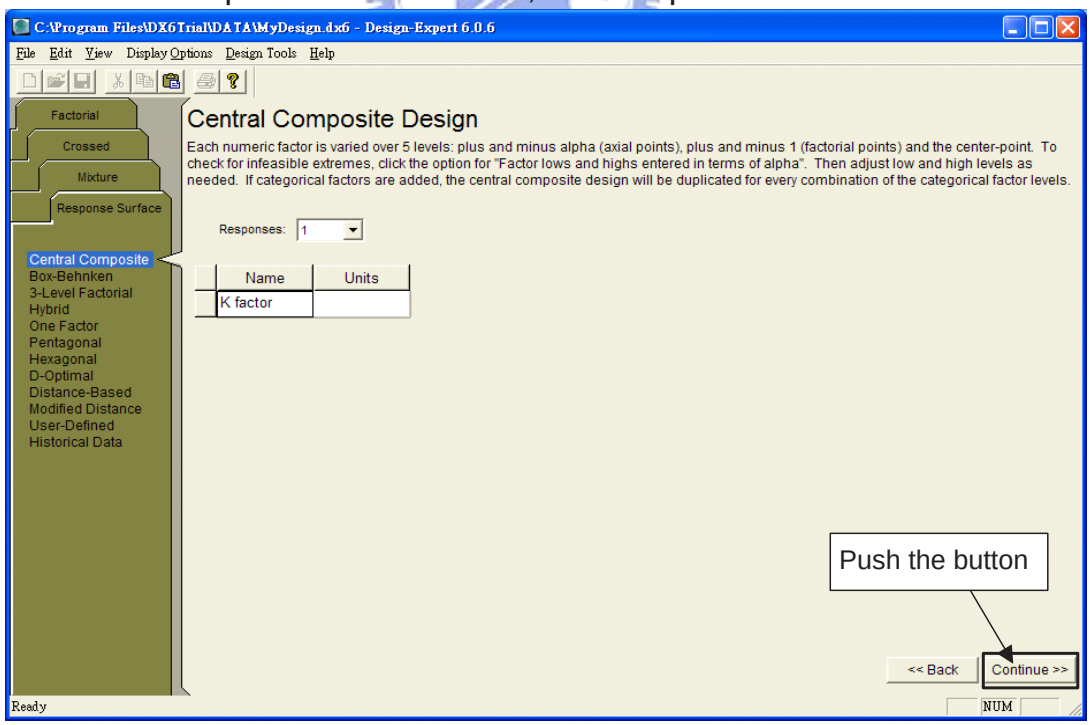

13. Key in the response values according to design matrix

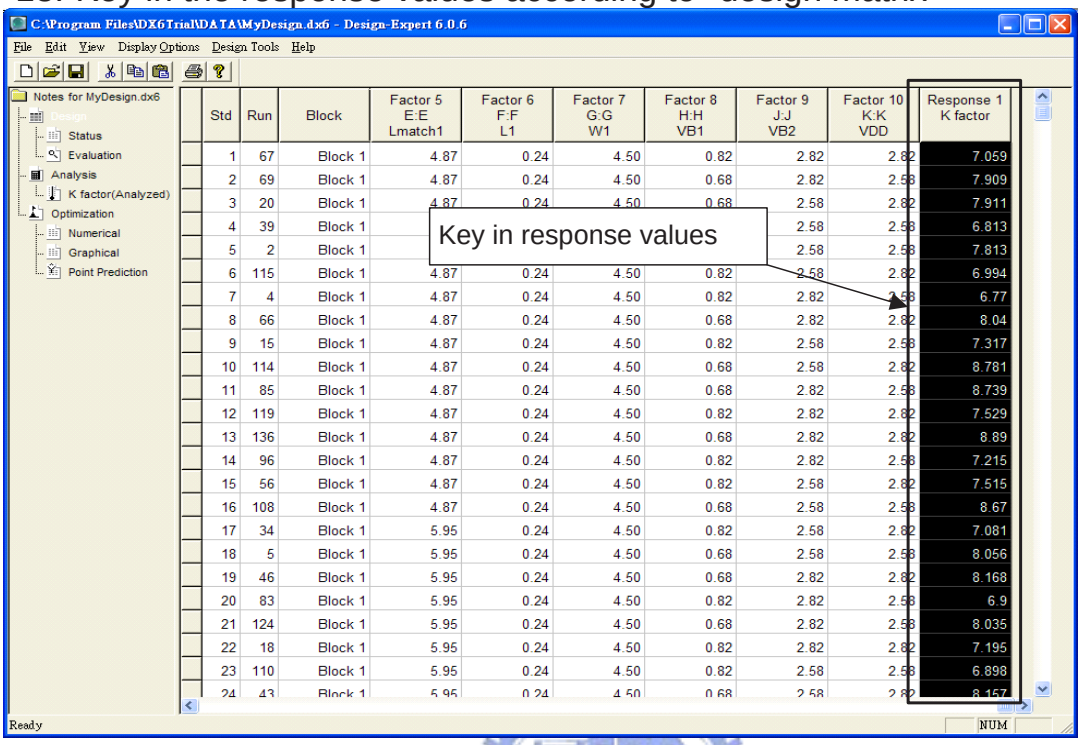

Std	Run	Block	Factor 5 E:E Lmatch1	Factor 6 F:F L1	Factor 7 G:G W1	Factor 8 H:H VB1	Factor 9 J:J VB2	Factor 10 K:K VDD	Response 1 K factor
1	67	Block 1	4.87	0.24	4.50	0.82	2.82	2.82	7.059
2	69	Block 1	4.87	0.24	4.50	0.68	2.82	2.58	7.909
3	20	Block 1	4.87	0.24	4.50	0.68	2.58	2.82	7.911
4	39	Block 1					2.58	2.58	6.813
5	2	Block 1					2.58	2.58	7.813
6	115	Block 1	4.87	0.24	4.50	0.82	2.58	2.82	6.994
7	4	Block 1	4.87	0.24	4.50	0.82	2.82	2.58	6.77
8	66	Block 1	4.87	0.24	4.50	0.68	2.82	2.82	8.04
9	15	Block 1	4.87	0.24	4.50	0.82	2.58	2.58	7.317
10	114	Block 1	4.87	0.24	4.50	0.68	2.58	2.82	8.781
11	85	Block 1	4.87	0.24	4.50	0.68	2.82	2.58	8.739
12	119	Block 1	4.87	0.24	4.50	0.82	2.82	2.82	7.529
13	136	Block 1	4.87	0.24	4.50	0.68	2.82	2.82	8.89
14	96	Block 1	4.87	0.24	4.50	0.82	2.82	2.58	7.215
15	56	Block 1	4.87	0.24	4.50	0.82	2.58	2.82	7.515
16	108	Block 1	4.87	0.24	4.50	0.68	2.58	2.58	8.67
17	34	Block 1	5.95	0.24	4.50	0.82	2.58	2.82	7.081
18	5	Block 1	5.95	0.24	4.50	0.68	2.58	2.58	8.056
19	46	Block 1	5.95	0.24	4.50	0.68	2.82	2.82	8.168
20	83	Block 1	5.95	0.24	4.50	0.82	2.82	2.58	6.9
21	124	Block 1	5.95	0.24	4.50	0.68	2.82	2.58	8.035
22	18	Block 1	5.95	0.24	4.50	0.82	2.82	2.82	7.195
23	110	Block 1	5.95	0.24	4.50	0.82	2.58	2.58	6.898
24	43	Block 1	5.95	0.24	4.50	0.68	2.58	2.82	8.157

14. Design summary

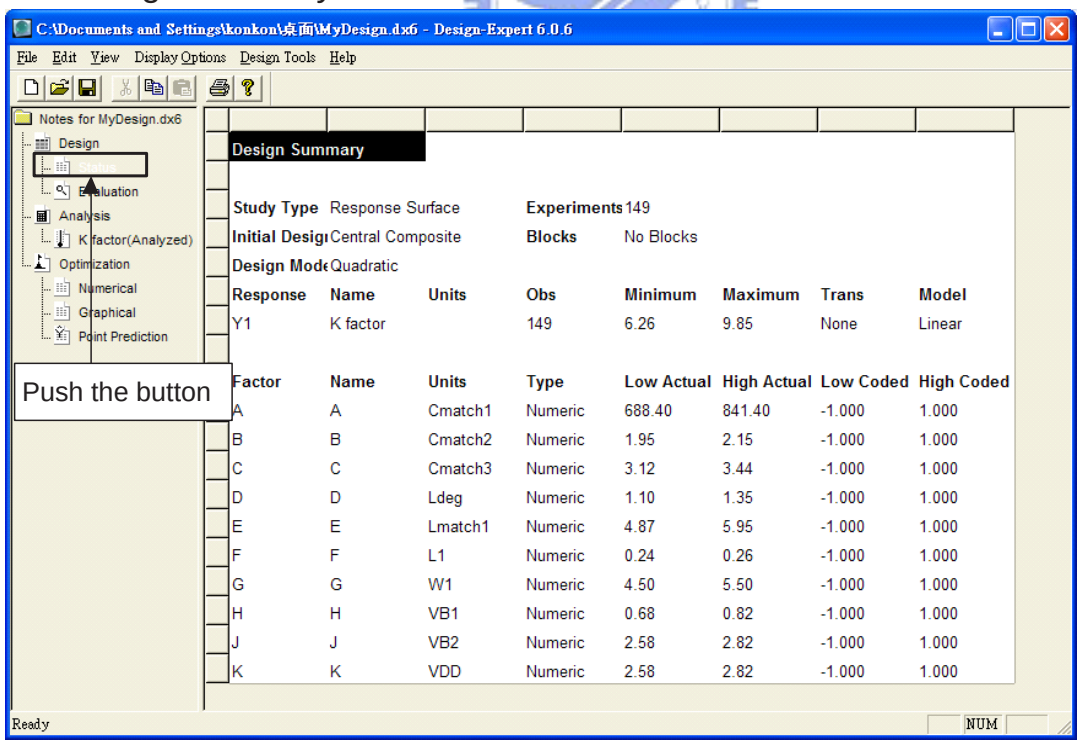

15. Construct model

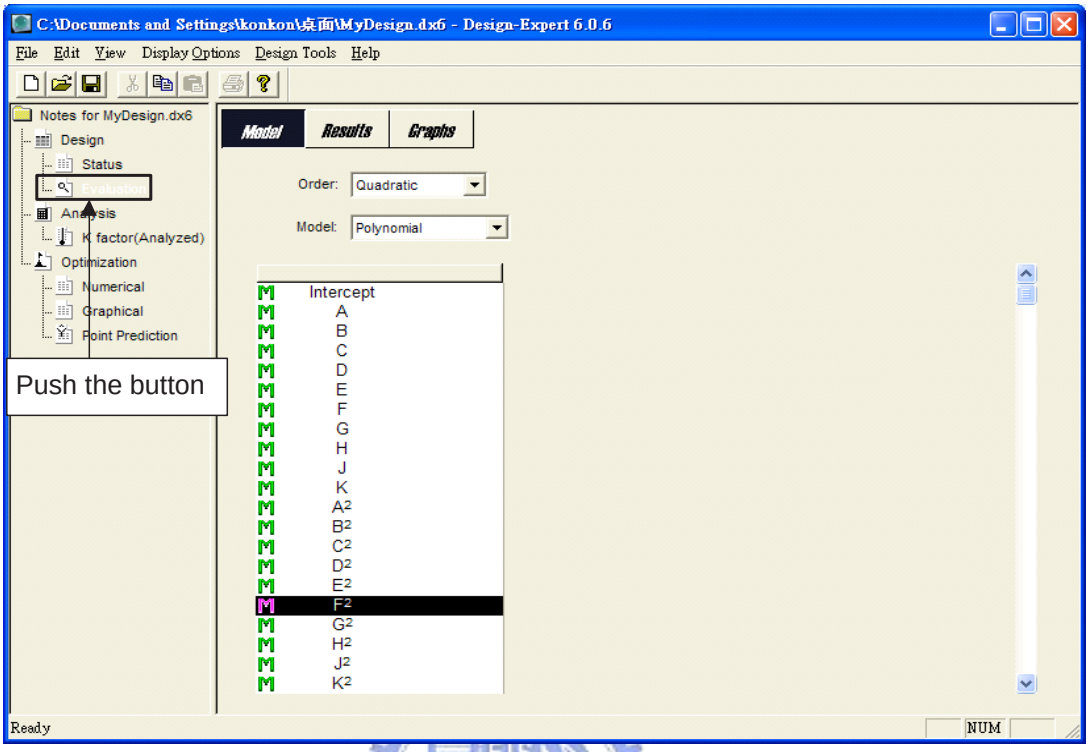

16. Choose one model type

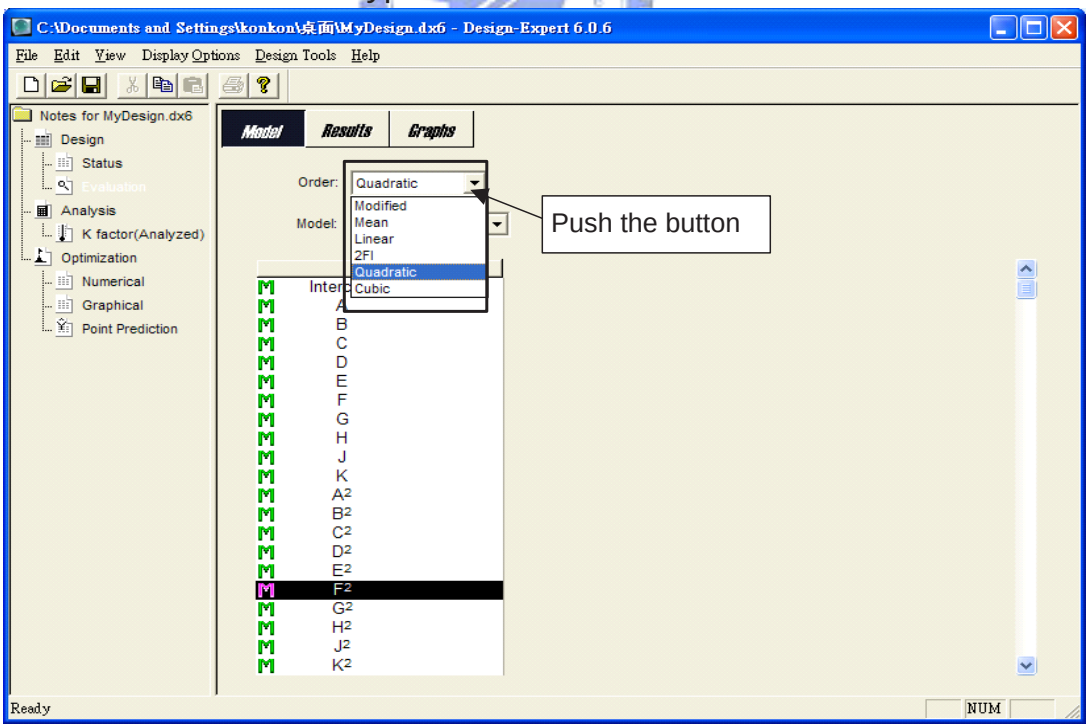

17. Model summary

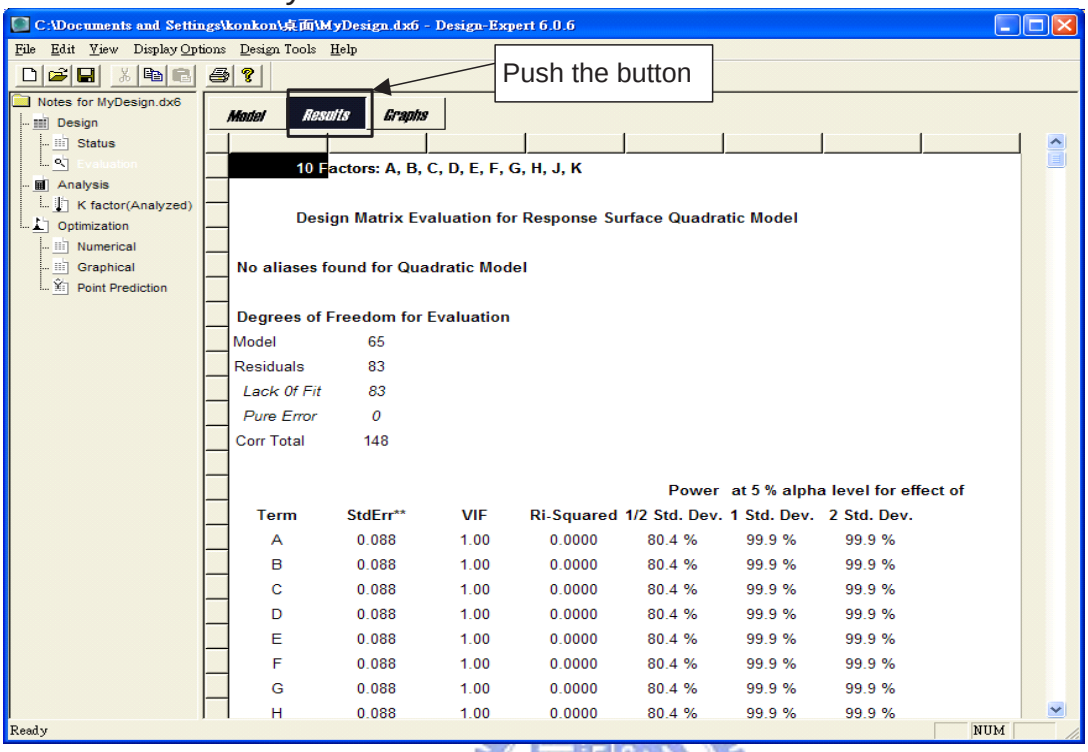

18. Graph of model summary

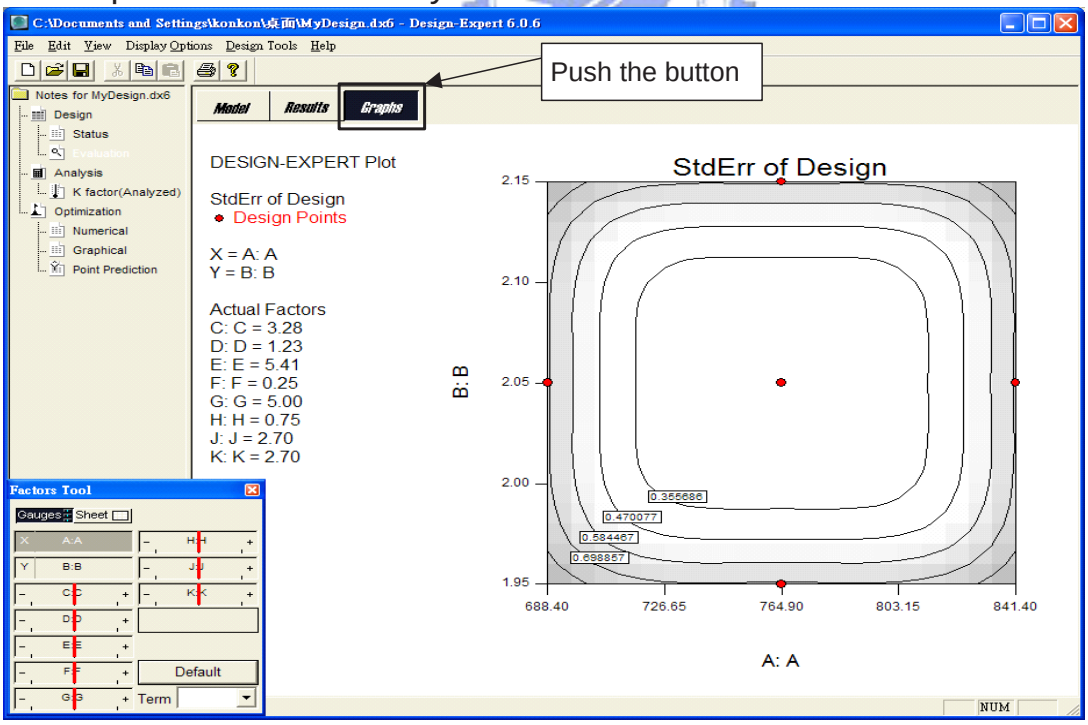

19. Start to estimate the surface response model

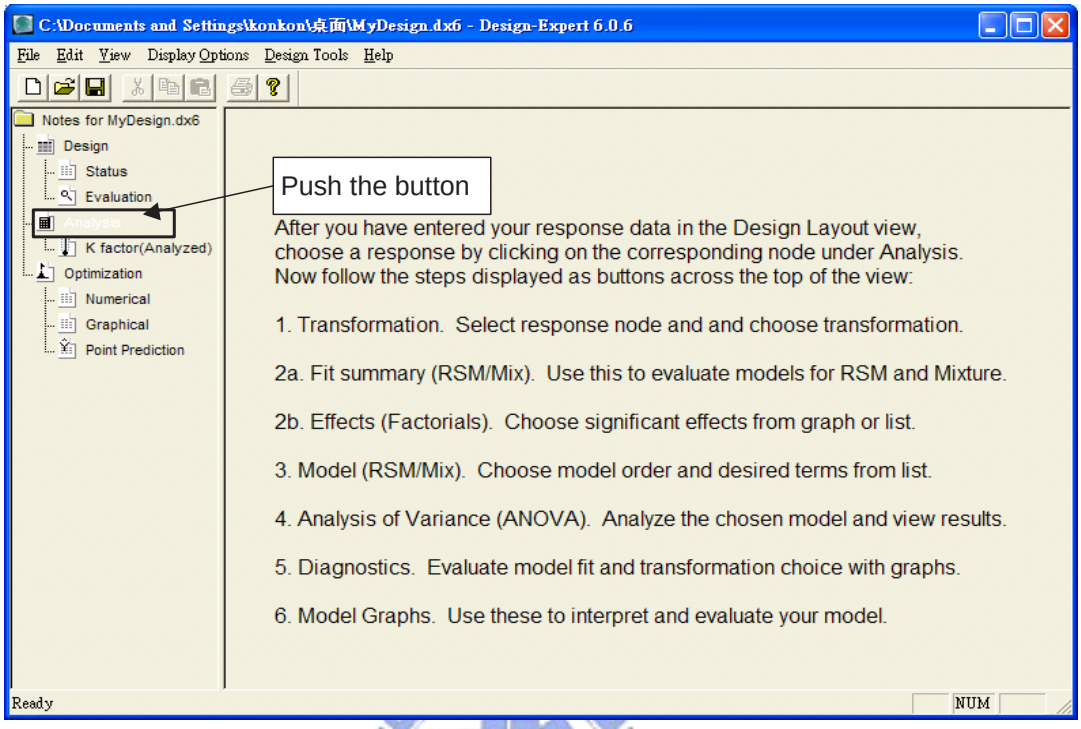

20. Transformation of the response or not

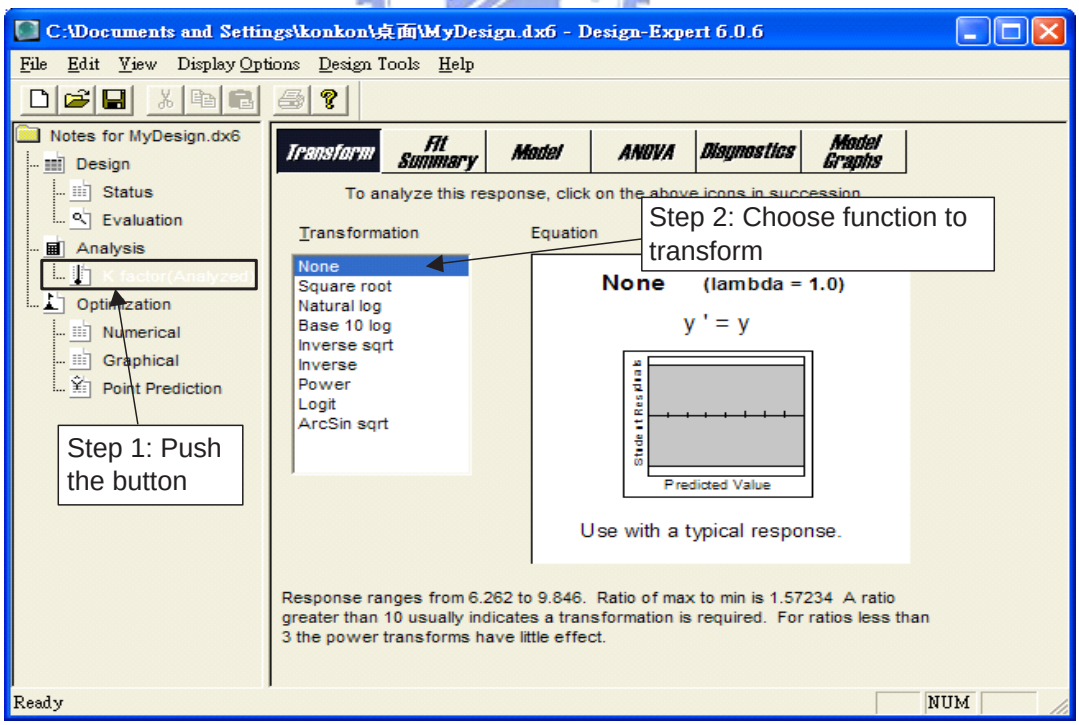

21. Observe the initial result

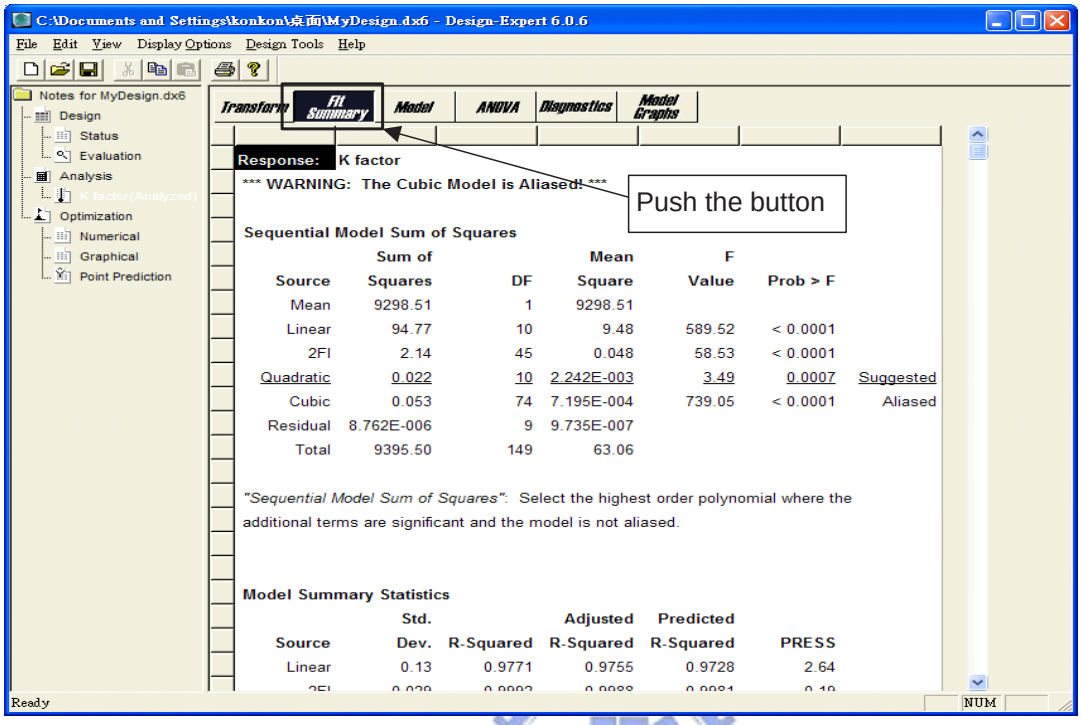

22. Choose one type of the response surface model

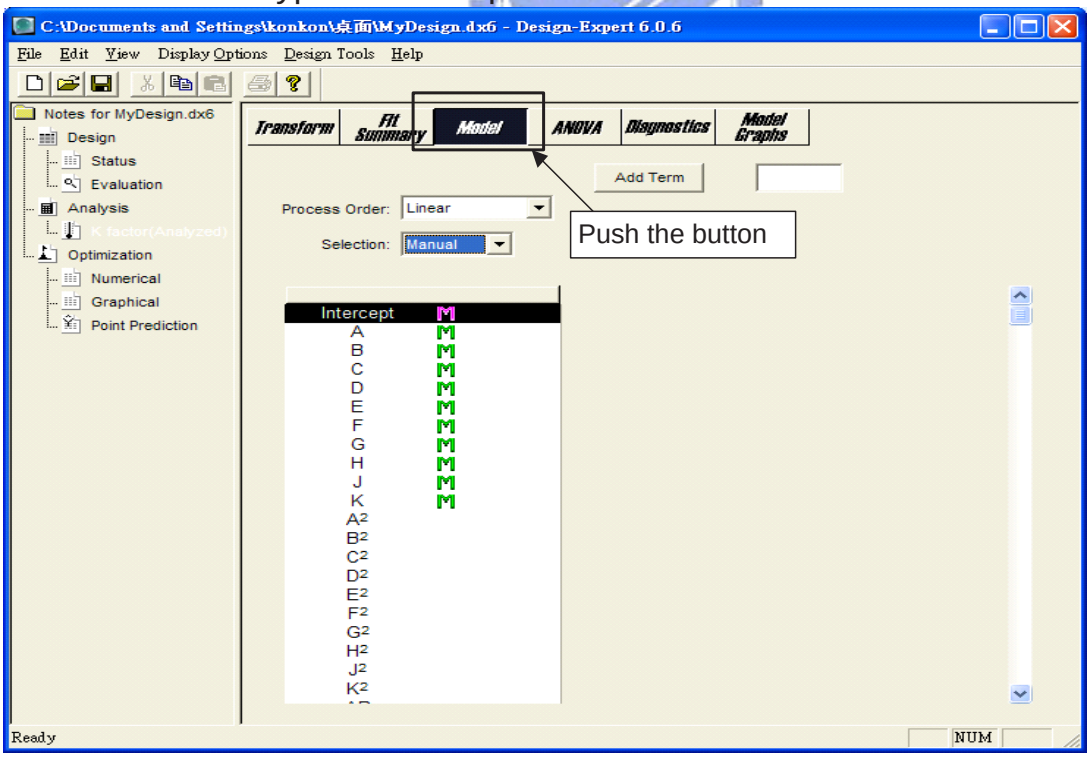

23. Change linear model to a 2 nd order model

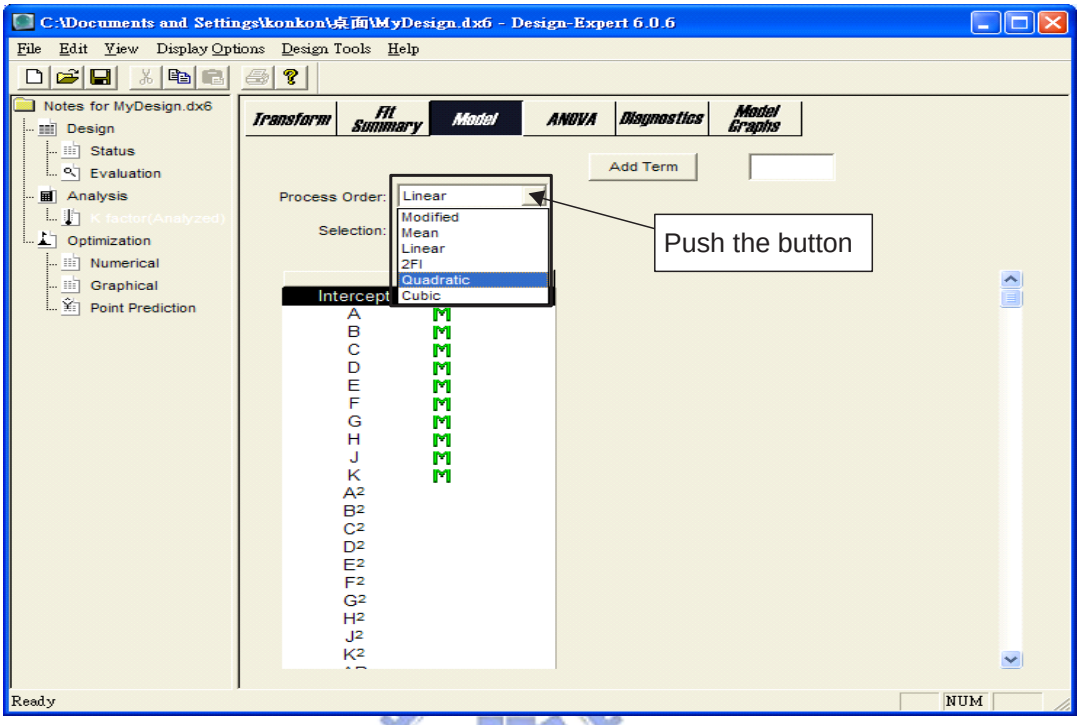

24. Complete the 2 order model construction

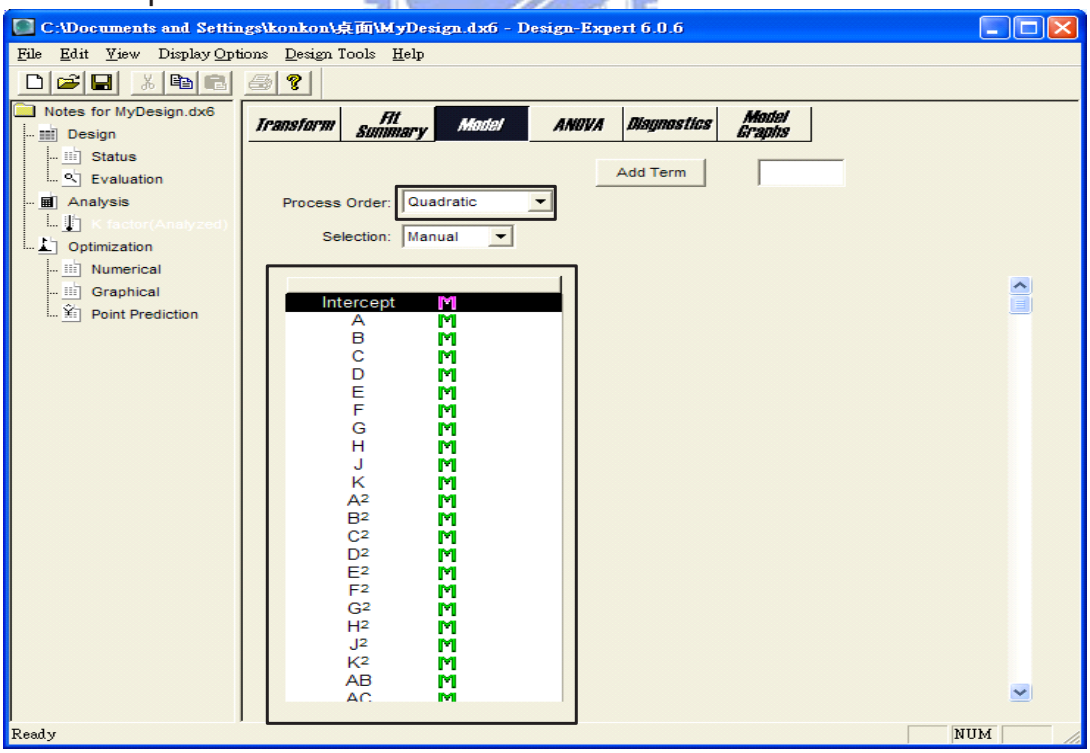

25. Observe the ANOVA table

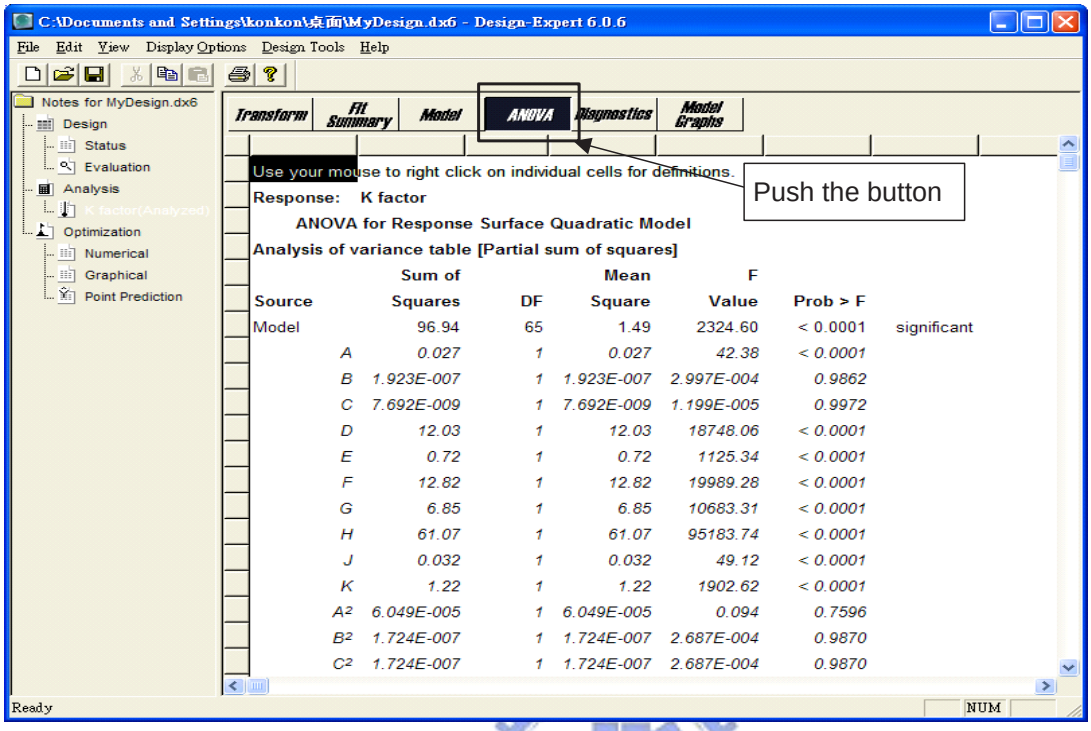

26. Normal plot of residuals

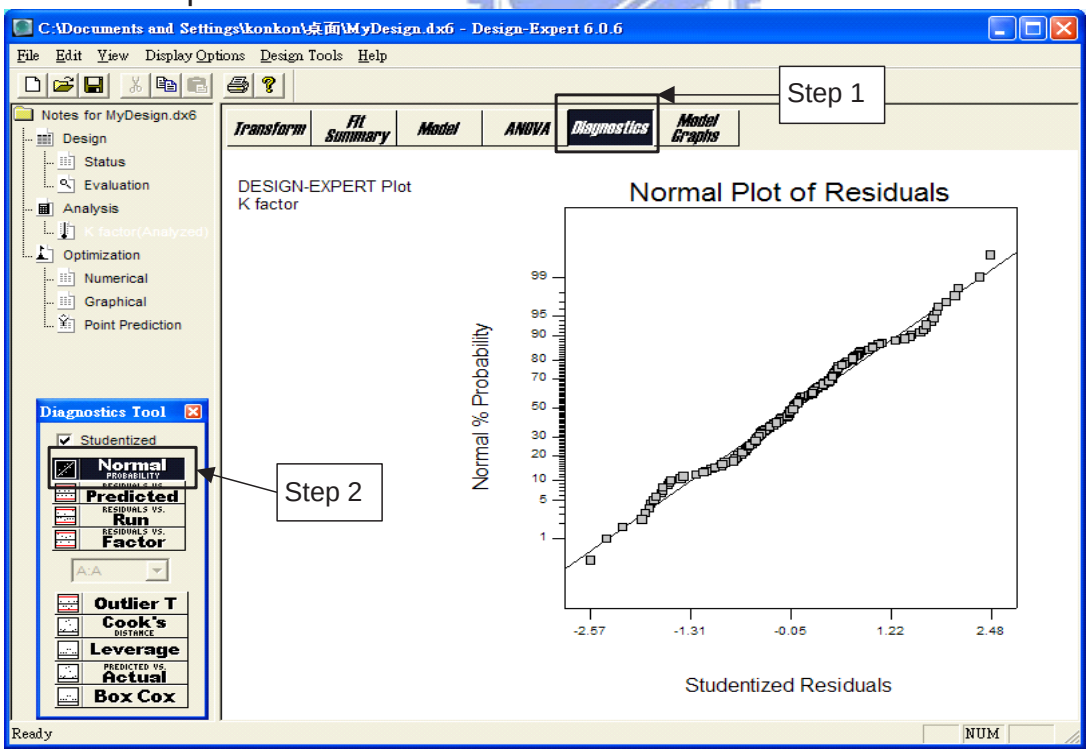

27. Scatter plot of residuals versus the predicted values

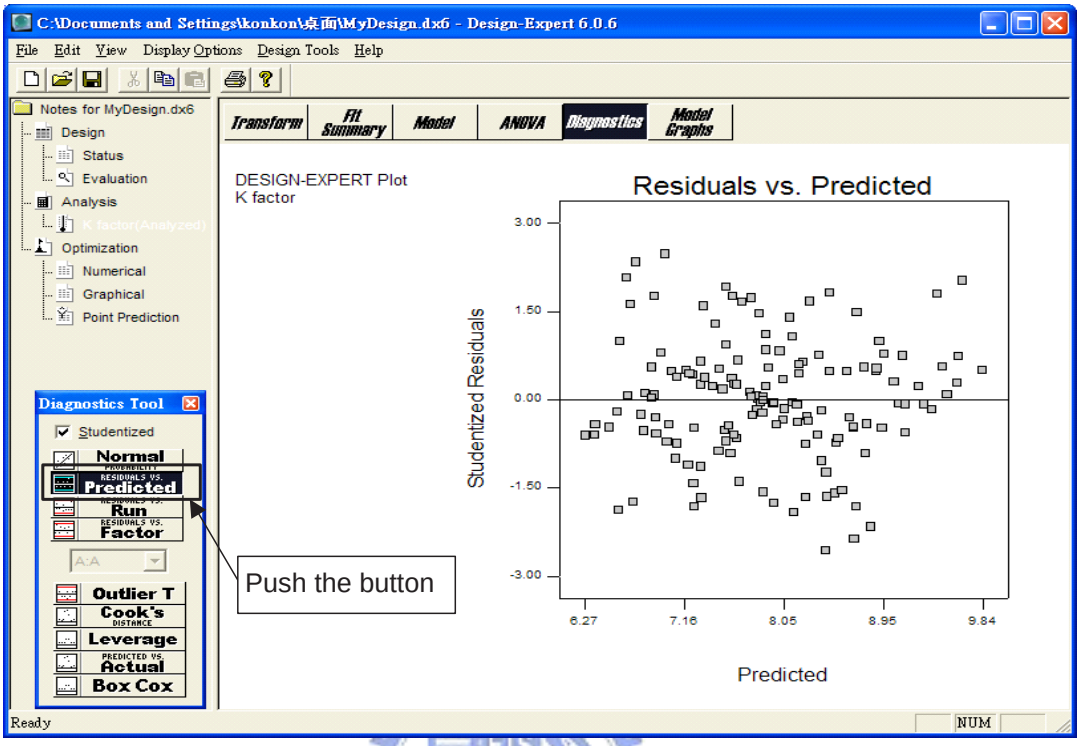

28. Other plots

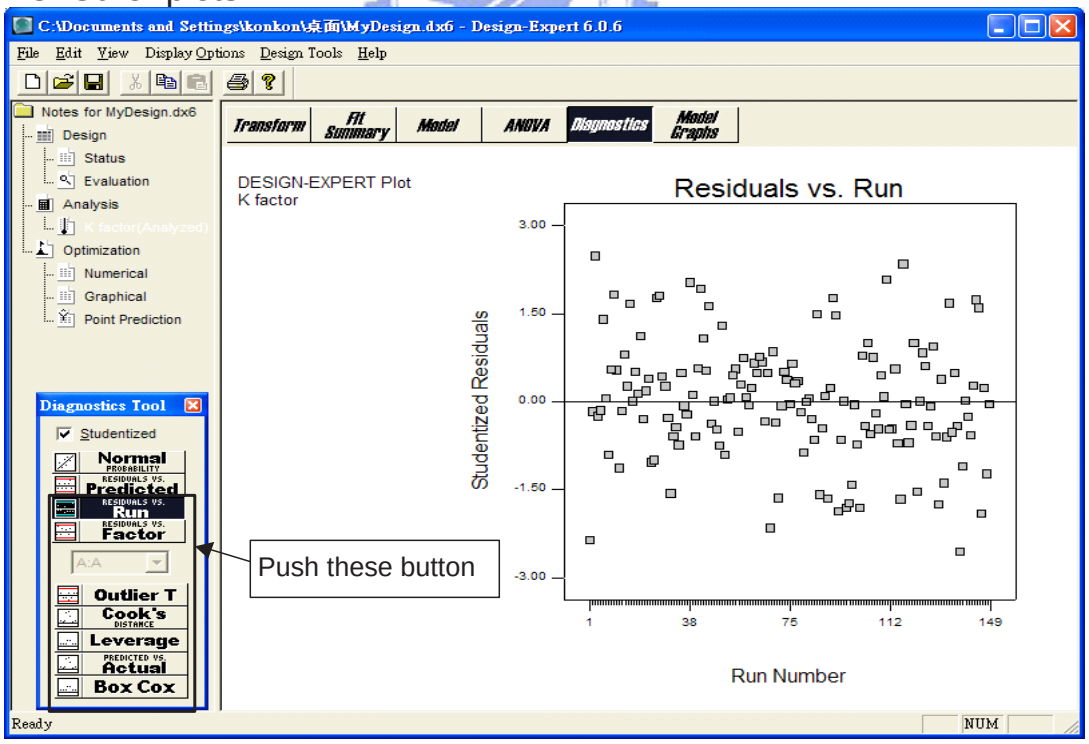

29. Contour plot - AB factors

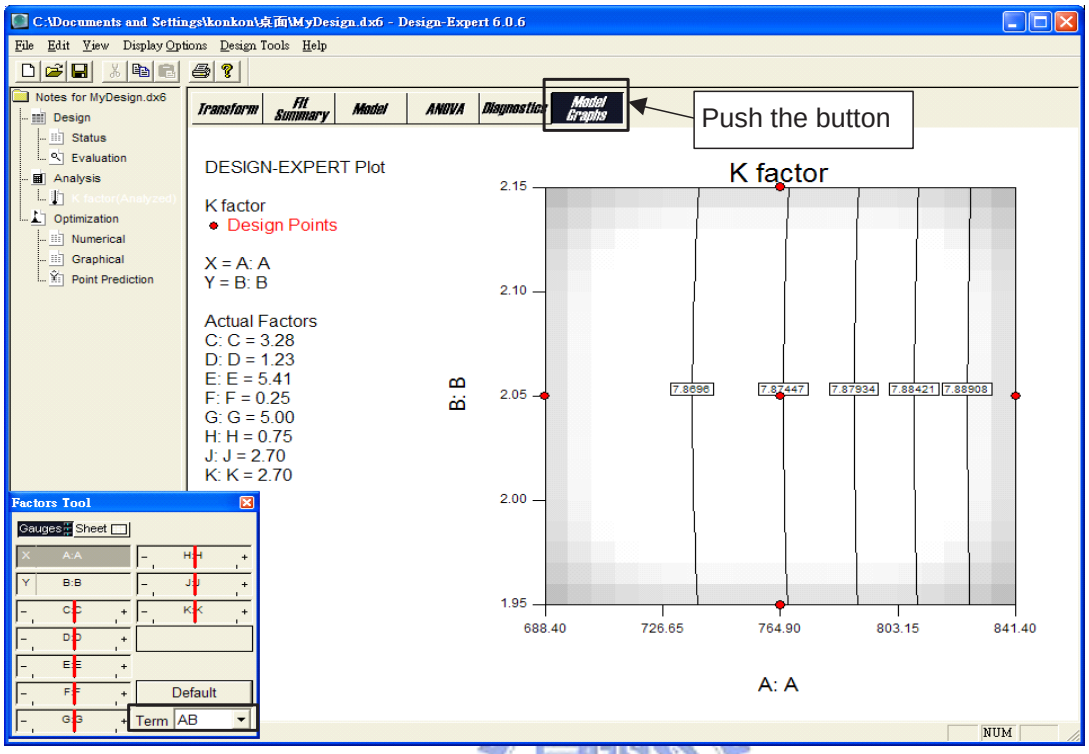

30. Change other contour plots of factors

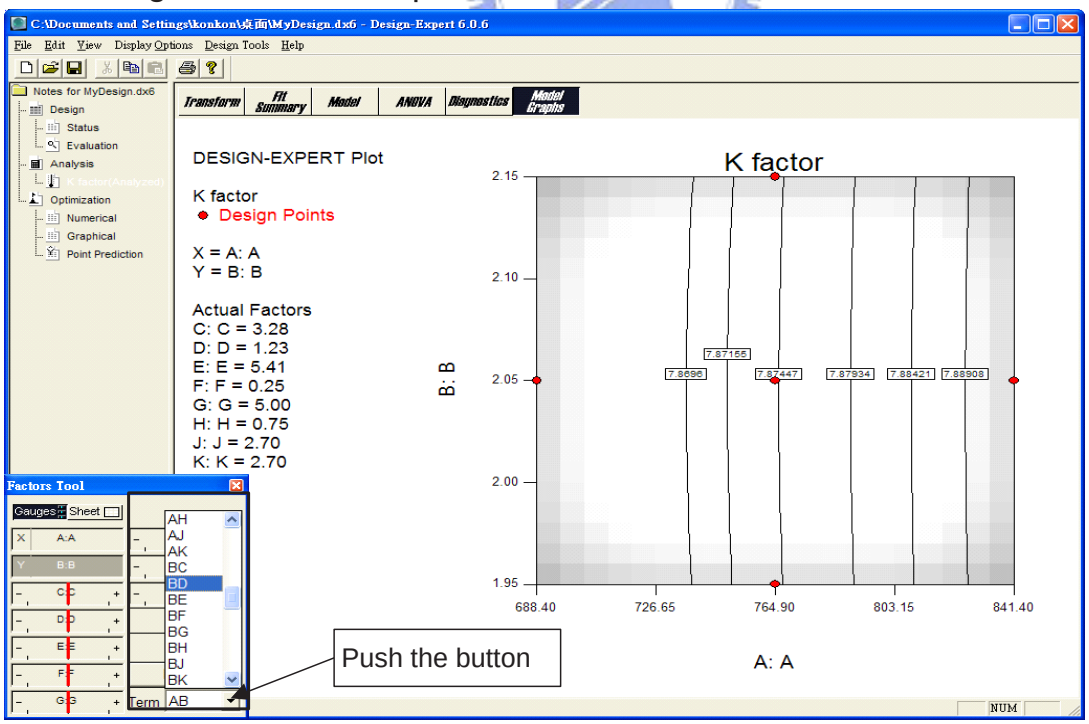

31. Optimization

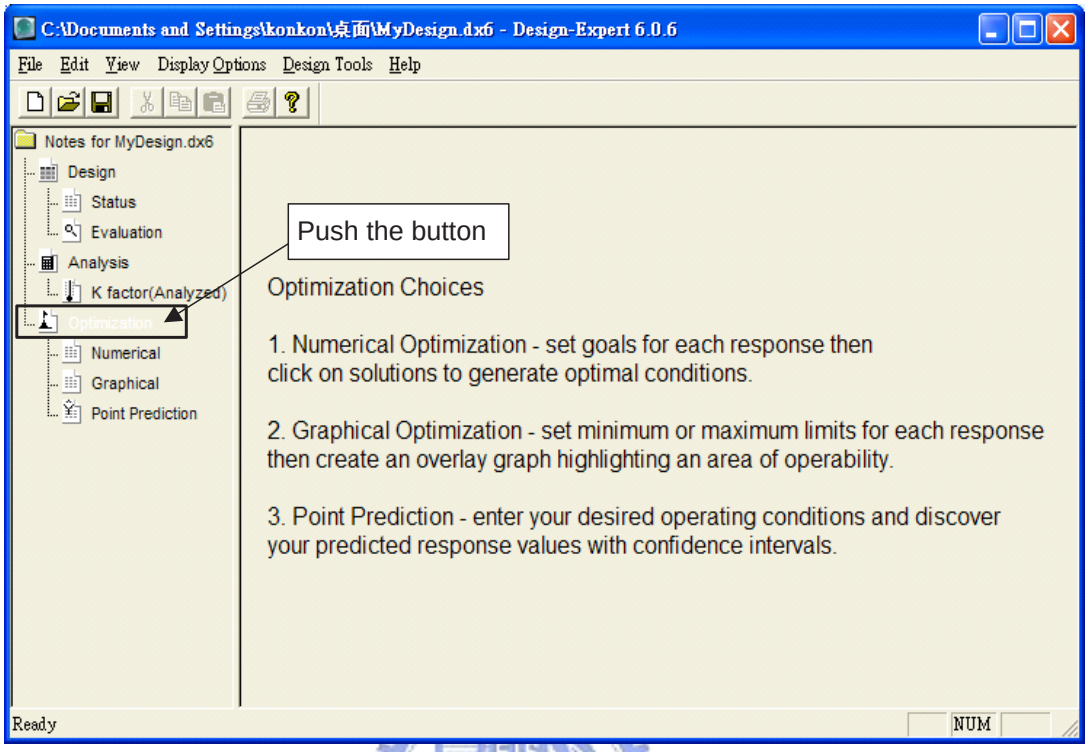

32. Determine the range of factor A

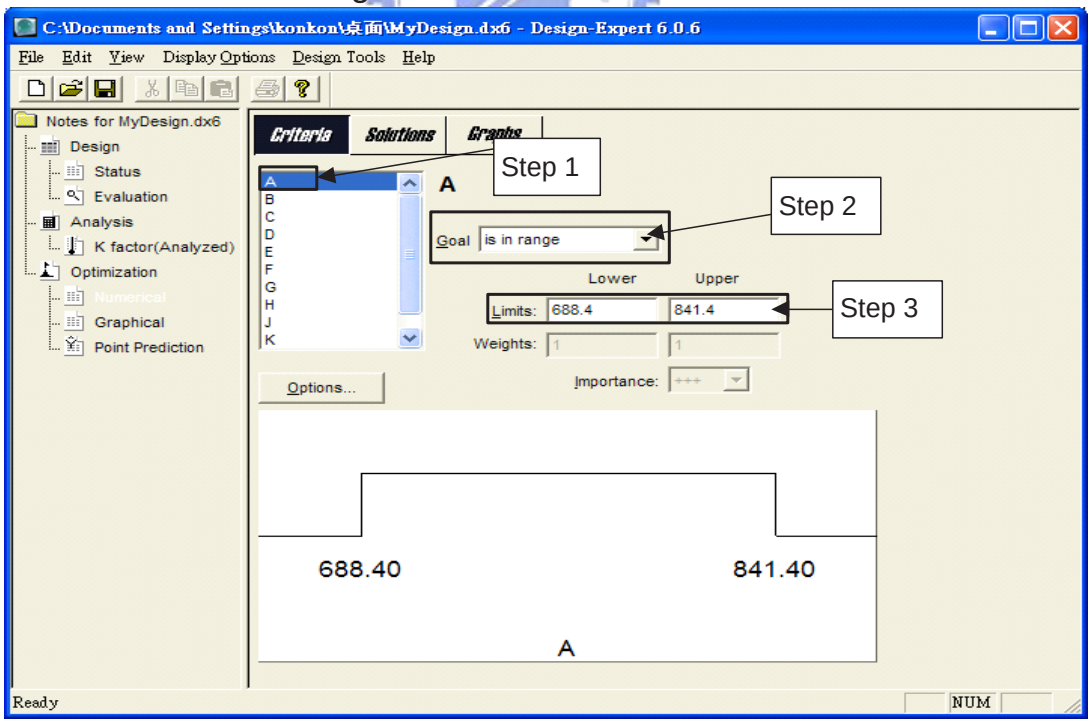

33. Determine the target value of K factor response

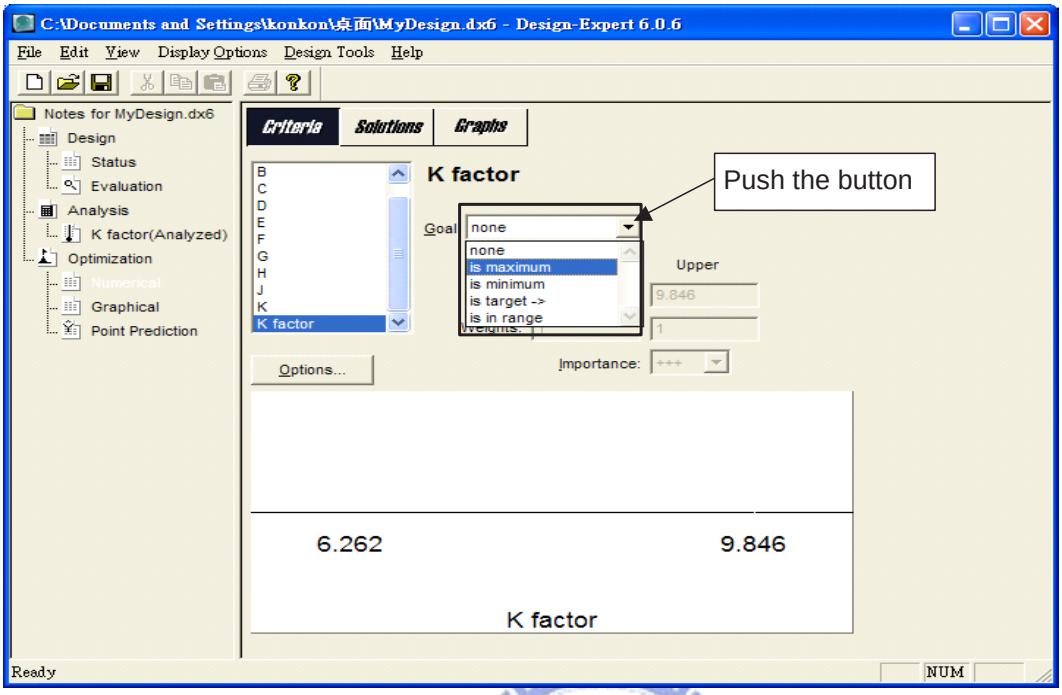

34. Determine the upper value, lower value, and weights of K factor response

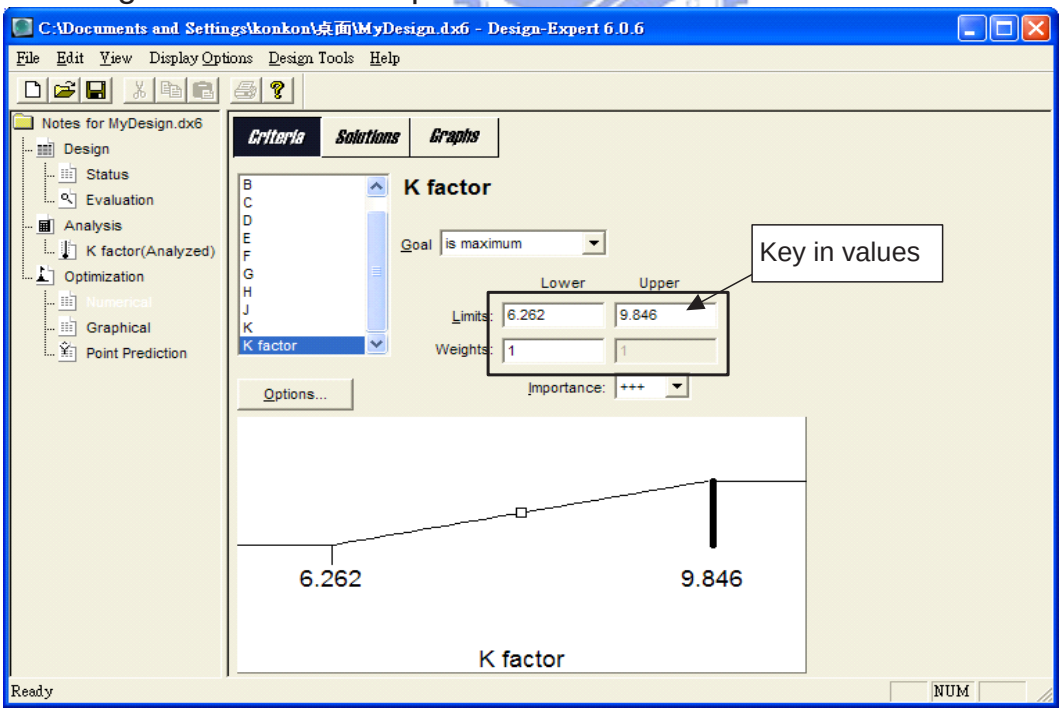

35. Summary of ten numerical solutions

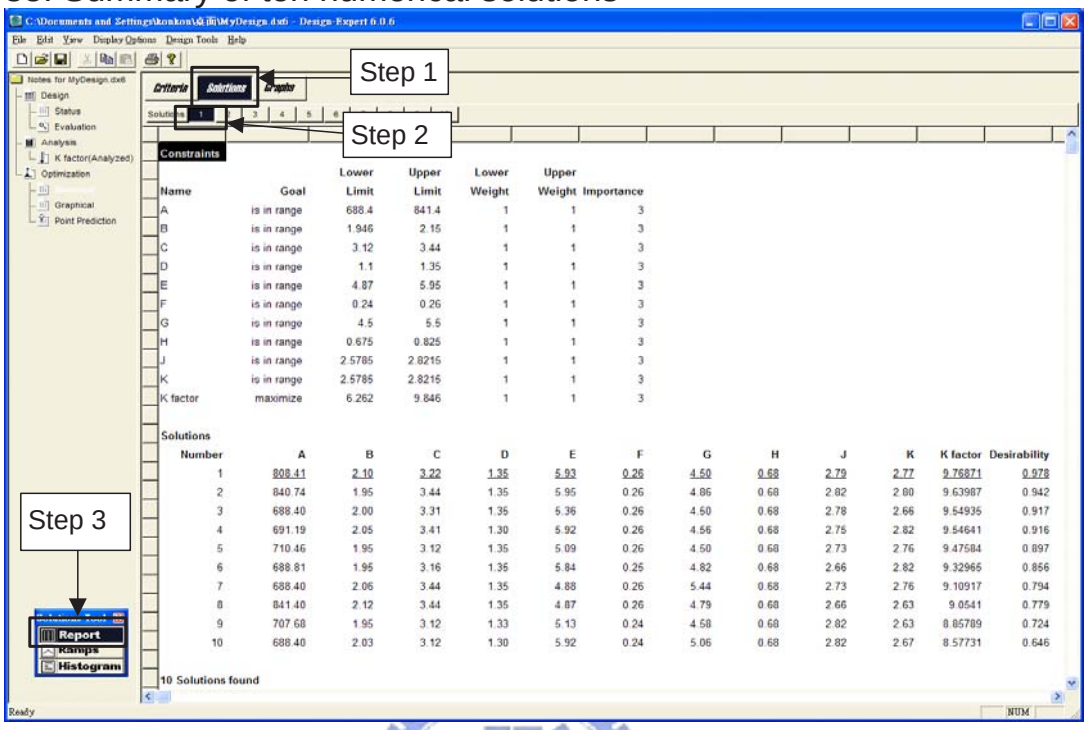

36. The number one solution, desirability is close to 1 as better

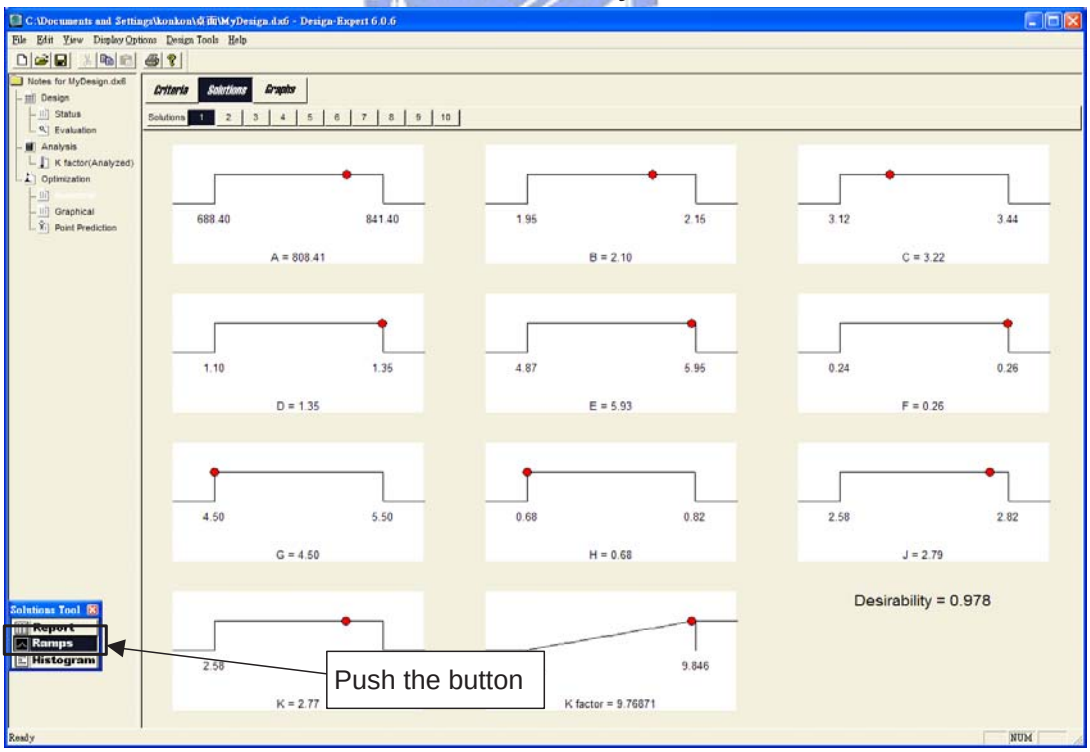

Appendix E

Sensitivity Analysis by Varying Ten Factors for the LNA Circuit

In this appendix, statistical distributions obtained by the sensitivity analysis on the models for the S11, S12, S21, S22, K ,NF, and IIP3 have provided here. we generate 100 normally and independently distributed pseudo-random numbers for 10 factors and seven responses obtained is calculated by the response surface model.

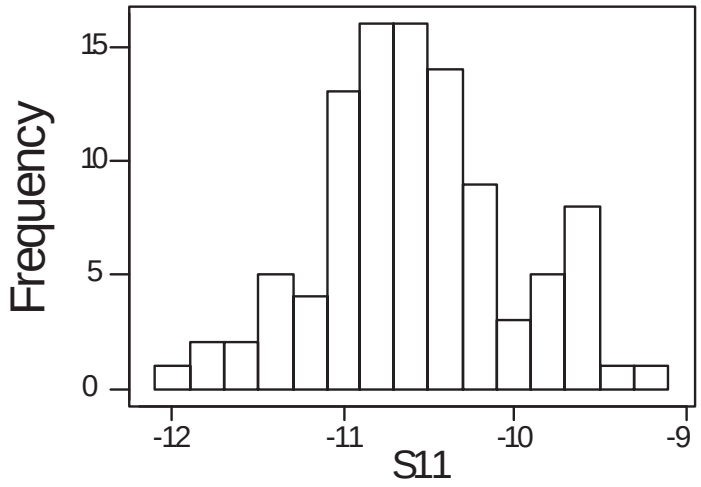

Figure E.1: Statistical distribution of the model for S11, which is calculated by the sensitivity analysis and using the full 2^{nd} order response surface model by varying 10 factors.

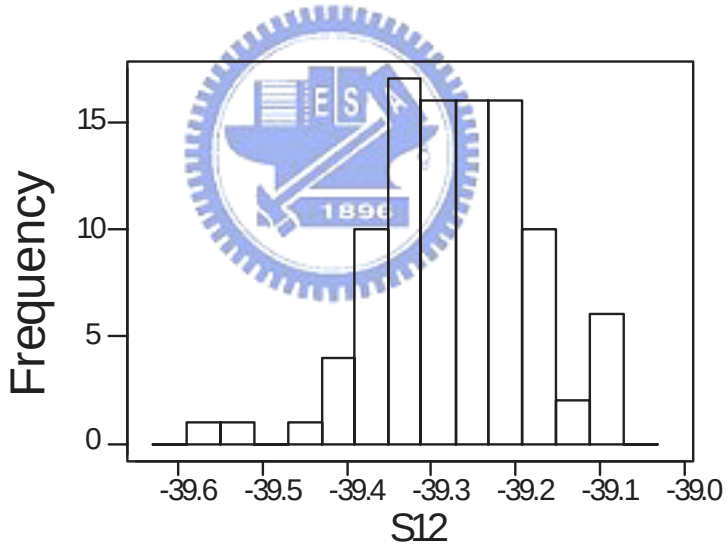

Figure E.2: Statistical distribution of the model for S12, which is calculated by the sensitivity analysis and using the full 2^{nd} order response surface model by varying 10 factors.

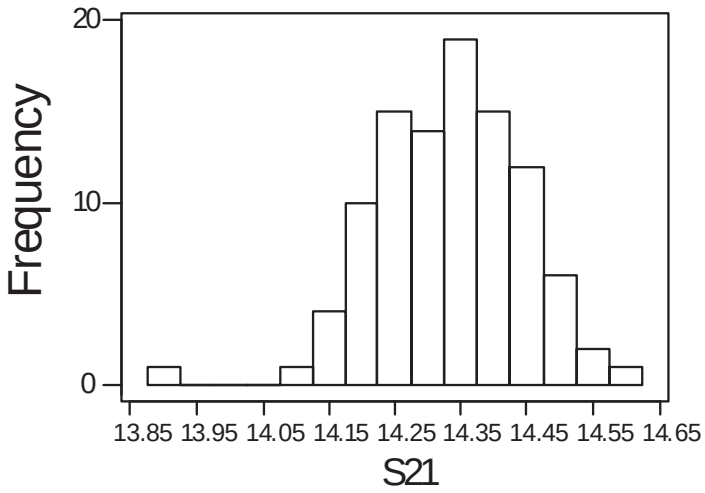

Figure E.3: Statistical distribution of the model for S21, which is calculated by the sensitivity analysis and using the full 2^{nd} order response surface model by varying 10 factors.

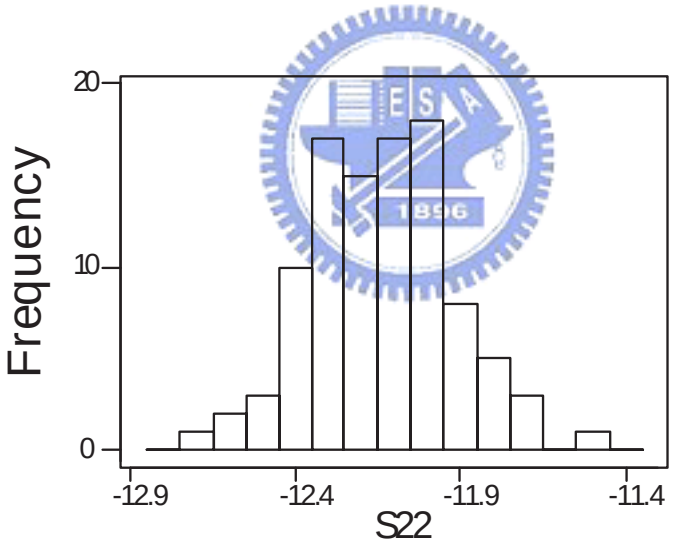

Figure E.4: Statistical distribution of the model for S22, which is calculated by the sensitivity analysis and using the full 2^{nd} order response surface model by varying 10 factors.

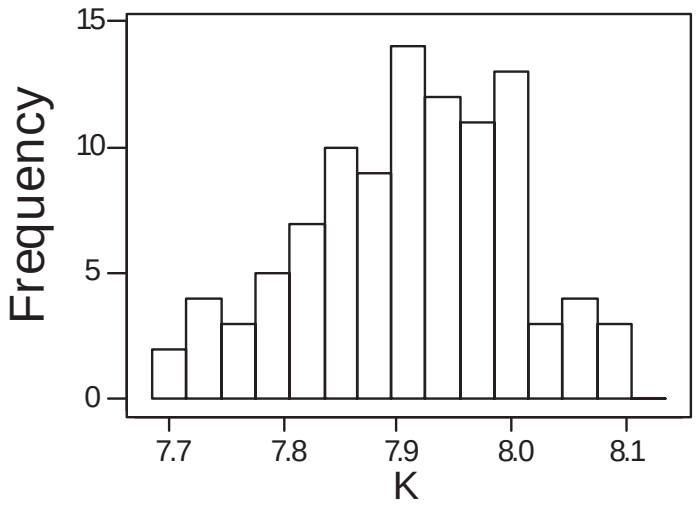

Figure E.5: Statistical distribution of the model for K, which is calculated by the sensitivity analysis and using the full 2^{nd} order response surface model by varying 10 factors.

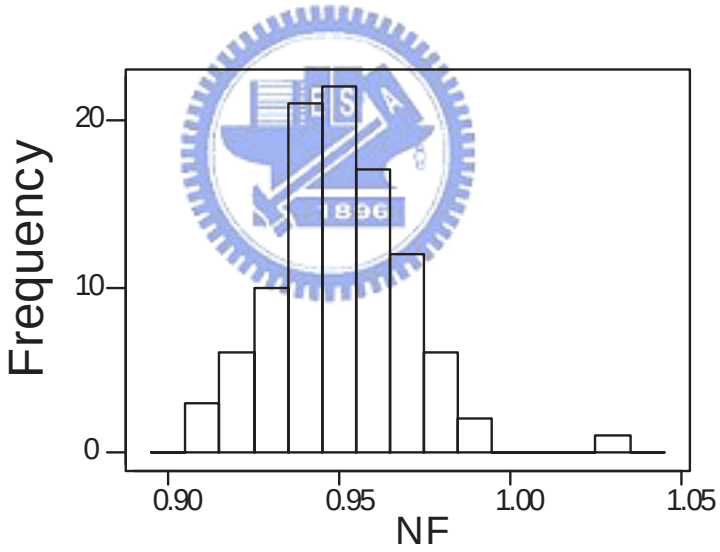

Figure E.6: Statistical distribution of the model for NF, which is calculated by the sensitivity analysis and using the full 2^{nd} order response surface model by varying 10 factors.

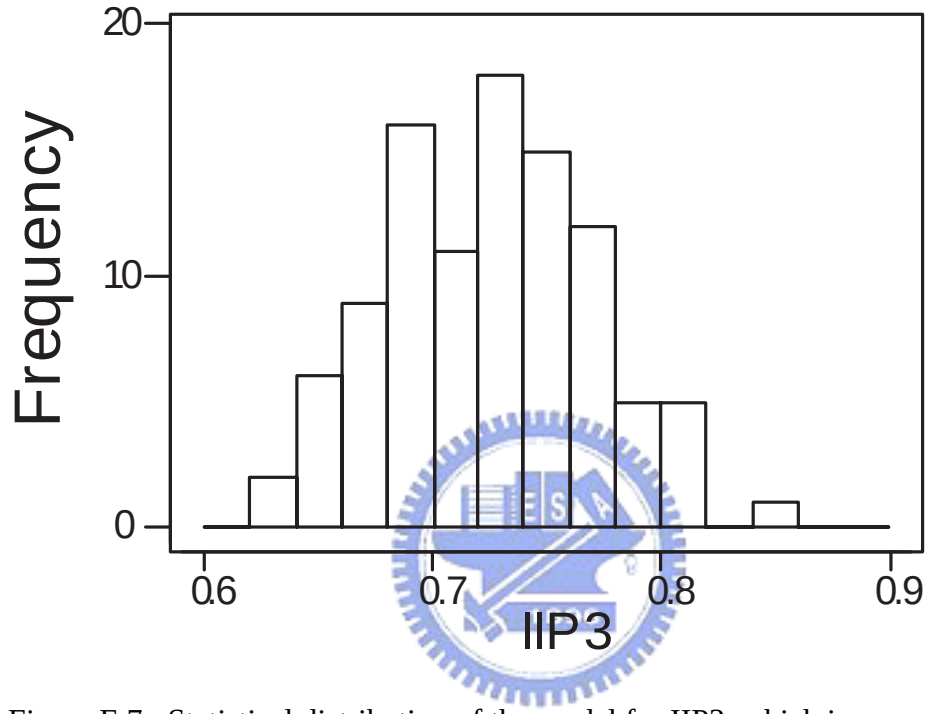

Figure E.7: Statistical distribution of the model for IIP3, which is calculated by the sensitivity analysis and using the full 2^{nd} order response surface model by varying 10 factors.

VITA

Name: Wan-Wen Lo, 羅婉文

Permanent address: No.276, Pingsin 2nd Rd., Tongsiao Township, Miaoli County 357, Taiwan

Degree and date to be conferred: Master of Statistics, July, 2006

Date of birth: August 11st, 1982

Place of birth: Miaoli, Taiwan

Collegiate institutions attended	Degree	Date of graduate
National Tsing Hua University Department of Mathematics	BS	June, 2004
National Chaio Tung University Institute of Statistics	MS	July, 2006

Master thesis title: Computational Statistics Approach to Integrated Circuit Design Optimization and Sensitivity Analysis

Publication List:

[1] Yiming Li, Chien-Sung Lu, Wan-Wen Lo, Meng-Jia Tsai, and Tung-Yu Wu,“Sensitivity Analysis of Static Noise Margin in SRAM Cells with 65 nm CMOS Devices,” Accepted by International Conference of Scientific Computing in Electrical Engineering (SCEE 2006), Sinaia, Romania, 17-22 September 2006.

[2] Yiming Li and Wan-Wen Lo, "A Unified Methodology for Characteristic Sensitivity Analysis of Analog and Digital Integrated Circuits," Submitted to International Conference on Solid State Devices and Materials, Sep. 12-15, 2006, Yokohama, Japan

[3] Yiming Li, Wan-Wen Lo, Tung-Yu Wu, and Yu-Tzu Chen, "Statistical Algorithm for Circuit Design Optimization," Submitted to International Conference of Computational Methods in Sciences and Engineering, Oct. 27-Nov. 1, 2006, Crete, Greece.